NASA CR-135327
CASD-NAS-77-025



NASA

National Aeronautics and Space Administration

# CONCEPTUAL DESIGN FOR SPACELAB TWO-PHASE FLOW EXPERIMENTS

December 1977

Prepared by
R. D. Bradshaw
C. D. King

Prepared for
National Aeronautics and Space Administration
LEWIS RESEARCH CENTER
21000 Brookpark Road
Cleveland, Ohio 44135
Contract NAS3-20389

Prepared by
GENERAL DYNAMICS CONVAIR DIVISION
P.O. Box 80847
San Diego, California 92138



GENERAL DYNAMICS
*Convair Division*

| 1. Report No. | 2. Government Accession No. | 3. Recipient's Catalog No. |
|---|---|---|
| NASA CR-135327 | | |

| 4. Title and Subtitle | 5. Report Date |
|---|---|
| Conceptual Design for Spacelab Two-Phase Flow Experiment | December 1977 |
| | 6. Performing Organization Code |
| 7. Author(s) | 8. Performing Organization Report No. |
| R. D. Bradshaw and C. D. King | CASD-NAS-77-025 |
| | 10. Work Unit No. |
| 9. Performing Organization Name and Address | 11. Contract or Grant No. |
| General Dynamics Convair Division<br>P.O. Box 80847<br>San Diego, CA 92138 | NAS3-20389 |
| | 13. Type of Report and Period Covered |
| 12. Sponsoring Agency Name and Address | Contractor Report |
| National Aeronautics and Space Administration<br>Washington, DC 20546 | 14. Sponsoring Agency Code |

15. Supplementary Notes

Project Manager, Thomas H. Cochran, Space Propulsion & Power Division
NASA Lewis Research Center, Cleveland, Ohio 44135

16. Abstract

A conceptual design for a two-phase flow experiment for Spacelab was prepared. The NASA-mission propulsion applications, cryogenic storage in space and advanced cryogenic vehicles, constitute the major volume user. Space power stations using the Rankine cycle have large potential application. The status of the existing empirical correlations justifies the experiment scientifically. KC-135 aircraft tests confirmed the gravity sensitivity of two-phase flow correlations. The prime component of the apparatus is a 1.5 cm dia by 90 cm fused quartz tube test section selected for visual observation. The water-cabin air system with water recycle was a clear choice for a flow regime-pressure drop test since it was used satisfactorily on KC-135 tests. Freon-11 with either overboard dump or with liquid-recycle will be used for the heat transfer test. The two experiments use common hardware. The experimental plan covers 120 data points in six hours with mass velocities from 10 to 640 kg/sec-$m^2$ and qualities 0.01 to 0.64. The apparatus with pump, separator, storage tank and controls is mounted in a double Spacelab rack. Supporting hardware, procedures, measured variables and program costs are defined. It is highly recommended that a design phase be initiated now and include the integration of these two-phase flow experiments with additional heat transfer/fluids experiments being considered. Our proposed configuration supports the integrated experiment concept.

| 17. Key Words (Suggested by Author(s)) | 18. Distribution Statement |
|---|---|
| Two-Phase Flow<br>Boiling<br>Reduced Gravity<br>Spacelab<br>Manned Orbital Research Laboratories | Unclassified - Unlimited |

| 19. Security Classif. (of this report) | 20. Security Classif. (of this page) | 21. No. of Pages | 22. Price* |
|---|---|---|---|
| Unclassified | Unclassified | 88 | |

* For sale by the National Technical Information Service, Springfield Virginia 22151

# FOREWORD

This conceptual design study was conducted by General Dynamics Convair Division at San Diego, California under Contract NAS3-20389. The program was under the direction of the NASA Project Manager, Mr. Thomas H. Cochran, Gravitational Environment Section, NASA Lewis Research Center. The study was completed under the direction of Convair project leader, Dr. Robert D. Bradshaw in the Convair Thermodynamics Group. A co-author of the report is Mr. C. Douglas King of the same group. These authors acknowledge the assistance provided by Robert E. Drowns in Mission Analysis, Robert E. Bradley in Economic and Cost Analysis, and Danial T. Chu and Walter O. Johnston in Design. The authors further acknowledge the capable direction and assistance provided by Mr. Cochran.

TABLE OF CONTENTS

TABLE OF CONTENTS, Contd.

LIST OF FIGURES

LIST OF FIGURES, Contd

LIST OF TABLES

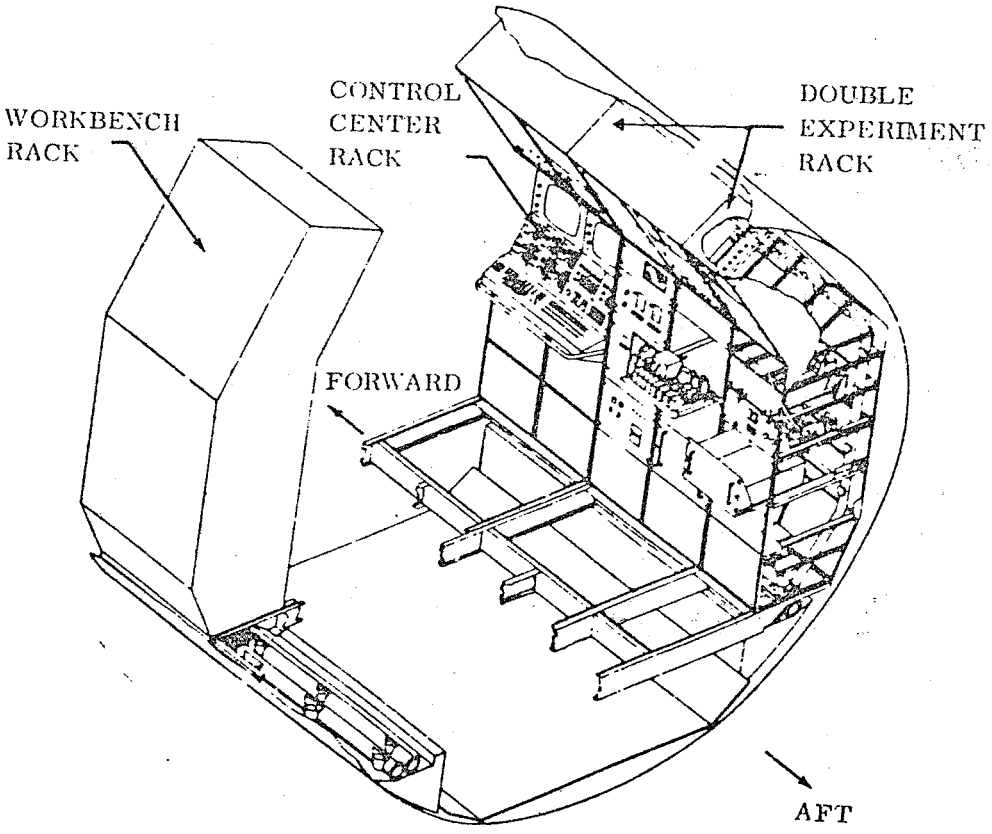

## SUMMARY

A conceptual design for a two-phase flow experiment for Spacelab was prepared. The NASA-mission applications were defined and a scientific justification for the study was established. An experimental test apparatus is described; the prime component being a tubular fused quartz test section selected for visual observation. The definition of flow-regimes and pressure drop will be achieved with an air-water fluid system while the heat transfer data will be taken in the same test configuration using only Freon-11. The apparatus with pump, separator, storage tank and controls is mounted in a double Spacelab rack. Other study achievements included a definition of supporting hardware, procedures, measured variables and program costs.

The proposed experiment is to be performed in the early 1980's. A search of the literature revealed many NASA missions in the remainder of this century which can benefit from improved design data for two-phase flow in reduced-gravity. The applications include propulsion, automated spacecraft, power generation, experiment support and life support systems. The propulsion applications constitute the major volume user. Cryogenic storage in space and advanced cryogenic vehicles are major applications in this area. Space power stations which use the Rankine cycle have a large potential application. For the remaining applications, a variety of cryogenic liquids will be able to be more effectively used with improved knowledge of the heat-transfer correlations.

The experiment is justified scientifically when we examine the existing empirical correlations for flow regime, pressure drop, and heat transfer. A correlation which contains the Froude number has been used in one investigation to indicate a shift in the flow regimes with a change in gravity level to $10^{-2}$ g's. Although a shift in the flow regime boundaries was observed, the magnitude of the shift did not agree with predictions. For pressure drop, no valid reduced-gravity correlations exist. Here the approach is to identify the flow regime and use existing one-g pressure drop correlations. Preliminary data at $10^{-2}$ g's indicates a 50% increase in pressure drop occurs at reduced-gravity. The heat transfer correlations are even more complex; a super-position of forced convection and boiling data has been used to correlate data on earth. It is accepted that boiling data is sensitive to gravity-level thus a sensitivity in these correlations is anticipated. However, no reduced-gravity two-phase flow data has been obtained.

Two-phase flow correlations are typically regime sensitive. An air-water test is planned so that the regimes can be clearly identified at the low gravity levels. This will also provide the most reliable pressure drop data since steady-state conditions will persist in the tube. Conversely, heat transfer data with Freon will cover a range of conditions depending on mass velocity and wall heat flux as controlled

by heater power. The experimental plan covers a range of mass velocities from 10 to 640 kg/sec-$m^2$ (7400 to 472,000 lb/hr-$ft^2$) and the quality range from 0.01 to 0.64.

A test section 1.5 cm in diameter by 90 cm long is recommended to provide L/D > 60. The circular test section is a fused quartz tube enclosed in a square Lucite block with an axial cylindrical hole. Visual observations with photographic coverage provides a prime data source. As indicated above, air-water and Freon-11 were selected as test fluids. Freon-11 boils at ambient temperature and lower as the outlet pressure is decreased below 100 kN/$m^2$ (1 atm). The test section is heated by a copper-nickel resistance wire providing 679 watts. A total of 80 data points are planned for the air-water system while 40 data points are planned for the Freon tests, these points requiring one and two minutes for data collection, respectively. Total test time is six hours allowing for changes in hardware settings. Total heater energy usage is 933 watt-hours. Total experiment energy usage is 2929 watt-hours in the six hours.

Experimental concepts considered test fluids of water, air, nitrogen, and Freon with the fluid loops or paths of overboard dump, total recycle, batch collection, and liquid-only recycle. Only three of ten concepts appeared promising. The water-cabin air system with water recycle was a clear choice for a flow regime-pressure drop test since it had been proven satisfactory on a KC-135 test program. Freon-11 with overboard dump or with liquid-recycle were selected alternatives for the heat transfer test. The former is preferred for simplicity, however the latter avoids dumping excess Freon, only 14 kg (30 lbs) versus 111 kg (245 lbs) and is more volume efficient. The liquid is pumped through the test loop from a storage tank or for recycle from a rotating separator which removes the liquid from the mixed-phase outlet flowstream of the test section.

As indicated earlier, the two experiments use common hardware and test section. Water is the first test fluid and is dumped overboard; the system is dried by a vacuum blowdown and next the Freon test is conducted. The test section is instrumented with thermocouples to measure wall and fluid temperatures. Quality is determined from flowmeters and energy input. Capacitance-type quality meters will also be used at the inlet and outlet. The Freon is stored in a tank with fluid control by bladders or capillary devices. The latter may be desirable if a transparent test tank is to be used for other integrated heat transfer/fluid dynamics tests.

A scientific layout design has been prepared for both experimental concepts in a double Spacelab rack. The experimental controls are very accessible and space still exists for integrating additional small fluid experiments in this rack. Several elements of the test hardware such as cameras, lights, electronics/signal conditioning and controls can be shared. The Freon-11 hardware, except for the test section, is contained within a Lexan enclosure for safety. The crew task performance and experimental procedures have been outlined. The data acquisition and reduction approach is briefly covered.

The experimental costs were defined through Level IV integration. Several high cost items including the test section, blower/motor, Freon tank, sensors/signal conditioning, quality meters, film magazines, and secondary structure were identified to have development costs of 147K and total costs of 276K dollars. For the program costs through Level IV integration, the development costs were 604K with production and operational costs of 314K for a program cost of 918K dollars.

In view of the results of this study, it is highly recommended that a design study be initiated at this time to integrate these two-phase flow experiments with additional heat transfer and fluids experiments being considered. The proposed configuration will support the integrated experiment concept.

# 1

# TECHNOLOGICAL JUSTIFICATION

As the Space Transportation System becomes operational in the early 1980's, the number of payloads placed in orbit annually will increase as will the complexity of these systems. By the mid 1980's we anticipate several new systems will be flowing numerous fluids in the low-gravity environment. The design and performance of these systems can be improved with proven correlations of two-phase fluid behavior in reduced-gravity. Cryogenics are unique in that initial line transients involve chilldown and the occurrence of two-phase flow. A second major application is space power systems or radiators in space where boilers or condensors involve the flow of two-phase fluids.

The literature for space systems has been reviewed and the specific applications which are discussed have been tabulated in this section. The importance of two-phase flow to these processes has been examined. Finally, the availability of data from a Spacelab experiment to support the design requirements of future systems has been assessed.

## 1.1 MISSIONS AND APPLICATIONS

A survey of NASA-missions has been completed and the results are presented in the following paragraphs and tables. The results support the conclusion that two-phase flow phenomena will be an increasingly significant element in space operations in the last two decades of this century. The NASA missions and vehicles for which two-phase flow may be important are listed under five functional categories as follows:

Propulsion
Automated Spacecraft
Power Generation
Experimental Support (Spacelab and Space Station)
Environmental Control/Life Support Systems (EC/LSS)

These functional categories are presented in Tables 1-1 through 1-5, respectively. Each program/vehicle listed includes the identification of the fluid, fluid function, quantity used, and the source of the data which is presented. Additionally, the number of men that the EC/LSS is to support is listed. There are many other potential applications for two-phase flow that have been proposed for automated spacecraft and spacelab experiments but were not included herein because of duplication of fluid application and quantity.

## Table 1-1. Propulsion Applications

| Program/Concept | Fluid | Fluid Function | Quantity lbs | Line Size Dia × L cm | Liquid Flow Rate, $G_l$ kg/m²-sec | Vapor Flow Rate, $G_g$ kg/m²-sec | Quality x | Inlet Pressure kN/m² | Temperatures Liquid K | Gas K | Wall K | Data Source |
|---|---|---|---|---|---|---|---|---|---|---|---|---|
| Propellant Depot (Orbital Fluid Transfer) | $LO_2$ | Re-supply | 600K/yr-360M/yr | ~4 × 10000 | - | - | 0 → 1 | 170 | 90 | - | - | Ref. 1 |
| | $LH_2$ | Re-supply | 100K/yr-60M/yr | ~8 × 10000 | - | - | 0 → 1 | 140 | 20 | - | - | |
| Orbital Transfer Vehicle (OTV) | $LO_2$ | Propulsion | 47K-89K | 6 × 760 | < 12000 | < 12000 | 0 → 1 | 170 | 90 | - | - | Ref. 1, Ref. 2 |
| | $LH_2$ | Propulsion | 8K - 150K | 12 × 760 | < 100 | < 100 | 0 → 1 | 140 | 20 | - | - | |
| Logistics Tank | $LO_2$ | Re-supply | 47K-4.6M | 3 × 100 | < 8000 | < 8000 | 0 → 1 | 170 | 90 | - | - | Ref. 1 |
| Logistics Tank | $LH_2$ | Re-supply | 8K-1.6M | 4.3 × 1300 | < 600 | < 600 | 0 → 1 | 140 | 20 | - | - | Ref. 1 |
| Electric Propulsion OTV for SPS (Alternative Fluids Listed) | LAr | Propulsion | 10M-92M/yr | ~0.65 × - | < 45 | < 45 | 0 → 1 | 1460 | 90 | - | - | Ref. 1 |
| | $LO_2$ | RCS Prop. | 3.4M-32M/yr | ~ 6.5 × - | < 1060 | < 1060 | 0 → 1 | TBD | 90 | - | - | |
| | $LH_2$ | RCS Prop. | 570K-5.3M/yr | ~ 1 × - | < 120 | < 120 | 0 → 1 | TBD | 20 | - | - | |
| Lunar Transfer Vehicle | $LO_2$ | Propulsion | 62K | ~ 3 × ~ 100 | ~ 8000 | ~ 8000 | 0 → 1 | 170 | 90 | - | - | Ref. 3 |
| | $LH_2$ | Propulsion | 10K | ~ 4 × ~ 1000 | ~ 700 | ~ 700 | 0 → 1 | 140 | 20 | - | - | |
| Solar Electric Propulsion Stage | LAr | Propulsion | 1K | ~ .3 × - | ~ 400 | ~ 400 | 0 → 1 | TBD | 90 | - | - | Ref. 1 |
| Propellant Depot/ Liquefaction | $LO_2$ | Generate Propellants for OTV | 700K/yr-420M/yr | TBD | 0.86 kg/sec | 0.86 kg/sec | 0 → 1 | TBD | 90 | - | - | Ref. 1, Convair in house |
| | $LH_2$ | | | TBD | 0.1 kg/sec | 0.1 kg/sec | 0 → 1 | TBD | 20 | - | - | |
| SPS/Reaction Control System | LAr | Prop. | 121K/yr-496K/yr | TBD | $1.7\times10^{-5}$ kg/sec | $1.7\times10^{-5}$ kg/sec | 0 → 1 | - | - | - | - | Ref. 4, p IV - B-4-15 |
| Cargo OTV: (Concepts) | | | | | | | | | | | | |
| -Chemical Propulsion | $LO_2$ | Propulsion | 151M/flt. | TBD | 21.3 kg/sec | 21.3 kg/sec | 0 → 1 | - | 90 | - | - | Ref. 4, p VI-D-1-13 |
| | $LH_2$ | | | TBD | 3.6 kg/sec | 3.6 kg/sec | 0 → 1 | - | 20 | - | - | |
| -Resistojet (Elect. Concept) | $LH_2$ | Propulsion | 47M/flt. | TBD | 4.5 kg/sec | 4.5 kg/sec | 0 → 1 | 100 | 20 → | - | - | |
| -Arc Jet (Elect. Concept) | $LH_2$ | Propulsion | 10.3M/flt. | TBD | .00015 kg/sec | .00015 kg/sec | 0 → 1 | 100 | 20 → | - | - | |
| Nuclear Shuttle | $LH_2$ | Fuel | 360K | 15 × - | 3.2 kg/sec | 3.2 kg/sec | 0 → 1 | 190 | 20 | - | - | Ref. 5 |
| | $LO_2$ | Prop. | 5560 | - × - | .25 kg/sec | .25 kg/sec | 0 → 1 | 190 | 90 | - | - | |
| Advanced Vehicle (General) | $LH_2$ | Thermal Manage-ment | TBD | 1 × 1000 | ~ 2 | ~ 2 | 0 → 1 | 140 | 20 | - | - | Ref. 1 |
| | $LO_2$ | | TBD | 1 × 1000 | ~ 30 | ~ 30 | 0 → 1 | 210 | 90 | - | - | |

## Table 1-2. Automated Spacecraft Applications

| Program/Concept | Fluid | Fluid Function | Quantity lbs | Line Size Dia × L cm | Liquid Flow-Rate, $G_l$ kg/m²-sec | Vapor Flow-Rate, $G_g$ kg/m²-sec | Quality x | Inlet Pressure kN/m² | Temperatures Liquid K | Gas K | Wall K | Data Source |
|---|---|---|---|---|---|---|---|---|---|---|---|---|
| Large High Energy Observatory B (HE-09A) | LHe | Cooling of Superconducting Magnetic Coils | 950 | 0.55 × 4500 | 0.5 | - | 0 → 1 | 24 | 3 | - | - | Ref. 6, pg. 46 Ref. 7 |
| Large X-Ray Telescope (HE-01A) | $LH_2$ | Detector Cooling | - | - | - | - | - | | 20-78 | - | - | Ref. 8, HE-01A |
| Gravity Coarse Monitoring Payload | LHe | Precision Gyroscope Cooling Cryogenic Dewar | 298/hr | - | - | - | - | 3 | 1.6-2 | - | - | Ref. 8, AP-01A |
| Flare Coarse Monitoring Payload | $LN_2$ | Detector Cooling Refrigerator | | 300 W Refrig. 1 $M^3$ | - | - | 0 → 1 | - | 78 | - | - | Ref. 6, p. 64 |
| Ocean Resources & Dynamics System (CO-4) (1985 | $LN_2$ | Detector Cooling Refrigerator | | - | - | - | - | - | - | - | - | Ref. 9, V. 1. III p. 13 |



## Table 1-3. Power Generation Applications

| Program/Concept | Fluid | Fluid Function | Quantity lbs | Line Size Dia × L cm | Liquid Flow-Rate, $G_l$ kg/m²-sec | Vapor Flow-Rate, $G_g$ kg/m²-sec | Quality x | Inlet Pressure kN/m² | Temperatures Liquid K | Gas K | Wall K | Data Source |
|---|---|---|---|---|---|---|---|---|---|---|---|---|
| SPS/Rankine Cycle | Under Evaluation (Type A: Water, Ammonia, Liquid Metals) (Type B: Freons, Diphenzl, etc.) | Power Generation in Boilers, Condensers | TBD | TBD | TBD | TBD | 0 → 1 | - | - | - | - | Ref. 4 p. IV-B-1-C-6 |
| SPS/Superconducting Generators and Cables | LHe | Power Generation Cryogenic Cooling | TBD | - | - | - | - | - | 4 | - | - | Ref. 4 p. IV-B-1-C-37 |

## Table 1-4. Experimental Support (Spacelab and Space Station) Applications

| Program/Concept | Fluid | Fluid Function | Quantity lbs | Line Size Dia × L cm | Liquid Flow-Rate, $G_l$ kg/m²-sec | Vapor Flow-Rate, $G_g$ kg/m²-sec | Quality x | Inlet Pressure kN/m² | Temperatures Liquid K | Gas K | Wall K | Data Source |
|---|---|---|---|---|---|---|---|---|---|---|---|---|
| Bioprocessing (Urokinase Production) | $LN_2$ | Refrigeration | 44 | 0.12 m³ | - | - | 0 → 1 | - | - | - | - | Ref. 10, p. 3-35 p. 5-85 |
| | Waste Med. | Waste Recycle Cryogenic Storage | | | | | | | | | | |
| Liquid Xenon Compton Telescope | LXe | X-Ray Detection | - | - | - | - | - | - | - | - | - | Ref. 11 |
| | LAr | Cool LXe | - | - | - | - | - | - | - | - | - | |
| Atmospheric, Magneto-spheric, & Plasma in Space (AMPS) (AP-06-S) | LHe | Radiometer IR Detector Cooling | 4 | TBD | TBD | - | 0 → 1 | - | 4 | - | - | Ref. 12, AP-06-S |
| | LHe | Spectrometer IR Detector Cooling | 44 | TBD | TBD | - | 0 → 1 | - | 4 | - | - | |
| | $LN_2$ | Spectrometer SWIR Detector Cooling | 18 | TBD | TBD | - | 0 → 1 | - | 77 | - | - | |
| Automated Furnace/ Levitation | $LO_2$ | Fuel Cell Reactants | 877 | TBD | TBD | - | 0 → 1 | - | 90 | - | - | Ref. 12 |
| | $LH_2$ | Fuel Cell Reactants | 111 | TBD | TBD | - | 0 → 1 | - | 20 | - | - | SP-14-S, SP-15-S |
| Shuttle IR Telescope Facility (AS-01-S) | LHe | Detector Cooling | 132 | TBD | TBD | - | 0 → 1 | - | 4 | - | - | Ref. 12, AS-01-S |
| Deep Sky UV Survey Telescope (AS-03-S) | LHe | Detector Cooling | 23 | TBD | TBD | - | 0 → 1 | - | 4 | - | - | Ref. 12, AS-03-S |
| Magnetic Spectrometer (HE-15-S) | LHe | Magnet Cooling | 40 | TBD | TBD | - | 0 → 1 | - | 4 | - | - | Ref. 12, HE-15-S |
| Bioprocessing (SP-01-S) | $LO_2$ | Fuel Cell Reactants | 291 | TBD | TBD | TBD | 0 → 1 | - | 90 | - | - | Ref. 12, SP-01-S |
| | $LH_2$ | Fuel Cell Reactants | 36 | TBD | TBD | TBD | 0 → 1 | - | 20 | - | - | |
| Bioprocessing (SP-31-S) (First Spacelab Mission) | $LN_2$ | Cryogenic Refrigeration | 13 | TBD | TBD | TBD | 0 → 1 | - | 77 | - | - | Ref. 12, SP-31-S |
| $CO_2$ Laser Data Relay Link (CN-05-S) | $LN_2$ | Cooling | 22 | TBD | TBD | TBD | 0 → 1 | | 77 | - | - | Ref. 12, CN-05-S |

## Table 1-5. Environmental Control/Life Support System Applications

| Program Concept | Men | Fluid | Fluid Function | Quantity lbs | Line Size Dia × L cm | Liquid Flow-Rate, $G_\ell$ kg/m²-sec | Vapor Flow-Rate, $G_g$ kg/m²-sec | Quality x | Inlet Pressure kN/m² | Temperatures Liquid K | Gas K | Wall K | Data Source |
|---|---|---|---|---|---|---|---|---|---|---|---|---|---|
| Shuttle | 4-6 | Waste Water | Reject Heat With Ammonia Boilers | 495 | 1.2 × - | 250 | 250 | 0 → 1 | - | - | - | - | Ref. 13 |
| OTV Crew Module | 4 | $LN_2$, $LO_2$, $H_2O$ | Environmental Control | (7 days) | Typ/man | Typ/man | Typ/man | 0 → 1 | - | - | - | - | Ref. 10, V1-E-7 |
| Passenger Module (POTV) SPS LEO Const. | 68 | $LN_2$, $LO_2$, $H_2O$ | Environmental Control | (7 days) | Typ/man | Typ/man | Typ/man | 0 → 1 | - | - | - | - | Ref. 10, V1-E-10 & V1-F-6 |
| Passenger Module (POTV) SPS GEO Const. | 230 | $LN_2$ $LO_2$ $H_2O$ | Environmental Control | (7 days) | Typ/man | Typ/man | Typ/man | 0 → 1 | - | - | - | - | Ref. 10, p. V1-F-5 |
| Space Station | 4 | Waste Water | Water Recovery by Vapor Compression Distillation | 40/day | TBD | - | - | 0 → 1<br>1 → 0 | - | - | - | - | Ref. 14, Book 3, p. 97 and F5 |
| Space Station | 6 (Growth -12-24) | Waste Water | Water Recovery by Vapor Compression Distillation | 60/day 120-240/ day | TBD | - | - | 0 → 1<br>1 → 0 | - | - | - | - | Ref. 14, Book 3, p. 195 and Appendix F |
| SPS Construction (Construction and Support) | 200-800 | | Environmental Control | | Typ/man | Typ/man | Typ/man | - | - | - | - | - | Ref. 4, p. V-C-13 |
| Space Taxi | 1 | $LN_2$ | Environmental Control | 4 | 2.5 × - | - | - | - | - | 78 | - | - | Ref. 15 |
| | | $LO_2$ | | 11 | 2.5 × - | - | - | - | - | 90 | - | - | |
| | | $LH_2$ | Fuel Cell Reactants | 1 | < 1 + - | - | - | - | - | 20 | - | - | |
| | | $LO_2$ | | 6 | < 1 + - | - | - | - | - | 90 | - | - | |
| | | Freon | Cooling | 9 | - | - | - | - | - | 275 | - | - | |
| Lunar Transfer Crew Module | 4-8 | $LN_2$, $LO_2$, $H_2O$ | Environmental Control | 20-80 days | - | - | - | - | - | - | - | - | Ref. 3, p. 150, p. 227 |

## 1.2 TWO-PHASE FLOW PERFORMANCE PARAMETERS

In the technoligical applications presented in the previous section, the applications can be divided into cryogenic and non-cryogenic. The non-cryogenic applications primarily involve a heat exchange fluid loop. Cryogenics involve the flow for fluid transfer as well as lower flows for heat exchanger/cooling applications. The fluids include helium, hydrogen, argon, nitrogen, oxygen, xenon, Freons, water, ammonia and liquid metals.

Most flow passages will be of circular-cross section and made of aluminum or stainless steel. Line lengths will be in excess of 100 meters for some of the future applications such as propellant depots.

A list of the parameters for the applications cited in Section 1.1 are presented in Table 1-6.

## 1.3 ROLE OF TWO-PHASE FLOW IN THESE APPLICATIONS

Propulsion applications constitute the major volume application of two-phase flow. The flow of propellants through warm lines during initial flow conditions requires the analysis of two-phase flow heat transfer. The resupply of propellants in space

Table 1-6. Application Ranges of Two-Phase Flow Correlation Parameters

| | | |
|---|---|---|
| Line Size, D | 0.3 - 15 cm | (0.11 - 6 in) |
| Mass Velocity, G | 1 - 12000 $kg/m^2$-sec | (737-8.85×$10^6$ $lb_m/ft^2$-hr) |
| Aspect Ratio, L/D | 20 - 10000 | |
| Pressure, P | 1 - 400 $kN/m^2$ | (0.14 - 60 psia) |
| Gravity Level, $g/g_o$ | 5 to $10^{-8}$ | |
| Reynolds No., $Re_\ell$ | 1000 - 3.6 × $10^6$ | |
| Nusselt No., $Nu_\ell$ | 1 - 5000 | |
| Prandtl No., $Pr_\ell$ | 0.5 - 2.15 | |
| Froude No., $Fr_\ell$ | 1 × $10^6$ - 4 × $10^9$ | |
| Heat Flux, q | $10^3$ - 4 × $10^5$ watts/$m^2$ | (315 - 1.3 × $10^5$ Btu/hr $ft^2$) |
| Viscosity, $\mu_\ell$ | 0.029·$10^{-4}$-1.35×$10^{-4}$ N·s/$m^2$ | (6×$10^{-8}$-28×$10^{-8}$ lbf-sec/$ft^2$) |
| Viscosity, $\mu_g$ | 0.012×$10^{-4}$-0.06×$10^{-4}$ N·s/$m^2$ | (2.5×$10^{-8}$-12×$10^{-8}$ lbf-sec/$ft^2$) |
| Density, $\rho_\ell$ | 0.067 - 1.36 gm/$cm^3$ | (4.2 - 85 $lb_m/ft^3$) |
| Density, $\rho_g$ | 0.0018-0.012 gm/$cm^3$ | (0.30 - 0.75 $lb_m/ft^3$) |

similarily involves initially warm lines for cryogenic transfer applications. Recent concepts to process fluids in space to produce cryogenic $H_2$ and $O_2$ involves broad application of heat exchange design. Storage techniques for cryogens in space involve vent systems with heat exchangers operating in low-g; vapor-cooled shields are another thermal protection system where two-phase flow occurs. Both pressure drop and heat transfer data are of importance in these applications. Providing the thermal control for a cryogenic environment for instruments aboard spacecraft involves the design of heat exchangers where two phase flow is occurring. A major application will arise in Rankine power generation systems in the high volume heat exchange systems involved.

The experimental support requirements for Spacelab and Space Station operations may well lead to application of a larger system in space than may be apparent from the data presented. The fuel cell used to supply power for the automated furnace, automated levitation, and some bio-processing may be more extensively used since output requirements will grow as these space processing/manufacturing facilities become commercially utilized. The cryogenics used for detectors cooling may also be more extensively used as longer duration viewing times are desired, further reduction in internal noise is purused, or the sensing of longer wavelength or far infrared is attempted.

## 1.4 TIMELINESS OF PROPOSED RESEARCH

The timing of when the identified programs, vehicles, and experiments will take place cannot be stated with certainty; however, some insight as to occurrence of these activities may be gained from Figure 1-1 which reflects NASA thinking (References 16, 17 and 18) and from Figure 1-2 which shows NASA near-term planning (Reference 19). Sortie flights (experiments) and automated spacecraft flights will occur in the near-term, and a low earth orbit (LEO) space station during this near-term is also envisioned. OTV usage, electric propulsion, orbital propellant transfer, initial space manufacturing, and solar power satellite (SPS) development is anticipated for the mid-term (Phase II). The far-term is envisioned to provide commercial solar power, space industrialization, and lunar operations. Thus, it is essential that the two-phase flow experiment be given high priority in the Spacelab experimental program to obtain the results in the early 1980's in order to support the applications in the remainder of that decade.

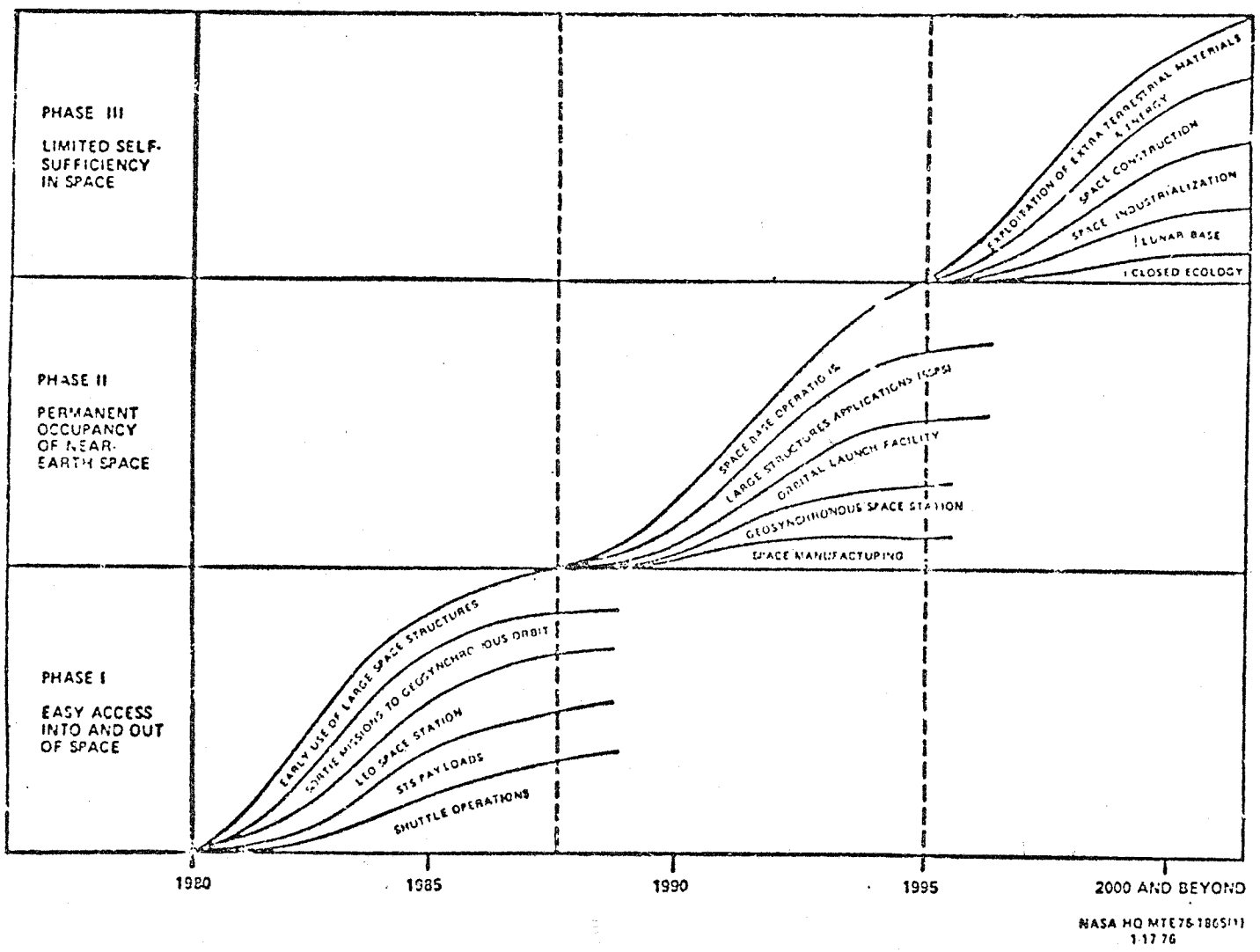


Figure 1-1. Man's Progress in Space Technological Development (Ref. 16)

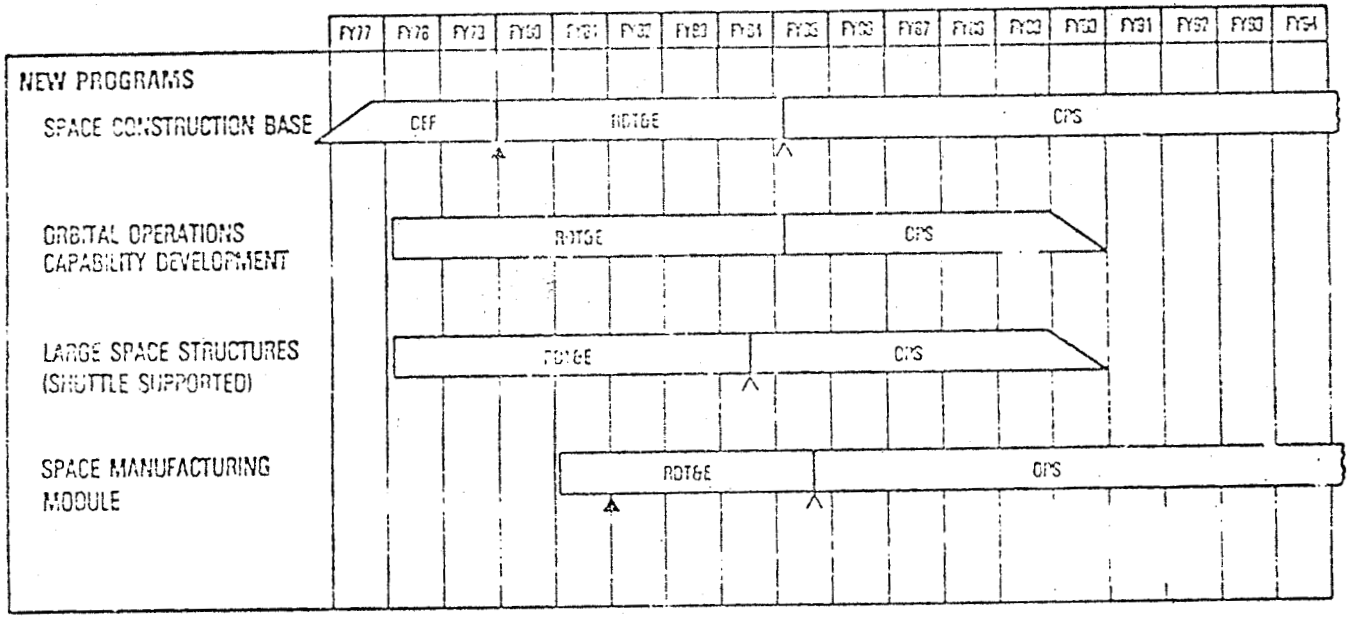


▲ Development Initiation

Λ Initial Operational Capability

| | |
|---|---|
| DEF | Definition Phase |
| RDT&E | Research, Development, Test and Evaluation Phase |
| OPS | Operations Phase |

Figure 1-2. Industrialization of Space Program Schedule (Ref. 19)

# 2

# SCIENTIFIC JUSTIFICATION

This study has determined that a scientific justification for experimentation in space exists in three specific areas of two-phase flow phenomena: flow regime definition, pressure drop, and flow boiling heat transfer. In each specific area, the status of existing correlations were examined and any indication of gravity-sensitivity was noted.

The physical process of two-phase flow is dominated by the gravity field; moreover specific regimes such as stratified flow or sedimentation exist solely because of the gravity field. It will be very interesting to approach the definition of this flow phenomena in the absence of a major variable such as gravity. The opportunity exists to achieve a better understanding of the mechanisms which influence the process. Preliminary work has shown regimes to be sensitive to gravity, however additional data is required to complete the assessment.

## 2.1 LOW GRAVITY EFFECTS ON TWO-PHASE FLOW REGIME BOUNDARIES

2.1.1 EXPERIMENTAL BACKGROUND IN REDUCED-GRAVITY. Earlier investigations by General Dynamics Convair (Ref. 20) showed analytically that for flow regime boundaries based on Froude number, a boundary shift could be calculated for any gravity level other than $g = g_o$ (normal earth gravity). The predicted shifts were expressed on coordinates of total mass velocity versus quality for gravity levels changing from $g = g_o$ to $g = 10^{-2}\ g_o$, and for boundaries corresponding to the Quandt classification zones I: pressure-gradient dominated (includes bubble and dispersed flows); II: gravity dominated with significant frictional drag, $Fr > 2/f$ (includes annular and wave flows); III: gravity dominated with minimal friction, $Fr < 2/f$ (includes plug, slug and stratified flows), where f is the friction factor for the liquid phase. Verification of the predicted shifts was pursued through two-phase flow experiments which were performed in a ground-based laboratory and then repeated aboard a KC-135 which was flown in "zero-g" trajectories. Experiment results showed that flow regime boundary shifts with reduced gravity were in the direction predicted but not to the extent expected. Figures 2-1a shows the location of $g = g_o$ boundaries and the predicted location of $g = 10^{-2}\ g_o$ boundaries. Figure 2-1b shows these same boundaries together with experimental results for $g = g_o$, and Figure 2-1c shows the data taken at a gravity level of approximately $g = 10^{-2}\ g_o$. The $g \quad g_o$ data points are seen to generally conform with $g \quad g_o$ boundaries, but the low gravity data points do not fall within the predicted $g = 10^{-2}\ g_o$ boundaries, i.e., the observed shift in the data was less than the predicted boundary shift. Limitations of the experiment such as time in reduced-gravity and test section length precluded precise resolution of this discrepancy.

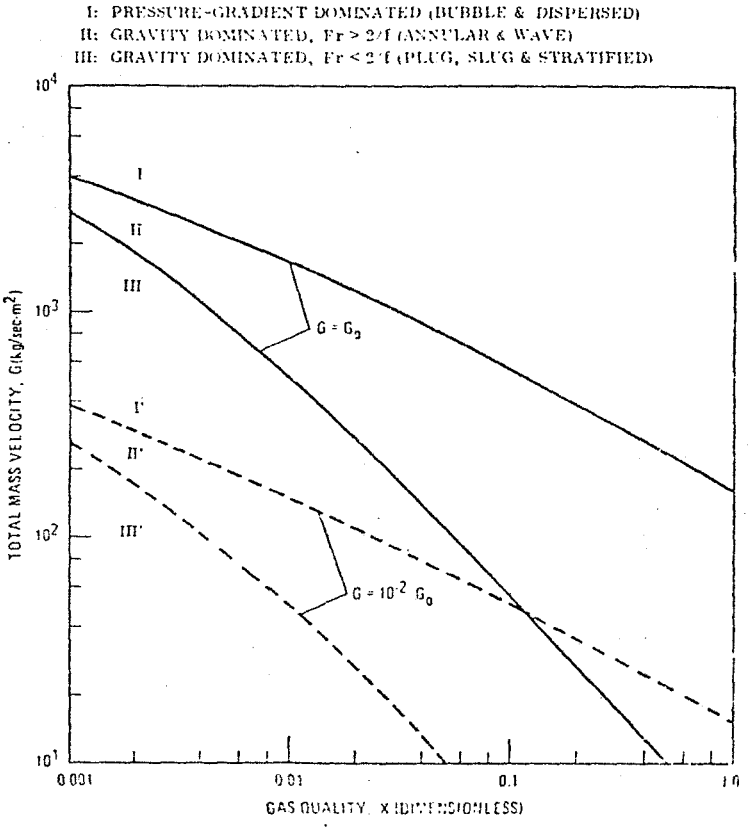


Figure 2-1a. Flow Regime Predicted Boundary Shift

2.1.2 EXISTING CORRELATIONS IN ONE-G. A literature review on the subject of flow regime definition has been pursued. The results, which are summarized in Table 2-1, revealed three approaches other than Quandt's in which the Froude number was a parameter, namely those of Kozlov, Haberstroh and Griffith, and Moissis. The same analytical method referred to in the General Dynamics Convair work was applied to each of the three approaches to derive boundary shifts with change from $g = g_o$ to $g = 10^{-2} g_o$. Data from the General Dynamics Convair laboratory experiments was then plotted against the $g = g_o$ boundaries and data from the aircraft flight experiments was plotted against the $g = 10^{-2} g_o$ boundaries.

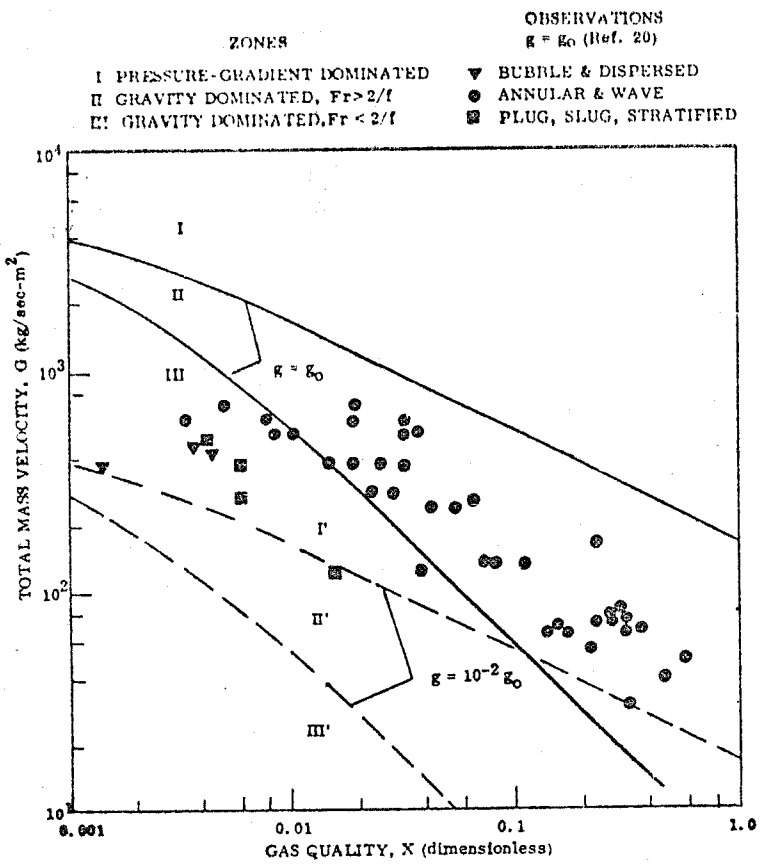


Figure 2-1b. Flow Regime Boundaries Segregate One-g Data at Higher Qualities

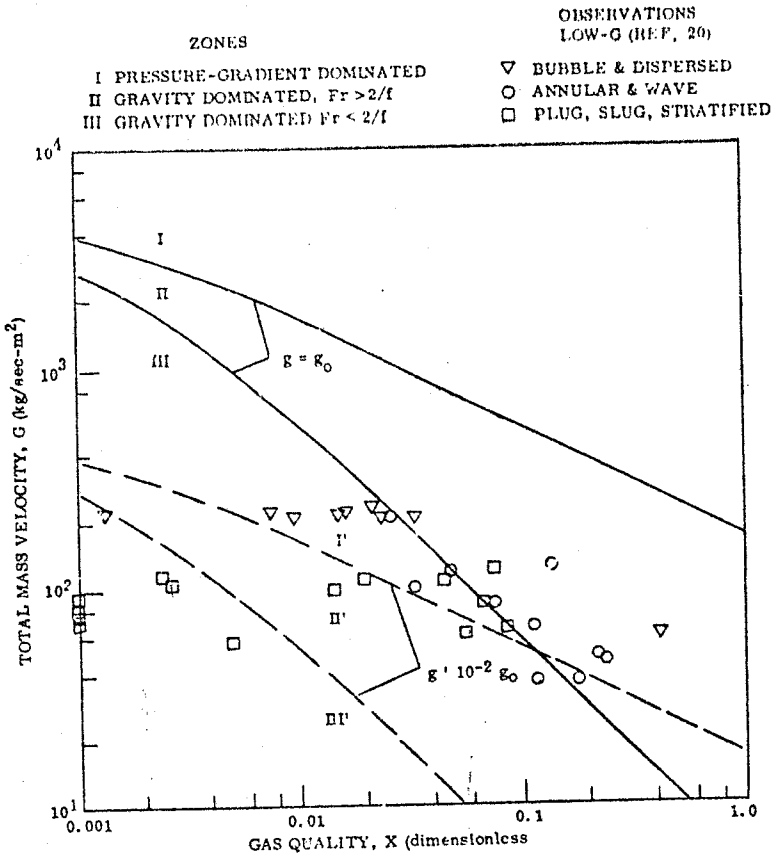


Figure 2-1c. Flow Regime Observed Boundary Shift Was Less Than Predicted: Reduced-Gravity Data

## Table 2-1. Flow Regime Definition Summary

| Work Cited & Approach | Fluids, Processes | Results | Discussion of Gravity Effects |
|---|---|---|---|
| Hubbard/Dukler,[21] power spectral density distribution for wall pressure fluctuations was calculated and verified with all regimes except froth. | Horizontal, air/water in 1-1/2 I.D. | 0 to $\zeta$ is bandwidth containing 68% of total energy:<br>$\zeta < 1$ Hz — Separated flow<br>0.1 Hz $< \zeta <$ 1.5 Hz — Transition<br>1.5 Hz $< \zeta$ — Dispersed flow<br>Also, for a bandwidth of $\pm \varepsilon$ around a mean frequency, containing 68% of energy; and with $\beta_L = Q_L/(Q_L + Q_V)$, then<br>$\varepsilon/\beta_L < 11$ — Intermittent flow<br>$11 < \varepsilon/\beta_L < 100$ — Transition<br>$100 < \varepsilon/\beta_L$ — Dispersed flow | The approach does not show any frequency shift (hence regime boundary shift) related to changes in gravity level. |
| Baker,[21] flow pattern map. Takes into account the fluid properties. Empirical graphical correlation from experimental data. | Air/water, adiabatic. Gas/oil. Horizontal. | Ordinate $G_g/\lambda$, abscissa $G_L \lambda \psi/G_g$<br>$\lambda = \left[\left(\frac{\rho_g}{0.075}\right)\left(\frac{\sigma_L}{\sigma 2.3}\right)\right]^{1/2}$<br>$\psi = \left[\frac{0.005}{\sigma}\right]\left[\left(\frac{\mu}{2.42}\right)\left(\frac{62.3}{\rho_L}\right)^2\right]^{1/3}$ | Empirical. All Results for normal earth gravity. No term for gravity sensitivity. |
| Bergles and Suo,[21] flow pattern map. Combined transition criteria of other investigators. | Steam/water, 500-1000 psia, saturated. | Ordinate $G_g$, abscissa X. | Empirical. Results are for normal earth gravity. |
| Kozlov. Later Griffith & Wallis,[21] Froude no. criteria for flow regime boundaries. Empirical and experimental. | Air/water, 1 atm Adiabatic. Pipe dia.: 0.5 in. to 2.34 in. | $\beta = Q_g/(Q_L+Q_g)$, Fr $\frac{[(Q_L + Q_g)/A_p]^2}{g D_p}$<br>Boundaries:<br>Bubble-plug — $\beta = 0.05\ (Fr)^{0.2}$<br>Plug-dispersed plug — $\beta = 0.12\ (Fr)^{0.15}$<br>Dispersed plug-emulsion — $\beta = 0.5\ (Fr)^{0.1}$<br>Emulsion-film emulsion — $\beta = 0.65\ (Fr)^{0.05}$<br>Film emulsion-drop — $\beta = 0.85\ (Fr)^{0.02}$ | Empirical. Assumes that all regime transitions are dictated by the same pair of flow parameters. Froude no. changes with change in g will cause boundary shift. Flow patterns do not readily relate to Baker regimes. |
| Quandt,[21] dimensional analysis. Flows classified as press. gradient controlled, gravity controlled, and surface tension controlled. | Air/water, others. 1 atm, adiabatic. | Boundaries:<br>Dispersed-annular $Fr > \frac{2}{f_{TP}}\left[\frac{\rho_L}{\rho_g} - \cos\theta\right]$<br>Slug-annular $Fr = \frac{u^2}{gD_e} < \frac{2}{f}$ | Froude no change with change in g will cause boundary shift. This was background for GDC experiments flown aboard KC-135. |
| Radovcich and Moissis,[21] transition from bubbly to slug flow is function of $\ell_c$, $D_b$, and $\alpha$. Experimental and empirical effort. | $N_2$/water. Bubble collision/coalescence transition mechanics. | Time for collision/coalescence to form cap bubble is:<br>$t = \frac{0.206}{P_{co}} \frac{D_b}{\bar{c}} \frac{(1+f)^2}{f}\left[\frac{D_p}{D_b}\right]^3\left[\left(\frac{0.74}{\alpha}\right)^{\frac{1}{3}} - 1\right]^5$ | Transition time is sensitive to void fraction. Long times imply incomplete transition in short tubes. No gravity sensitivity. |
| Haberstroh & Griffith,[21] transition between slug and annular regimes. Experimental effort with empirical correlations. | Air/water, steam/water, air/water & alcohol, air/water & glycerine, $CO_2$/water. Adiabatic | Tests showed $0.8 < \alpha < 0.9$ at transition. By force balance:<br>$u_g^+ = \alpha u_{gl}^+ = \left[\frac{2.5}{2 f_i}(1+\alpha) + \frac{f_s \alpha^{2.5}}{f_i (1-\alpha)^2} u_L^{+2}\right]^{1/2}$<br>$u_g^+ = \frac{u_{gs}}{[(\rho_L/\rho_g) g D]^{\frac{1}{2}}}$, $u_{gl}^+ = \frac{u_{gl}}{[(\rho_L/\rho_g) g D]^{\frac{1}{2}}}$,<br>$u_L^+ = \frac{u_{Ls}}{[(\rho_L/\rho_g) g D]^{\frac{1}{2}}} = [Fr_{Ls} (\rho_g/\rho_L)]^{\frac{1}{2}}$ | Dimensionless velocities $u^+$ contain gravity term. Therefore boundary will shift with change in g. Ordinate $\alpha$, abscissa $u_L^+$. Empirical correlation between $u_g^+$ and $u_L^+$. Correlation approach lacks gravity discrimination. |
| Wallis,[21] transition between annular and dispersed annular. Experimental and empirical. | Not reported | Ordinate $\tau$ entrainment, abscissa is<br>$\tau_2 = \frac{u_g \mu_g}{\sigma}\left[\frac{\rho_g}{\rho_L}\right]^{\frac{1}{2}}$ where $\tau_2 = 2.46 \times 10^{-4}$<br>at onset of entrainment. | Empirical correlation of data. Results are for normal earth gravity. No gravity sensitivity. |
| Moissis,[21] transition between slug and homogeneous fog and froth. Experimental with theoretical development. | Air/water, 1" D tube, 1 atm. press. vertical pipes. | Ordinate $\beta_g$, gas volumetric flow rate fraction; abscissa is Fr. Boundaries are a function of $L_b$, critical bubble length. | Fair agreement with Griffith & Wallis empirical results. Froude no. change with change in g will cause boundary shift. |
| Hall-Taylor & Hewitt,[22] annular flow pattern. | Air/water. 1-1/4" D vertical tube, 15 psia | Ordinate $W_g$, abscissa $W_f$. Boundaries of six subdivisions of annular flow. | No g effects. Parameters chosen are inadequate for boundary definition. |

a. Kozlov Criteria (Ref. 21). The boundaries given are:

| | | Quandt Classification Zones |
|---|---|---|
| Film emulsion-drop | $\beta = 0.85\ Fr^{0.02}$ | II - I |
| Emulsion-film emulsion | $\beta = 0.65\ Fr^{0.05}$ | I - II |
| Dispersed plug-emulsion | $\beta = 0.50\ Fr^{0.1}$ | III - I |
| Plug-dispersed plug | $\beta = 0.12\ Fr^{0.15}$ | III - III |
| Bubble-plug | $\beta = 0.05\ Fr^{0.2}$ | I - III |

where

$$\beta = \frac{Q_g}{Q_\ell + Q_g}$$

$$Fr = \frac{[(Q_\ell + Q_g)/A_p]^2}{gD_p}$$

The above boundaries are plotted in Figure 2-2a for $g = g_o$ and in Figure 2-2b for $g = 10^{-2}\ g_o$. Also plotted in the respective figures are some of the experimental results by General Dynamics Convair as referred to in Section 2.1.1 above. The above criteria are related to the Quandt classification zones with the provision that the dispersed plug flow is a transition phase to slug flow and remains in zone III. The emulsion flow resembles bubble flow of zone I while the film emulsion resembles the annular flow of zone II.

There does not appear to be any correlation between the Kozlov patterns and the experimental data as referenced to Quandt classification zones. However, a boundary shift is qualitatively confirmed by positions of the experimental data points. The foregoing suggests that the Kozlov coordinate parameters are useful for depicting flow regime boundary shifts, but the validity of the boundary definitions does not appear to be correct.

b. Haberstroh and Griffith Criteria (Ref. 21). A published boundary between annular and slug flow regimes was replotted in Figure 2-3a and 2-3b, along with the shifted boundary at $g = 10^{-2}\ g_o$. The coordinates are void fraction, $\alpha$, versus dimensionless liquid velocity $u_\ell^+$, where

$$u_\ell^+ = \frac{u_{\ell s}}{[(\rho_\ell/\rho_g)\ gD]^{1/2}} = [Fr_{\ell s}\ (\rho_g/\rho_\ell)]^{1/2}$$

and $Fr_{\ell s}$ is a Froude number based on superficial liquid velocity. Superficial liquid velocity is obtained by dividing the liquid volumetric flow rate, $Q_\ell$, by the total

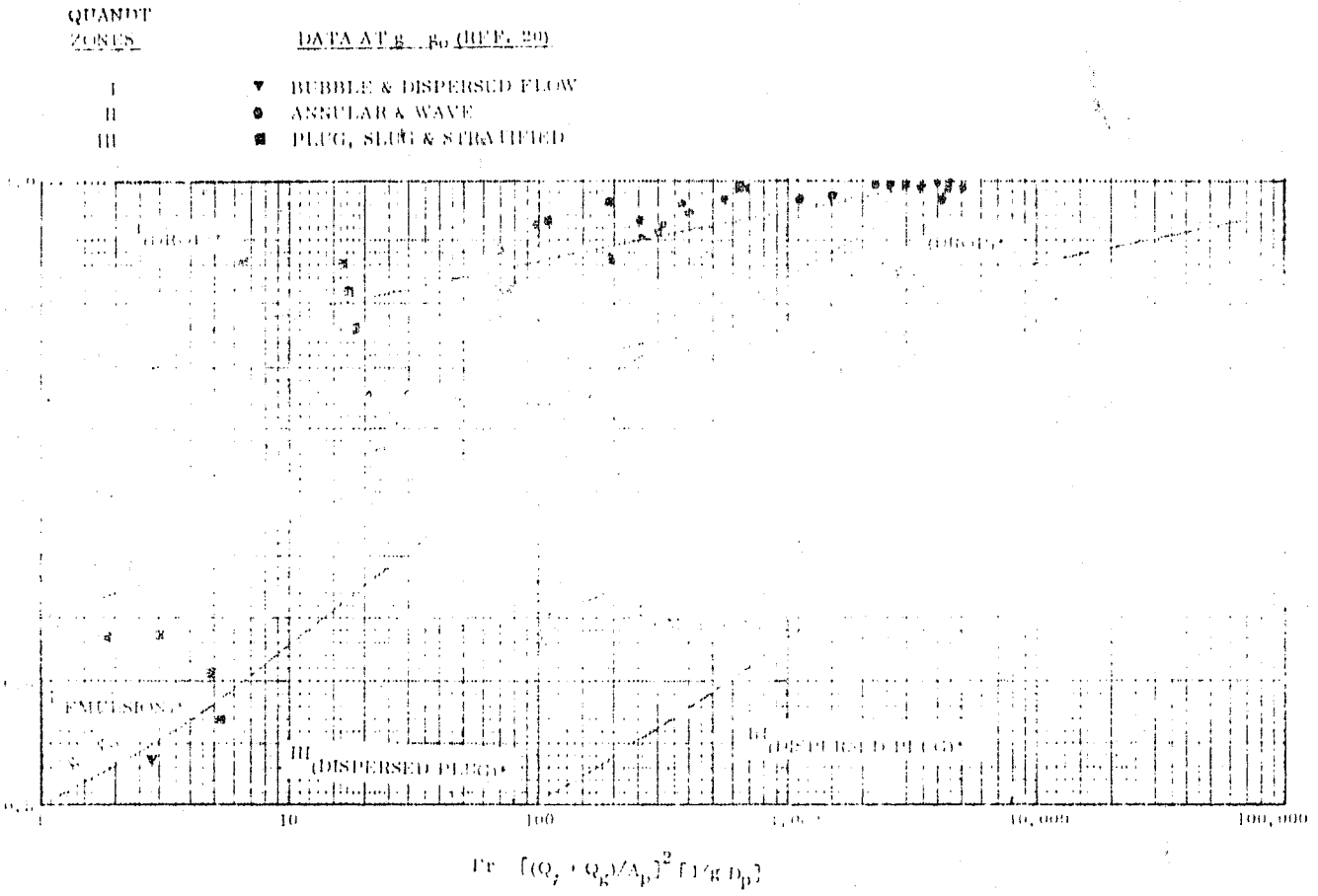


*Kozlov Classifications

Figure 2-2a. Kozlov Flow Regime Boundaries With One-G Data

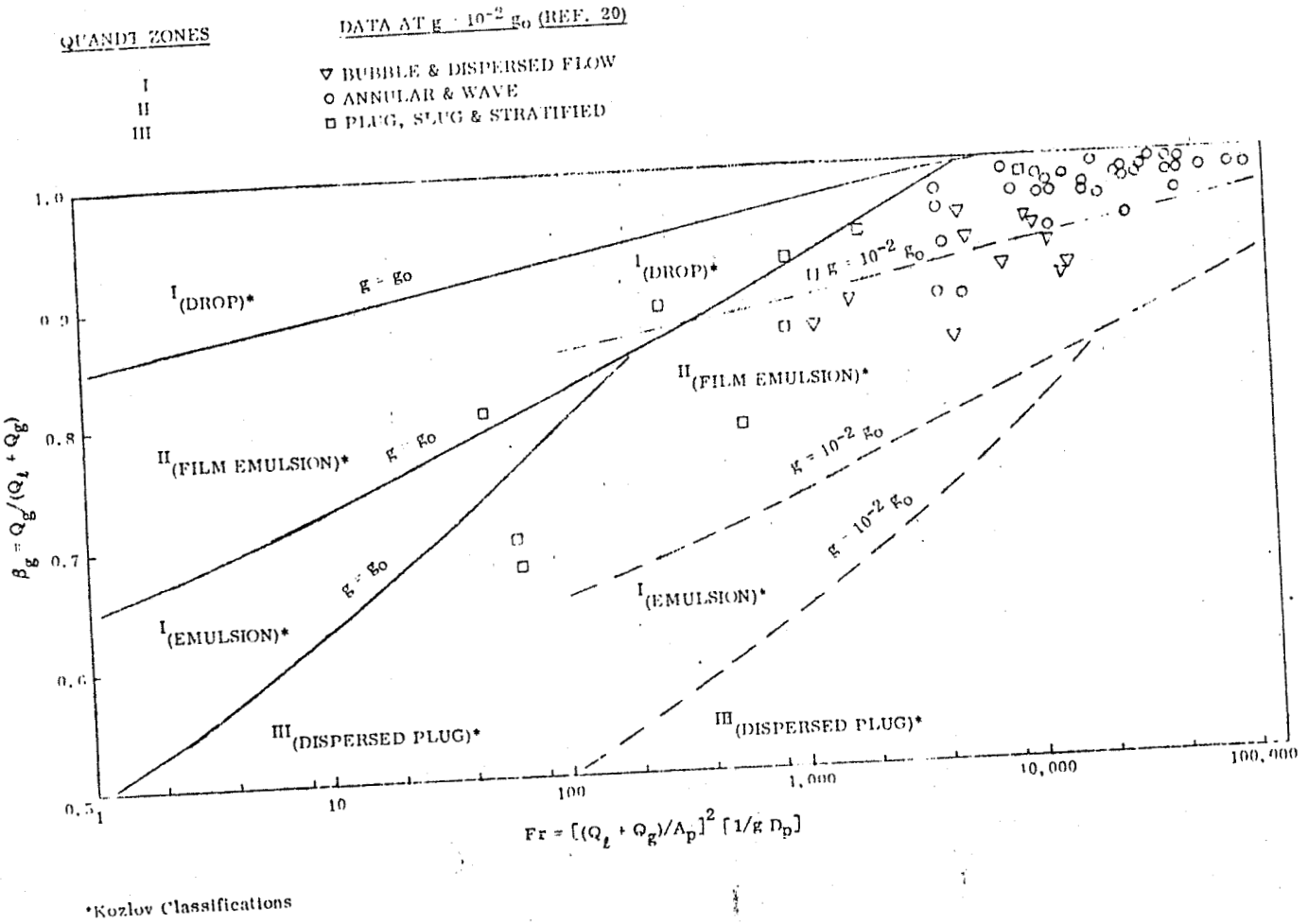


Figure 2-2b. Kozlov Flow Regime Boundaries With Reduced Gravity Data

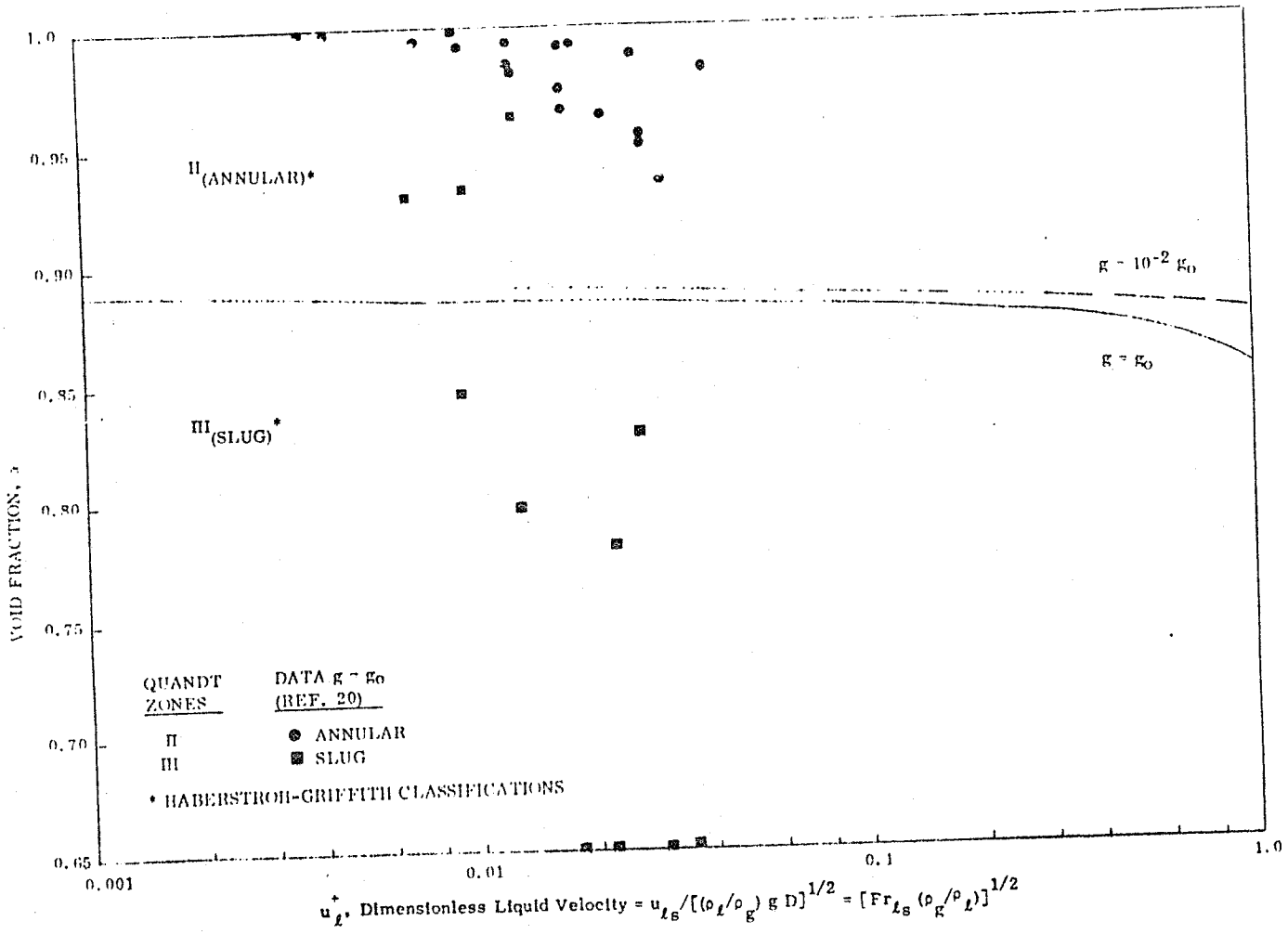


Figure 2-3a. Haberstroh-Griffith Flow Transition Boundaries are Gravity Insensitive: One-g Data

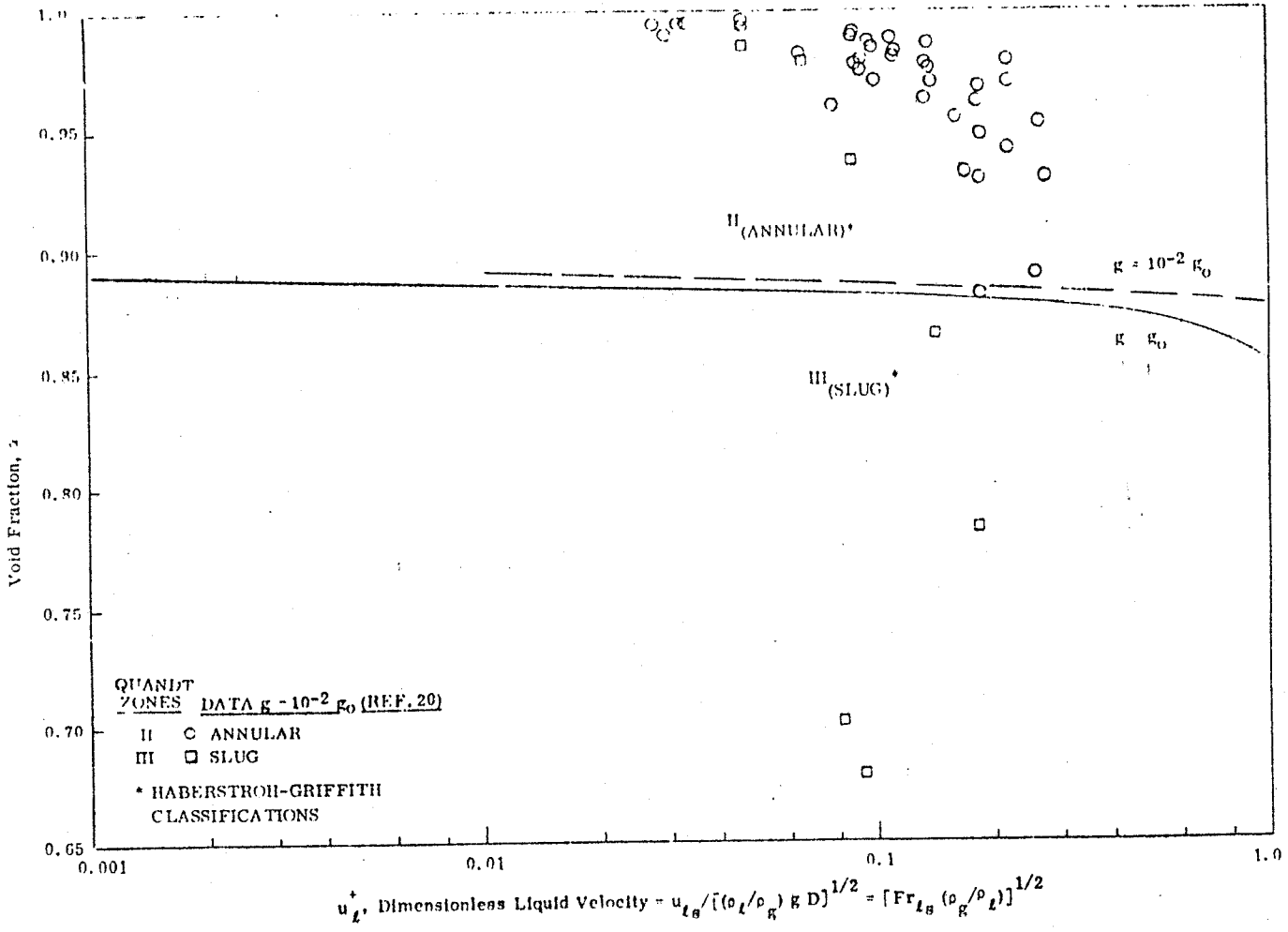


Figure 2-3b. Haberstroh-Griffith Flow Transition Boundaries are Gravity Insensitive: Reduced-Gravity Data

cross-sectional area of the channel. The near zero slope of the boundary suggested by Haberstroh and Griffith causes the boundary shift due to gravity field to be almost indistinguishable. The data points plotted are annular and slug at one-g and reduced-gravity from Reference 20. Local void fraction, $\alpha$, was not available from experimental data, so the points are plotted at a test section average $\alpha$ which is equal to $\beta$, the gas volumetric flow rate fraction. TheHaberstroh-Griffith boundaries approximate a separation of experimentally-determined annular and slug flow patterns, but are not effective in prediction of the $g = g_o$ to $g = 10^{-2}\ g_o$ shift.

c. Moissis Criteria (Ref. 21). A plot of $\beta$ versus Fr based on the criteria developed by Moissis results in ten curves which in effect represent a rather wide zone for the transition from slug to froth flow regimes. Only the centerline of this zone was replotted in Figure 2-4a and 2-4b. The shift of this boundary at $g = 10^{-2}\ g_o$ is also shown. The data points plotted are for bubble flow, which may be interpreted as equivalent to froth, and for slug flow. It is apparent from the plots that the Moissis correlation approach reflects the gravity sensitivity of the data; however, his regime boundaries do not clearly distinguish between the observed slug and bubble flow data.

d. Summary. Any attempt to correlate the fluid and flow parameters with boundaries between regimes is subject to a number of limitations, including the following:

1. A two-dimensional map may represent only two parameters, whereas a transition may be influenced by several more.

2. The same pair of parameters does not dictate all of the transitions between the several regimes.

3. Transitions occur over a zone, rather than a line boundary, and the zones of two kinds of transition may overlap.

4. Experiments have had limitations on scale and time and in the number of fluids employed.

5. Experimentally-produced flow patterns often appear to contain elements of two or more regimes, which necessitates subjective identification of the dominant regime.

Allowing for the limitations named, the work to date confirms the existence of a gravity-level shift of flow regime boundaries which are based on Froude number. However, the magnitude and nature of the changes caused by gravity have not been determined and require the long term test environment that a space experiment can provide.

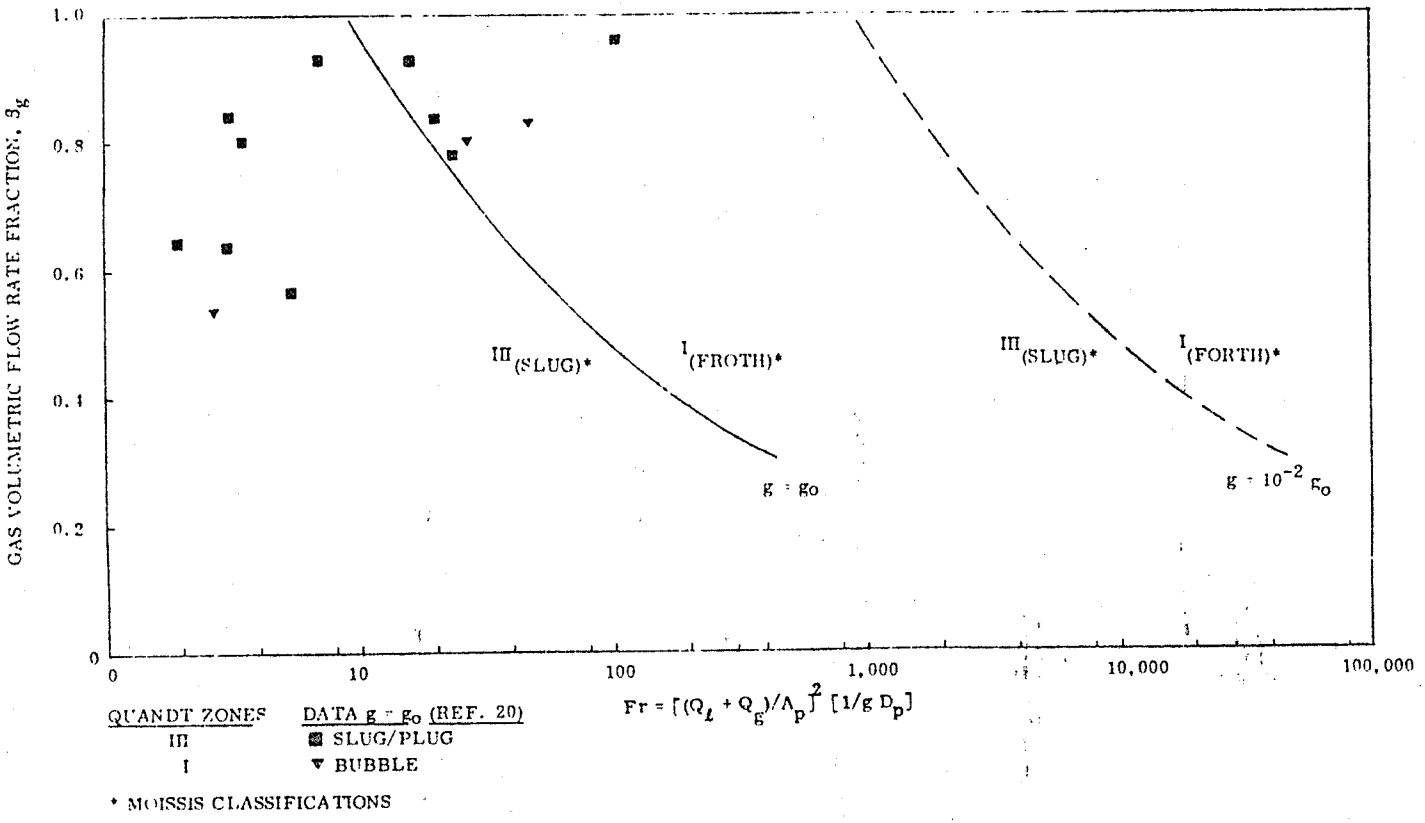


Figure 2-4a. Moissis Flow Transition Shows High Gravity Resolution and Fair Regime Definition: One-g Data

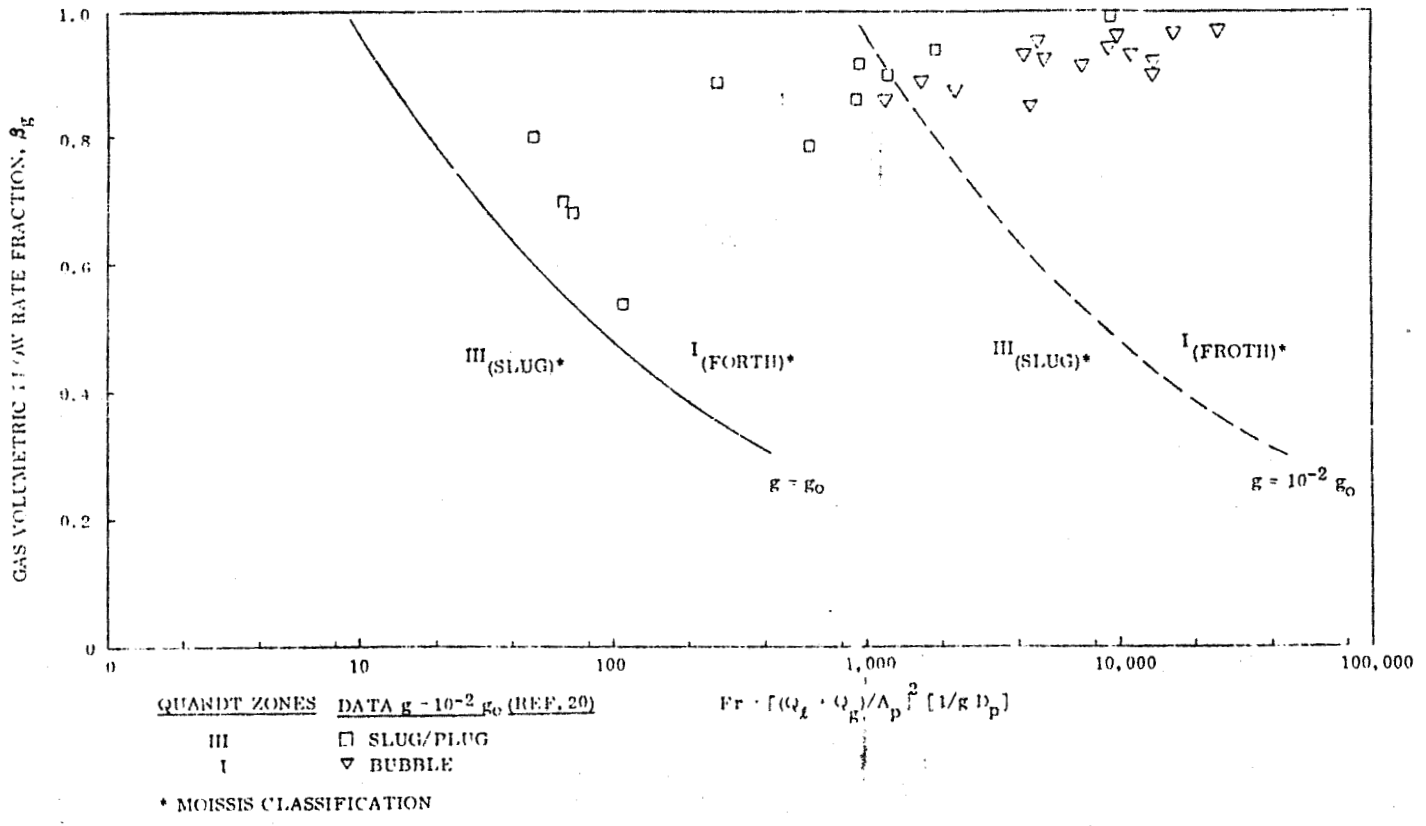


Figure 2-4b. Moissis Flow Transition Shows High Gravity Resolution and Fair Regime Definition: Reduced-Gravity Data

## 2.2 LOW GRAVITY EFFECTS ON PRESSURE DROP IN TWO-PHASE FLOW

In a literature survey addressed to the pressure drop in a flowing liquid/gas mixture, particular attention was given to approaches which included gravity effects. Reference 20 reports $\Delta P$ measurements in low-g (approximately $10^{-2}$ g) which were compared directly with measurement in $g = g_o$ for water/air mixtures flowing in a straight, horizontal, circular channel. For the same fluid and flow parameters, the low-g $\Delta P$ was higher than in $g = g_o$ by a factor of about 1.5 (Figure 2-5). Since it has been demonstrated that low-g had induced changes in flow regime, the higher $\Delta P$ was attributed to such change in flow regime.

An application of two-phase flow occurred in the Skylab shower waste water plumbing. It consisted of a water/air pickup head and a flexible hose which was connected from the pickup to a mechanical liquid/gas separator. Flight evaluation of the shower system (Reference 23) reported that pickup efficiency was poor, shower stall cleanup was very time consuming, and higher air flows would be required to improve performance. Reference 23 does not indicate whether this portion of the flight hardware had any instrumentation for $\Delta P$ measurements, however, the observations are consistent with the experiments conducted to date.

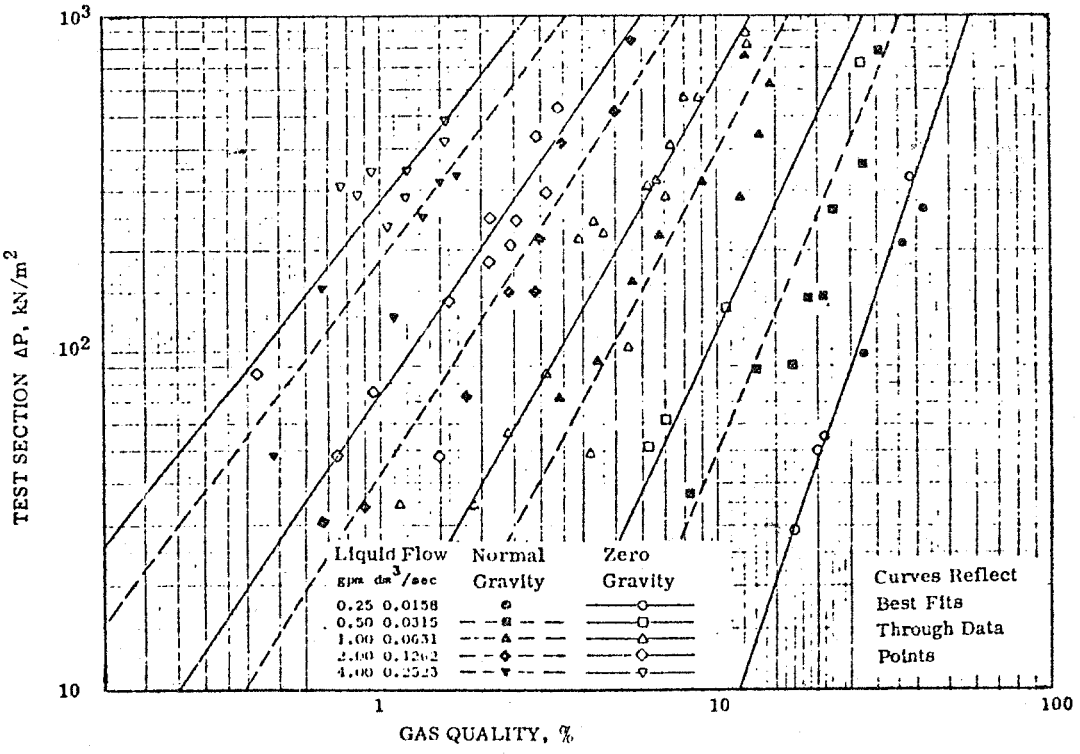


ORIGINAL PAGE IS
OF POOR QUALITY

Figure 2-5. Pressure Drop, Zero Gravity and Normal Gravity

A summary of the literature survey is shown in Table 2-2. Analytical development of pressure drop equations is typically based on energy, continuity, and momentum equations, and leads to dp/dz expressed as the sum of gravitational, accelerational, and frictional terms. The gravitational term is significant only for vertical or inclined piping in $g = g_o$, as it becomes zero for horizontal piping in $g = g_o$ or any piping in zero g. Thus the low-g case has a superficial similarity to horizontal flow in $g = g_o$, but equal pressure drops cannot be assumed. As stated previously differences in flow regime have an effect on pressure drop as well,so that changes in flow regime in low gravity should change the pressure drop.

## 2.3 LOW GRAVITY EFFECTS ON FLOW BOILING HEAT TRANSFER

Boiling is affected by the acceleration field as indicated in Reference 21. One effect is on the criterion for the incipient threshold of nucleate boiling. It is dependent on the thermal layer thickness which is proportional to $(a/g)^{-1/3}$ to $(a/g)^{-1/4}$. The thinner thermal layer requires a higher delta temperature for activating the nucleation site. Hsu and Graham (Ref. 21) report, although not with the concurrence of all investigators, that the mechanisms for nucleate boiling are considered to be inertia dominated including bubble evolution, thus implying that nucleate boiling phenomena is not significantly influenced by reduced-gravity. For the critical heat flux, investigators report it proportional to $(a/g)^{-1/3}$ and experimental data by Merte and Clark (Ref. 25) have verified the decrease in this value for $LN_2$. Lienhard (Ref. 26) suggests that the nucleate boiling region may vanish and can be replaced by a monotonic line in reduced-gravity fields. Merte (Ref. 27) confirms the gravity dependence of the heat flux in reduced-gravity in the film boiling regime. It is obvious that agreement on the effect of gravity on boiling does not exist today.

In flow boiling, reduced-gravity has been demonstrated (Ref. 21) to influence the flow regime through a reduction in buoyancy forces, which in turn modifies the heat transfer performance. Efforts in flow-boiling at reduced-gravity have been primarily qualitative in nature.

In an effort to determine existing correlation forms for the several conditions of heat transfer regions which sequentially occur in the flow-boiling process, the literature summarized by Collier (Ref. 28) was reviewed. In Figure 2-6 from Collier, the heat transfer regions are depicted with the two-phase regimes. The following paragraphs and Table 2-3 present the correlation forms for the various heat transfer conditions.

A partial subcooled boiling region exists, region B in Figure 2-6, where the heat flux is commonly expressed as the sum of the contributions of forced convection single-phase liquid heat transfer and subcooled pool-boiling heat transfer, $\phi = \phi_{SPL} + \phi_{SCB}$ The Dittus-Boelter equation is widely accepted for the former contribution and unique pool-boiling correlations are offered for the latter from the pool-boiling literature. Bowring's work is considered the most detailed for design.

Table 2-2. Pressure Drop Definition Summary

| Work Cited and Approach | Fluids, Processes | Correlations and Results | Discussion of Gravity Effects |
|---|---|---|---|
| Owens.[21] Assumes uniform homogeneous mixture (bubbly flow and dry-wall mist flow). Empirical. | Adiabatic. Friction loss only. Air-water and boiling water. | Two-phase $\Delta P$ related to $\Delta P$ for all liquid flow. For $f_{TP} \approx f_\ell$ $\left.\frac{dp}{dz}\right\|_{TP,f} = f_\ell \frac{G^2 v}{2Dg_c}$, where $v$ = specific vol. | Low g favors uniform mixing. Empirical basis for $f_{TP} = f_\ell$. No gravity effects. |
| Govier, Radford and Dunn[21] Experimental and empirical, effects of regimes on dP/dx. | Adiabatic, air/water. | Plot shows $\Delta P$ is irregular function of flow pattern and liquid/gas volume fraction. | Empirical. Data does not enable display solely of flow pattern effects. Since flow pattern is g-sensitive, therefore $\Delta P$ is g-sensitive. |
| Bankoff.[21] Radial distribution in void is modelled. Mixture treated as single phase flow using synthetic $\rho$ and $\mu$. Applicable to dispersed flow patterns. | Adiabatic. Air/water and steam/water K parameter correlations. | Based on Blasius equation. $\frac{\tau}{\tau_\ell} = \left[1 - \bar{\alpha}\left(1 - \frac{\rho_v}{\rho_\ell}\right)\right]^{3/4}\left[1 - X\left(1 - \frac{\rho_\ell}{\rho_v}\right)\right]^{7/4}$ where $X = \left[\left(1 - \frac{\rho_\ell}{\rho_v}\right) + \frac{\rho_\ell K}{\rho_v \bar{\alpha}}\right]^{-1}$ and several empirical correlations of K are available. | Good match with experimental data is reported. There is no modelling of gravity effects. |
| Levy.[21] Mixing length Model. Experimental. | Adiabatic. Homogeneous, steam/water | Tabular presentation of parameters including friction factors, shear stress, densities, Re. | No modelling of gravity effects. |
| Martinelli, et al.[21] Equal static pressure drops of liquid and gas phases. $(dp/dz)_{TP}$ is found by relationship with pressure drop of either phase as if it flowed alone. Exper. and emptrical. | Adiabatic. Various two-component mixtures. Parallel coexistence of liquid flow and vapor flow. Low pressures. Oil/air, horizontal pipes. | For both phases turbulent (TT), $(dp/dz)_{TP}/(dp/dz)_g = \phi^2_{TT,g}$, where $\phi_{TT,g}$ is correlated as a function of $X_{TT} = (\mu_\ell/\mu_g)^{0.111}(\rho_g/\rho_\ell)^{0.555}(w_\ell/w_g)$ | Similar correlations were given for TL, LT, and both phases laminar LL, and for ratio of two-phase pressure drop to liquid-phase pressure drop. No modelling of gravity effects. |
| Martinelli & Nelson.[21] Above method extended by interpolating between low pressure and critical pt. Exper. and empirical. | High pressure, water-steam mixtures, other single component mix. | Parameters, $\phi_{\ell,TT}$ and $\sqrt{X_{TT}}$ as a function of pressure. | Independent of gravity. |
| Levy.[21] Simplified approximation of pressure drop ratio. Empirical | Not restricted to any one fluid. | $\frac{(dp/dz)_{TP}}{(dp/dz)_\ell} = \frac{1}{(1-\alpha)^2}$ | Pressure drop can be integrated if $\alpha$ is known as a function of Z. No gravity sensitivity. |
| Chien and Ibele.[21] Modification of Martinelli correlation for other flow domains. Empirical correlations. | Annular and annular mist regimes. | Annular: $\phi^2_g = 3.885 \times 10^{-6} Re_{gp}^{0.71} Re_{\ell p}^{0.725}$ Annular Mist: $\phi^2_g = 3.425\, Re_{gp}^{-0.34} Re_{\ell p}^{0.517}$ | No modelling of gravity effects, but boundaries between regimes are g-sensitive. |
| Baroczy.[21] Modifications of Martinelli correlation for flow rates, qualities, and fluid properties. Experimental and empirical. | Water-air, water-stream, Hg-$N_2$, liquid metals, organic oils. | Correlations of $\phi$ with parameters depending on G, x, and a "properties index." Extensive verification of Martinelli approach. | No gravity parameter involved. |

Table 2-2. Pressure Drop Definition Summary (Continued)

| Work Cited and Approach | Fluids, Processes | Results | Discussion of Gravity Effects |
|---|---|---|---|
| Brown and Govier.[21] Slug flow pressure drop attributed to liquid only, neglecting gas phase $\Delta P$. Empirical. | Slug flow. Vertical flow. | $(\Delta P/\Delta Z)_{TP} = (\Delta P/\Delta Z)_{\ell,m}\,(1 - C_A\,\alpha)$, where $C_A$ ranges from 1.1 for low-viscosity fluids to 1.4 for highly viscous fluids. | Requires knowledge that regime will be slug flow. Regime is subject to gravity effects. |
| Hughmark[21] Empirical correlation. Extensive data correlation | Slug flow. Horizontal flow. | $\left[\frac{\Delta P}{\Delta Z}\right]_{TP} = \frac{2f\,\bar{u}_\ell^{\,2}}{g_c\,D}$, $\bar{u}_\ell = \frac{W_\ell}{A\,\rho_\ell\,(1-\alpha)}$ where f is friction factor at $Re = D\bar{u}\,\rho_\ell/\mu_\ell$. | Requires knowledge of regime, which is g-sensitive. |
| Continuity, energy and momentum equations. One-dimensional homogeneous equilibrium flow.[22] Theoretical. | Steady flow, any two-phase mixture. | Expression for dp/dz in which the only empirical factor is $C_f$, the homogeneous friction factor. | Gravity term, $g\cos\theta/(v_1 + v_2)$, will vary with variable g. |
| McAdams,[22] homogeneous viscosity. Empir. | Laminar flow, gas/liquid. | $1/\mu = (x/\mu_g) + [(1-x)/\mu_f]$ (an averaging model) | $\mu$ used in Re which is related to $C_f$. Gravity insensitive. |
| Cicchitti,[22] homogeneous viscosity. Empir. | Laminar flow, gas/liquid. | $\mu = x\,\mu_g + (1-x)\,\mu_f$ (an averaging model) | $\mu$ used in Re which is related to $C_f$. Gravity insensitive. |
| Dukler,[22] homogeneous viscosity. Empirical. | Laminar flow, gas/liquid. | $\mu = (J_f/J)\,\mu_f + (J_g/J)\,\mu_g$ (an averaging model) | $\mu$ used in Re which is related to $C_f$. Gravity insensitive. |
| "Rule of Thumb,"[22] Empirical. | Turbulent flow. | $C_f = 0.005$ | Accuracy within factor of 2, relative to measurements. Gravity insensitive. |
| McAdams, et al; also Owens.[22] $C_f$ calculated from an equivalent single phase flow. Experimental and empirical. | Turbulent flow. Water/steam 0.118 in I.D. and 30-in long. Horizontal. | $\frac{-(dp/dz)_F}{-(dp/dz)_{Fo}} = 1 + X\left[\frac{\rho_f}{\rho_g} - 1\right]$ where subscript fo denotes case that liquid flow in same pipe with same mass velocity as the combined flows. | Accuracy about +10%/-30% relative to measurements Gravity insensitive. |
| Blasius equation[22] Experimental correlation. | Turbulent flow, smooth pipe. | $C_f = 0.079\,Re^{-0.25}$ | Expression for equivalent $\mu$ used to determine Re. Gravity insensitive. |
| Continuity, energy, and momentum equations with time-dependent terms (unsteady flow).[22] Basic theoretical developments. | Evaporator, negligible pressure changes and viscous dissipation. | $X(t,t_o) = v_f/v_{fg}\,(e^{\Omega(t-t_o)} - 1)$ where $\Omega = \frac{4\,v_{fg}\,\varphi}{D\,h_{fg}}$ and $\varphi$ = wall heat flux | Applicable to horizontal tube. Requires identification of $t_o$, the time when a liquid particle starts to evaporate. Gravity insensitive. |
| $\Delta P$ measurements, horizontal pipe with 90° bends, tees, valves, expansions, contractions.[24] Experimental with empirical correlations. | Water/steam, X = 0 to 21%, p = 800 to 1600 psia. G = (1 to 2) × $10^6$ lb/hr-ft$^2$. | Straight pipe: Fair correlation with Levy momentum exchange model. Bends: Ratio of two-phase to single-phase $\Delta P$ was different for various bend radii. Diameter changes: two-phase to single-phase $\Delta P$ ratios same for expansion and contractions and same as straight-pipe ratios. | Negligible gravity forces in test configuration. Experiment hardware design provided L/D ratios of 3 to 89 to promote recovery from upstream disturbances. |

Table 2-3. Heat Transfer Definition Summary

| Work Cited and Approach | Fluids, Processes | Correlations and Results | Discussion of Gravity Effects |
|---|---|---|---|
| Dittus[28]-Boelter. Standard for forced convective heat transfer in a tube, used for convective portion of superposition. Empirical. | Water, forced convective boiling single phase. Heating in vertical upflow, Re > 10000. | $\frac{h_{fo}D}{k_f} = 0.023\left[\frac{GD}{\mu_f}\right]^{.8}\left[\frac{C_p\mu}{k}\right]_f^{1/3}$ | Forced convection effects dominate gravity. Turbulent $GD/\mu > 10,000$, $L/D > 50$ |
| Bowring[28] Superposition of convective and nucleate boiling. Experimental plus empirical correlation. | Steam 0 to 140 atm<br>q,0 to 200 W/cm$^2$<br>u,0 to 200 cm/sec<br>Subcooled boiling | $q = q_{SPL} + q_{SCB}$<br>$q_{SPL} = h_{fo}\left[T_{SAT} - T_f(Z)\right]$<br>for $T_{SAT} \le T_w \le T_{FDB}$<br>for $T_w > T_{FDB}$, $q_{SPL} = 0$<br>$q_{SCB} = 1/\psi\left[(T_w)_{SCB} - T_{SAT}\right]^{1/n}$<br>$n = 0.25$ to $0.5$, $\psi$ = f (prop.) | Gravity effects not considered. |
| Rohsenow[28] Superposition of convective and nucleate boiling. Experimental with empirical correlation. | Water, subcooled boiling | $q = q_{SPL} + q_{SCB}$<br>$q_{SPL} = h_{fo}\left[T_w - T_f(Z)\right]$<br>$\frac{C_p\Delta T_{SAT}}{i_{fg}} = C_{sf}\left[\frac{q_{SCB}}{\mu_f i_{fg}}\sqrt{\frac{\sigma}{g(\rho_f-\rho_g)}}\right]^{.33}\left[\frac{C_p\mu_f}{k_f}\right]^{1.7}$<br>where $C_{sf} = 0.006 \rightarrow 0.020$ | Gravity effects not considered. |
| Bergles and Rosehow[28] Superposition of convective and nucleate boiling. Experimental with empirical correlation. | Water, 15-2000 psia.<br>Subcooled boiling. | As above except<br>$q = q_{SPL}\left[1 + \left(\frac{q_{SCB}}{q_{SPL}}\left(1 + \frac{q_{c''}}{q_{SCB}}\right)\right)^2\right]^{1/2}$<br>$q_{c''}$ defined from $q_{ONB}$ on curve $q_{SCB}$<br>$q_{ONB} = 15.60\,p^{1.156}(\Delta T_{SAT})_{ONB}^{(2.30/p^{.0234})}$ | Gravity effects not considered. |
| Thom[28]. Modification to the work of Jennes and Lottes. | Water only. Fully developed subcooled boiling. | $\Delta T_{SAT} = 22.65\,q^{.5}\,e^{-p/87}$<br>$\Delta T$ °C, q MW/m$^2$, p in bars | Gravity effects not considered. |
| Dengler and Addoms[28]. Vertical tube saturated boiling. Exper. and emp. | Water, annular flow, saturated nucleate boiling. | $h_{TP} = h_L\,3.5\,F_{DA}\,(1-X)^{-.8}\,(x_{tt})^{-.5}$ | Gravity effects not considered. |
| Macbeth[28]. Empirical correlation. | Water, low mass velocity region. | $q_{crit} = A - \frac{B}{i_{fg}}\left[\frac{4q_{crit}Z}{DG} - (\Delta i_{SUB})\right]$ | Gravity effects not considered. |
| Thompson and Macbeth[28]. Empirical correlation. | Water, high mass velocity region | $q_{crit} = \frac{A + DG\,(\Delta i_{SUB})}{C + Z}$<br>where A and C fcn (G, D, p) | Gravity effects not considered. |
| Swenson[28]. Empirical correlation. Exp. eval. of wall temperature profiles in saturated nucleate boiling. | High pressure steam water, liquid deficient region | $\frac{h_c D}{k} = 0.023\left[\frac{GD}{\mu_g}\left[X + \frac{\nu_f}{\nu_g}(1-X)\right]\right]^{.8}\left[\frac{C_p\mu}{k}\right]^{.8} Y$<br>where $Y = 1 - .1\left[\frac{\nu_g}{\nu_f} - 1\right]^{.4}\left[1 - X\right]^{.4}$ | Gravity effects not considered. |

Table 2-3. Heat Transfer Definition Summary (Continued)

| Work Cited and Approach | Fluids, Processes | Correlations and Results | Discussion of Gravity Effects |
|---|---|---|---|
| Hughmark.[21] Experimental correlation for horizontal tube – slug flow. | Air-water, air-oil, gas-oil; turbulent and laminar. Horizontal slug flow. | $(26,000 < Re_\ell < 4,500,000)$<br>$\frac{h_{TP}}{(C\rho u)_\ell} = \frac{f_\ell}{2q}$ $\qquad u_\ell = \frac{w_\ell}{\rho_\ell A(1-\alpha)}$<br>$f_\ell = \frac{(\Delta P_{TP}/\Delta L)\, g_c D}{2 u_\ell^2 \rho_\ell} = f(Du_\ell \rho_\ell/\mu_\ell)$<br>$1600 < Re_\ell < 4600$<br>$\frac{h_{TP} D \sqrt{1-\alpha}}{k_\ell} = 1.75 \left[\frac{w_\ell C_\ell}{(1-\alpha) k_\ell L}\right]\left[\frac{\mu}{\mu_w}\right]^{.14}$ | Although derived for two-component systems, applicable to single component system where mean void fraction obtained from quality. Independent of gravity except for slug regime identification. |
| McNelly[21] and Lavin and Young[21] correlated early-phase annular flow (Nucleate Boiling). | Annular flow. Part. nuc. boil. | $Nu = 0.225 \left[\frac{q\,De}{\mu\lambda}\right]^{.69}\left[\frac{C\mu}{k}\right]^{.67}\left[\frac{\rho_\ell}{\rho_v}\right]^{.31}\left[\frac{p\,D_e}{c}\right]^{.31}$ | No gravity effects. Restricted to apply to early annular flow regime. |
| Bennett[21] correlation for annular flow, uses Martinelli parameter and $h_{s\ell}$. Experimental. | Steam-water. Annular flow. Saturated nuc. boil. | $h_{TP} = h_{s\ell} \cdot 0.64\, q^{.11} (\chi_{tt})^{.74}$<br>q in BTU/hr ft$^2$ | Bubbles do not burst film. Mechanism convection and eddy diffusivity in liquid. No gravity effects. |
| Collier and Pulling[21] introduce a boiling number for two-phase annular flow. | Steam-water. Annular flow. Saturated nuc. boil. | $h = h_{s\ell} \cdot 6700 \left[\frac{q}{h_{fg} G} + 0.00035 (\chi_{tt})^{.66}\right]$<br>nucl. boiling number; forced conv. evaporation | No gravity effects; error derv. ± 30%. Combines nucleate boiling and forced conv. evaporation. |
| Chen[21] used superposition principle for boiling and forced convection effects in annular flow. Experimental effort with empirical correlations. | Water, benzene, pentane, heptane. Annular flow. Saturated nuc. boil. | $h = h_{\text{boil conv.}} + h_{\text{flow conv.}}$<br>$h_{bc} = .00122 \left[\frac{k_\ell^{.79} C_{p_\ell}^{.45} \rho_\ell^{.49} g_c^{.25}}{\sigma^{.25} \mu_\ell^{.29} h_{fg}^{.24} \rho_v^{.24}}\right] \Delta T^{.24} \Delta P^{.75} S$<br>$h_{fc} = .023 (Re_\ell)^{.8} (Pr_\ell)^{.4} \frac{k_\ell}{D} F$<br>where $F = F(1/\chi_{tt}) = (Re/Re_\ell)^{.8}$ and<br>$S = (Re_\ell \cdot F^{1.25})$<br>where $\frac{1}{\chi_{tt}} = \left[\frac{X}{1-X}\right]^{.9}\left[\frac{\rho_\ell}{\rho_v}\right]^{.5}\left[\frac{\mu_v}{\mu_\ell}\right]^{.1}$ | Range of data to qualities of 71% are correlated within ± 10%. No consideration is given to gravity effects. |
| Bennett[21] for film boiling regime with dry-wall mist flow. Experimental with empirical correlation. | Steam-water. Film boiling. Mist flow. | $\frac{hD_e}{k_\ell} = .0157 \left[\frac{D_e u_v \rho_v}{\mu_\ell}\right]^{.84} Pr_\ell^{1/3} \left[\frac{L}{D}\right]^{-.04} \quad 6 < \frac{L}{D} < 60$<br>$\frac{hD_e}{k_\ell} = .0133 \left[\frac{D_e u_v \rho_v}{\mu_\ell}\right]^{.84} Pr_\ell^{1/3} \quad \frac{L}{D} > 60$ | Impinging droplet evaporation neglected. Gravity effects not considered. |
| Merte and Clark[21] confirm Noyes[21] correlation for $(q/A)_{max}$ from $10^{-2}$ to 1 g for nucleate boiling. | $LN_2$ boiling from sphere. Pool boiling. | $(q/A)_{max} = .144\, h_{fg} \rho_v^{1/2} \left[\frac{(\rho_\ell - \rho_v)^2}{\rho_\ell} g g_o \sigma\right]^{1/4}$<br>$\times Pr^{-.245} (a/g)^{.25}$ | Authors add gravity effect to a 1-g correlation of Zuber (Noyes modif.), verify over two-fold change a/g. |

It is generally accepted that the correlation for the fully-developed forced-convection nucleate pool-boiling regions, C and D, can be established as an extrapolation of the pool-boiling curve. This suggests that the form of the equation from fully-developed pool boiling will be valid for flow boiling in a modified form. The pool-boiling curve thus is extended to higher delta temperatures and higher heat fluxes.

The transition to the forced convection pool boiling region is smooth and the form of the correlations for subcooling boiling are retained where $T_f$ is now replaced by $T_{SAT}$.

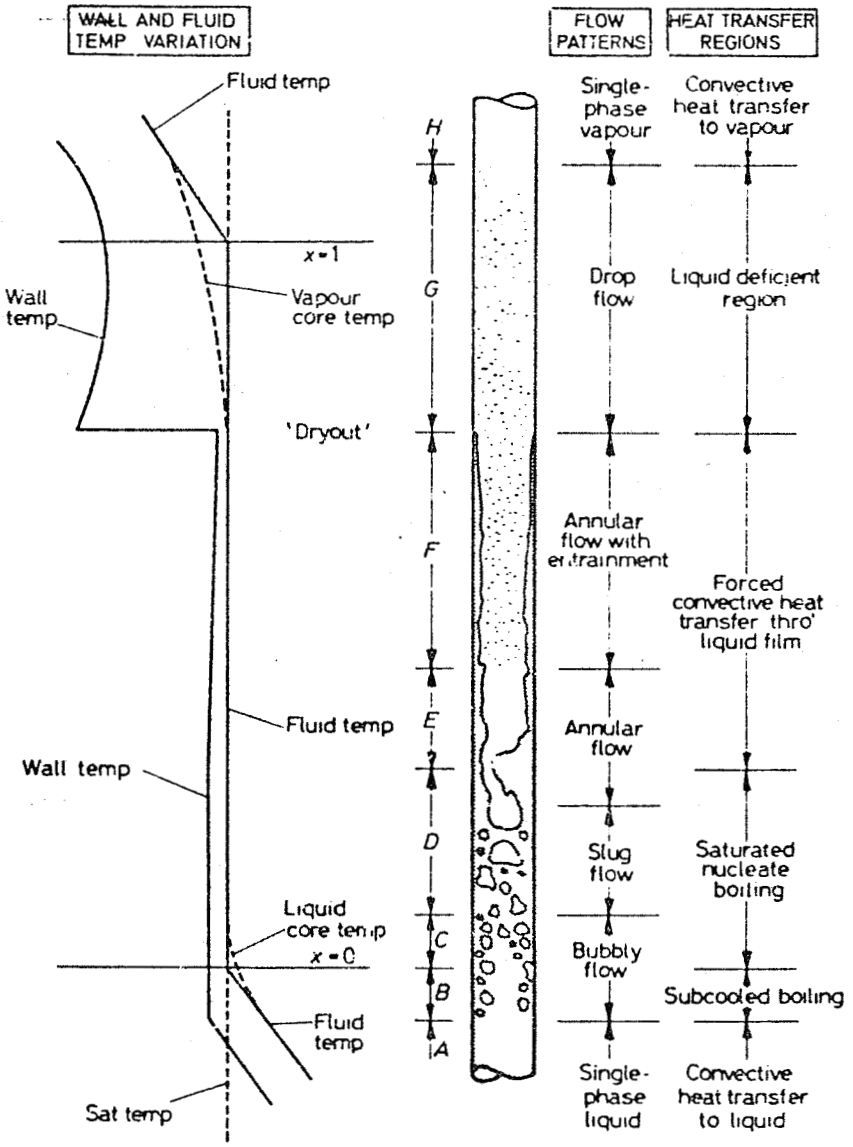


Figure 2-6. Heat Transfer Regions and Flow Regimes Progressively Change in Two-Phase Flow Forced Convection Boiling (From Collier, Ref. 28)

Correlations in this region are independent of mass quality and mass velocity. The condition of constant $\Delta T_{SAT}$ leads to a constant heat transfer coefficient.

The forced convection nucleate boiling region evolves to a two-phase forced convective region, E and F, as boiling continues and quality increases. Dengler and Addoms, Bennett and others offer correlations for the two-phase heat transfer coefficient $h_{TP}$ as a function of the liquid phase heat transfer coefficient $h_L$ and Martinelli's $\chi_{tt}$ turbulent factor.

Continuing the superposition principle clearly into the two-phase forced convective region (predominantly annular flow), the heat transfer coefficient is defined $h_{TP} = h_{NCB} + h_c$ by Chen (Table 2-3).

As heat flux increases in the nucleate boiling regions, B, C and D, and the generation of vapor increases, a critical heat flux regime may be reached. The nucleate boiling phenomena is inadequate to satisfy the existing wall heat flux. In the two-phase forced convective regions, E and F, the attainment of the critical heat flux coincides with "dry out" or the start of the liquid deficient region, G. Both empirical, Macbeth, and phenomenological approaches have been taken to correlate data in these regions. Separate correlations are offered for the low mass velocity region ($G < 5 \times 10^5$ lb/hr $ft^2$) and the high mass velocity region.

One of the merits of the proposed experiment lies in the opportunity to identify flow regimes in the reduced-gravity environment and confirm the applicability or non-applicability of the heat transfer correlations for each region.

## 2.4 PAST EXPERIMENTAL LIMITATIONS

Prior evaluation of gravity-effects on two-phase fluid flow has been limited by the inability to achieve adequate duration in reduced-gravity. The heat transfer process does not stabilize in a flowing system in the time period available in aircraft or drop tower tests. In one-g, rotation of the tube axis through 90° has lead to different flow regime and heat transfer performance but has done little to explain the anticipated performance in reduced gravity. Aircraft tests have been the most productive in verifying a sensitivity to gravity level; however time limitations and the level of the acceleration field were both unsatisfactory for heat transfer analysis. Drop tower tests, although providing the true low-gravity field, are limited in both time duration and size. Thus, the Spacelab environment will afford the first opportunity to examine the two-phase heat transfer process at two controlled gravity levels.

# 3

# SPACELAB EXPERIMENT CONCEPTUAL DESIGN

Having established technological and scientific needs for an orbital experiment to collect engineering data for two-phase fluid behavior, this section defines a conceptual experiment for Spacelab to achieve this end. The objectives for combined regime definition, pressure drop and heat transfer experiments are outlined. An experimental apparatus is described which uses the fluids water and Freon. The data to be collected is described and the experimental procedures are discussed. Finally, the costs to develop this experiment for Spacelab were determined.

## 3.1 OBJECTIVES

3.1.1 FLOW REGIME/PRESSURE DROP EXPERIMENT. The predicted shift of two-phase adiabatic flow regime boundaries with change from 1-g to a low-g environment was discussed in Section 2. Previous measurements of this shift were handicapped by brief duration of low-g available aboard an aircraft. An objective of this experiment is to determine flow regime boundaries for an environment of sustained near zero-g, as is characteristic of space flight. The sustained environment will provide steady-state data. Further, the range of flow parameters should encompass the complete range of flow regimes at both 1-g and near zero-g. Then the boundaries at 1-g and near zero-g can be compared so as to provide a reliable definition of the boundary shift.

Another objective is to relate two-phase frictional pressure drop to the influence of gravity. There is limited experimental evidence that frictional pressure drop increases with reduced-gravity due to changes in flow regime. A sustained low-g environment will enable a more reliable definition of this pressure drop increase.

3.1.2 FLOW BOILING EXPERIMENT. The objective of the heat transfer experiment is two-fold: to establish modified one-g correlations applicable to the reduced gravity environment and to develop insight into the mechanisms of heat transfer in the absence of gravity. Current correlations depend on contributions of nucleate boiling and forced flow to define the heat transfer process. The magnitude of these individual contributions in reduced gravity must be determined. The heat transfer process for fluid flow takes a long period to reach steady-state so that no suitable test environments have been available to date. The heat transfer is regime dependent therefore it is significant to both define the regimes and collect the heat transfer data in a reduced-gravity environment.

## 3.2 EXPERIMENT HARDWARE CONCEPTS ANALYSIS

The candidate concepts in subsequent discussion are premised on providing hardware for two experiments, namely (a) a "Flow Regime/Pressure Drop Experiment" similar to that reported in Reference 20, and (b) a "Flow Boiling Experiment" in which a single component fluid enters a heated test section either subcooled or at low vapor quality and exits at higher quality. The two experiments, and perhaps others, may share some hardware components where economical and feasible without compromising experiment objectives.

3.2.1 TEST SECTION SIZE. A small diameter tube has obvious advantages in terms of corresponding low flow rates and low mass, volume, and power requirements for the hardware. A limitation on size reduction is inherent in the requirement to visually identify flow patterns. Such identification may be by direct observation or by viewing still or motion pictures. General Dynamics Convair experience (Ref. 20) was that a 2.54 cm (1 inch) diameter flow channel was adequate in size for both direct observation and 16 mm motion pictures. Still photos were not made. It is estimated that the lower limit for direct flow pattern identification without optical aids is about 1 cm diameter. This does not preclude using a magnifier to view flow in a local area, but the value of an optical aid in these circumstances is minimal. Not only would the apparent speed of motion be magnified, but flow pattern identification would be further inhibited by the limited field of view.

Photographic recording is less subject to the restrictions noted above. Still photos can be enlarged several times without significant loss of resolution. Motion pictures can be projected in slow motion and on a screen sized according to viewing distance.

Considering geometric accuracy, larger size has advantages because there will be proportionally less effect from diameter measurement error, roughness measurement error, presence of contaminating particles, or the intrusion of sensors.

A test section L/D of 20 was used for the experiments reported in Reference 20. Observations were that the entrance disturbances could be seen to persist for various distances downstream of the entrance. At the higher flow rates, it appeared that the flow pattern changes were occurring up to the test section exit. It was concluded that an L/D of 20 was too low.

Fitzsimmons (Ref. 24 ) reported the effect of an upstream flow disturbance on pressure drop through a bend which was located 56 diameters straight downstream of the disturbance source. The measured $\Delta P$ was about 1.6 times higher when the flow disturbance was created than when it was not. This result contrasts with single-phase practice in which 15 to 20 diameters is recommended for the "recovery length." Recovery length is the length of straight pipe downstream of a disturbance (tee, bend, valve, orifice, contraction, expansion) for re-establishment of a fully-developed straight pipe flow.

Considering the foregoing, the test section size selected for further conceptual analysis is 1.5 cm (0.6 in) ID by 90 cm (36 in) long, thereby providing an L/D of 60. Although there is the option of different test sections of different sizes for the two experiments, the advantages of less space and more simplicity indicate that a single test section should serve both experiments if feasible.

3.2.2 TEST FLUIDS. The flow regime/pressure drop experiments reported in Reference 20 employed water and air. The more important criteria which supported this selection were safety; the ubiquitous use of both fluids in engineering practice; and the extensive background of ground-based analytical and experimental efforts with this fluid mixture, against which low-g flight results could be compared. Further, the gas being air was readily compatible with an open loop using the aircraft cabin air. These same criteria apply to an experiment aboard Spacelab and lead to the same recommendation.

If there is reason to abandon the concept of using cabin air in an open loop, then $N_2$ is essentially equivalent in meeting all other criteria and has a further advantage of being relatively inert.

Selecting a fluid for the flow boiling experiment also requires consideration of safety and of properties similarity to fluids expected to be used in space applications. Further, because it may be difficult to accurately measure heat exchange with the environment, it is desirable to approach zero heat exchange by operating at near room temperature. This also eliminates time delays for the fluid and apparatus to change from room temperature to operating temperature. A vapor pressure of about one atmosphere at room temperature is desirable to minimize problems of leakage and stress in the test section. A low freezing point may be desirable so that solid does not form in overboard discharge ports if there is overboard discharge.

Water is excellent in many respects, but has a high freezing point and a vapor pressure of only 2.48 $kN/m^2$ (0.36 psi) at room temperature. At such a low pressure and low vapor density, the void fraction, $\alpha$, and the vapor volumetric flow fraction, $\beta$, are very high for a given quality, x. Pressures so low, and void fractions so high, are not typical of expected applications. There is the possibility of operating with water at temperatures near 373K (212F) and a pressure near one atmosphere.

The various halogen compound refrigerant fluids offer a wide range of vapor pressure versus temperature characteristics. Considering safety, they are less desirable than water. Their toxicities range from low to moderate, and their flammabilities range from nonflammable to "capable of forming weakly combustible mixtures with air." Table 3-1 shows some properties of a selected few refrigerants in the range of interest. All have low freezing points. Of those shown, Freon-11 is nearest the desired characteristics discussed above.

Table 3-1. Some Candidate Fluids for Flow Boiling Experiment

| Fluid | | Vapor Pressure @ 294 K (70°F) kN/m² | Vapor Pressure @ 294 K (70°F) psia | Flammability | Toxicity* |
|---|---|---|---|---|---|
| Freon 113 | $CCl_2F\text{-}CClF_2$ | 37.9 | 5.5 | Nonflammable | Between Groups 4 & 5 |
| Freon E-1 | $(CHCF_2O)CBFCF_3$ <br> $\vert$ <br> $CF_3$ | 48.3 | 7.0 | Nonflammable | "Low", undefined |
| Freon 11 | $CCl_3F$ | 93.1 | 13.5 | Nonflammable | TLV** 1000 ppm Group 5a |
| Freon 21 | $CHCl_2F$ | 139 | 23 | Weakly Combustible | TLV = 1000 ppm Between Groups 4 & 5 |
| Freon 114 | $C_2Cl_2F_4$ | 156 | 27 | Nonflammable | Group 6 |

*On a scale of 1 to 6, with 6 least toxic
**Industrial "Threshold Limit Value"

Consideration was given to alcohols, hydrocarbons, and other materials of vapor pressure/temperature characteristics similar to the Freons of Table 3-1. The hydrocarbons and alcohols were rejected for reasons of safety, especially flammability and toxicity. A brief survey of glycols, light oils, various dielectric fluids, expendable coolants, and other refrigerants revealed properties generally less satisfactory than Freon-11. Cryogenics were rejected because of increased experimental complexity in departing from room temperature fluids.

3.2.3 EXPERIMENT OPERATING PARAMETERS.

3.2.3.1 Flow Regime/Pressure Drop Experiment. Figures 3-1 and 3-2 show a proposed range of operating parameters, namely total mass velocity, G, from 10 to 640 kg/sec-m$^2$ (7400 to 472,000 lb/hr-ft$^2$), and gas quality, x, from 0.01 to 0.64. It is desirable that the range of parameters encompass the distributed, segregated, and intermittent flow regimes for both 1-g and low-g operation. However, increasing the range increases the time and resources required to acquire enough data. Also, a preliminary calculation indicates that test section pressure drop will be excessive at combined maximum G and maximum x, and that pressure drop will be acceptable if the operating region omits the shaded area of Figures 3-1 and 3-2. The corresponding limits are then x = 0.16 at G = 640 kg/sec-m$^2$ (472,000 lb/hr-ft$^2$), x = 0.32 at G = 320 kg/sec-m$^2$ (236,000 lb/hr-ft$^2$), and x = 0.64 at G = 160 kg/sec-m$^2$ (118,000 lb/hr ft$^2$). The 46 grid intersections of the operating region represent 46 data points and would require about 16 minutes of operation. In the near zero-g environment of Spacelab the flow regime boundaries are expected to shift more than shown in Figure 3-2 for a $10^{-2}$ g-environment (Ref. 20). If the experiment operator (Payload Specialist) observes that such a shift occurs, he may extend the range by reducing G to a set of values below the matrix of Figure 3-2. To provide for this contingency, the time and resources should allow for about 80 data points.

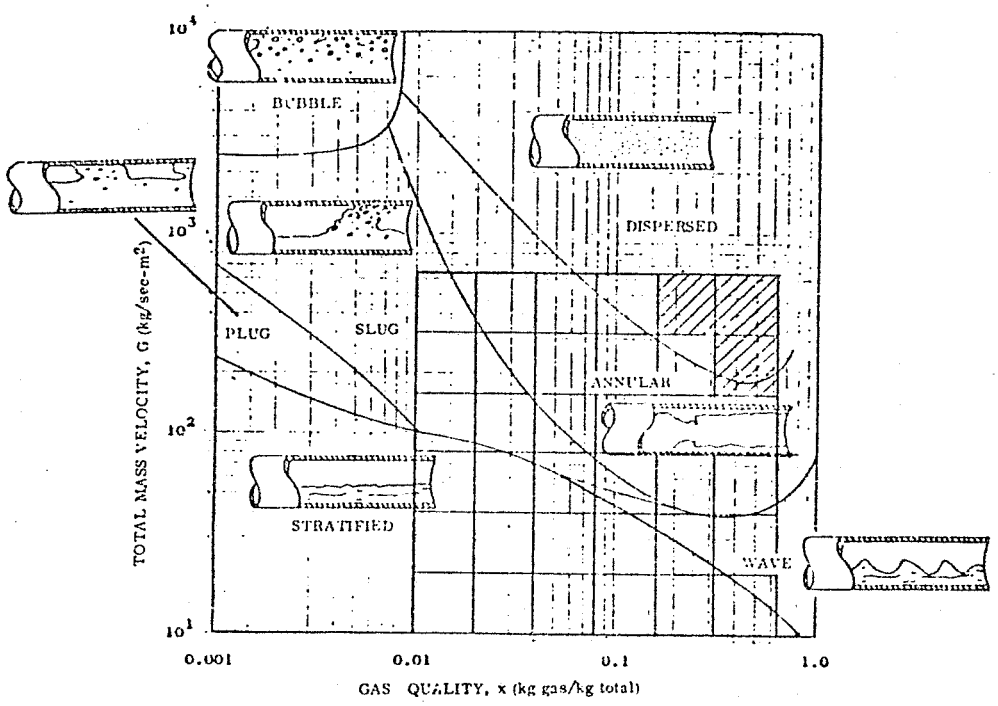


Figure 3-1. Baker Operating Regions, Flow Regime/Pressure Drop Experiment

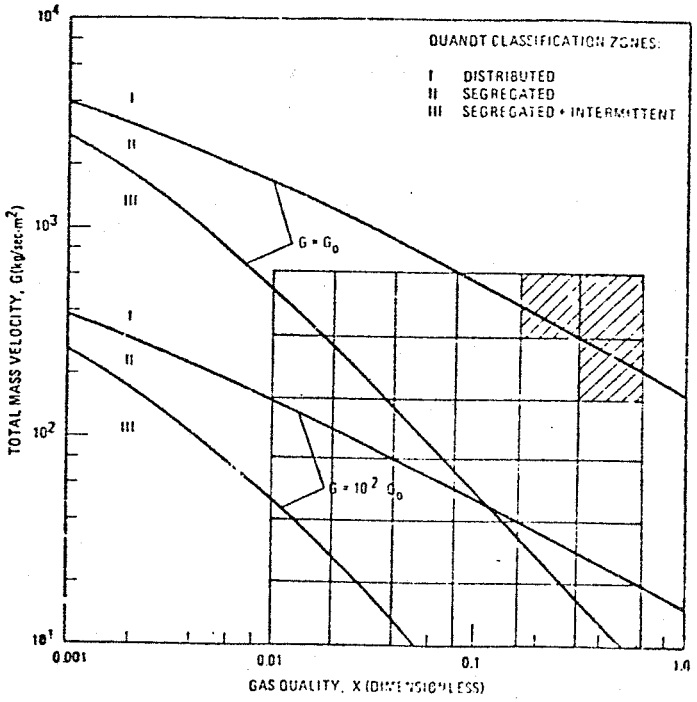


Figure 3-2. Quandt Operating Regions, Flow Regime/Pressure Drop Experiment

3.2.3.2 Flow Boiling Experiment. The operating range for the flow boiling experiment was based on generally the same criteria expressed for the flow regimes/pressure drop experiment; i.e., the range of mass velocities and qualities should encompass the distributed, segregated, and intermittent regimes for both 1-g and near zero-g. The operating region map in Figures 3-3 and 3-4 is based on liquid Freon-11 initially stored at Spacelab module ambient temperature and pressure (≈ 294K, 101 kN/m$^2$; 70F, 14.7 psia), then expanded isenthalpically upstream of the test section to a selected lower pressure and temperature. After entering at low vapor quality, the fluid flowing within the test section boils progressively and uniformly and isothermally. Discharge from the test section is at a quality higher than at entry by an amount directly proportional to heating rate and inversely proportional to mass flow rate. Parameters corresponding to paths at the boundaries of the operating region are maximum Q/A = 1.55 watts/cm$^2$ of test section inner surface, maximum Q = 679 watts, maximum mass velocity G = 690 kg/sec-m$^2$ (172,000 lb/hr-ft$^2$), maximum flow $\dot{w}$ = 0.12 kg/sec (925.2 lb/hr), minimum boiling temperature 270K (26F), and minimum test section pressure p = 34.5 kN/m$^2$ (5 psia).

The operating region shown in Figure 3-3 is structured on 23 "set points." It is estimated that the operating time required will be about two minutes per set point, or

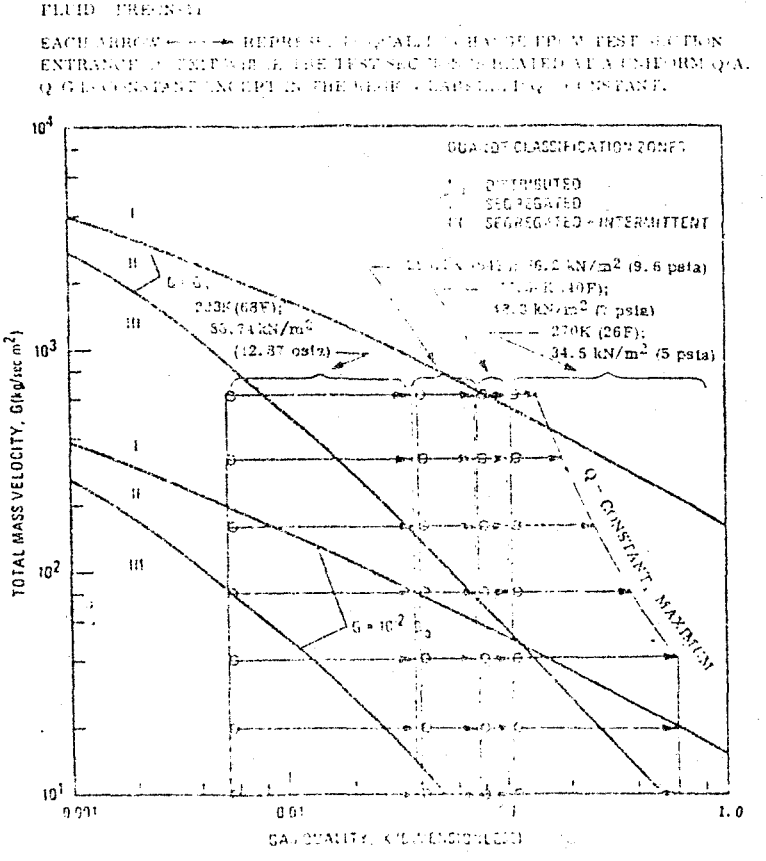


Figure 3-3. Operating Region, Flow Boiling Experiment

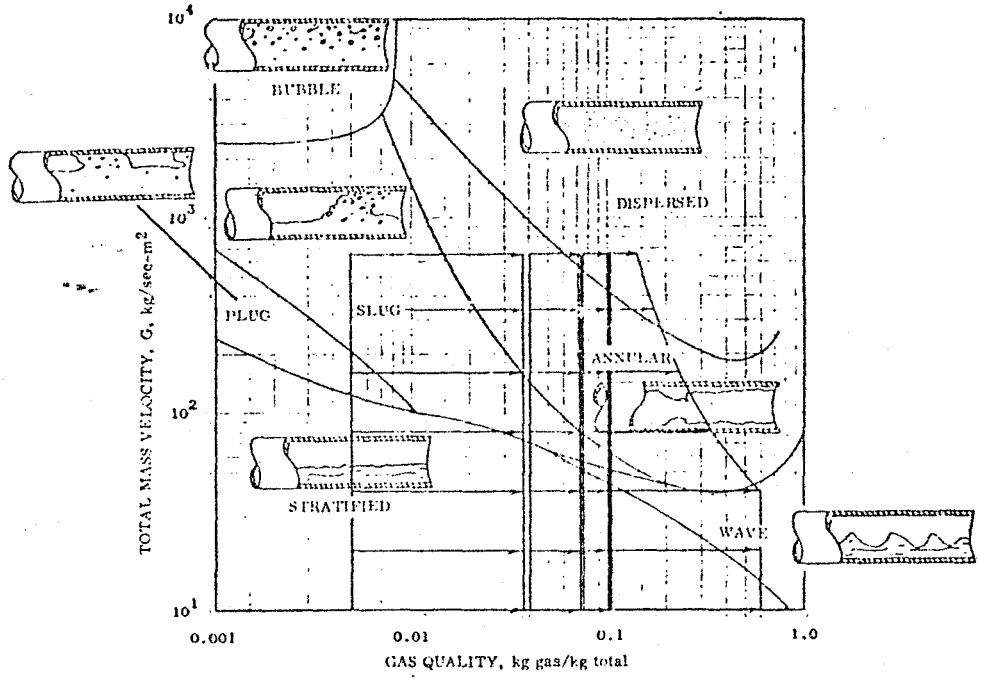


Figure 3-4. Baker Operating Regions, Flow Boiling Experiment

56 minutes total. As stated earlier, the experiment operator may observe reason to extend the operating region in the direction of lower flows. The option exists for extending the experimental range into the subcooled region. With Freon-11 stored at the pressure and temperature conditions stated above, the degree of initial subcooling available is 2.6K (4.7F). Time and resources for at least 40 set points should be provided. The proposed experimental data plan is limited to the single Spacelab environment of $10^{-4}$ g, however opportunities for data at a second level of $10^{-2}$ g should be considered as further experiment definition continues.

Examination of the operating region in Figure 3-3 also raises the question of data at qualities near one and in the superheated vapor region. Because of heater limitations (Section 3.2.4), dryout may not be achieved at the high mass velocities, however, this regime can be examined at the lower mass velocities. Figure 2-6 shows dryout occurring at qualities below one as the transition from the annular into the dispersed regime takes place (see also Figure 3-4).

Data from the literature (Kirby, Ref. 29) was found which indicates the quality at dryout under normal gravity conditions. At this condition, a large and discontinuous decrease in the heat transfer coefficient has been observed at the indicated axial location which corresponds to dryout of the annular film. This quality condition at dryout is shown in Figure 3-5 for Freon 12 tests (Ref. 29). The 16.1 mm curve with G of 49.3 gm/sec-cm$^2$ is close to our conditions, 15.2 mm tube with G of 54 gm/sec-cm$^2$ at the highest flow rate. The

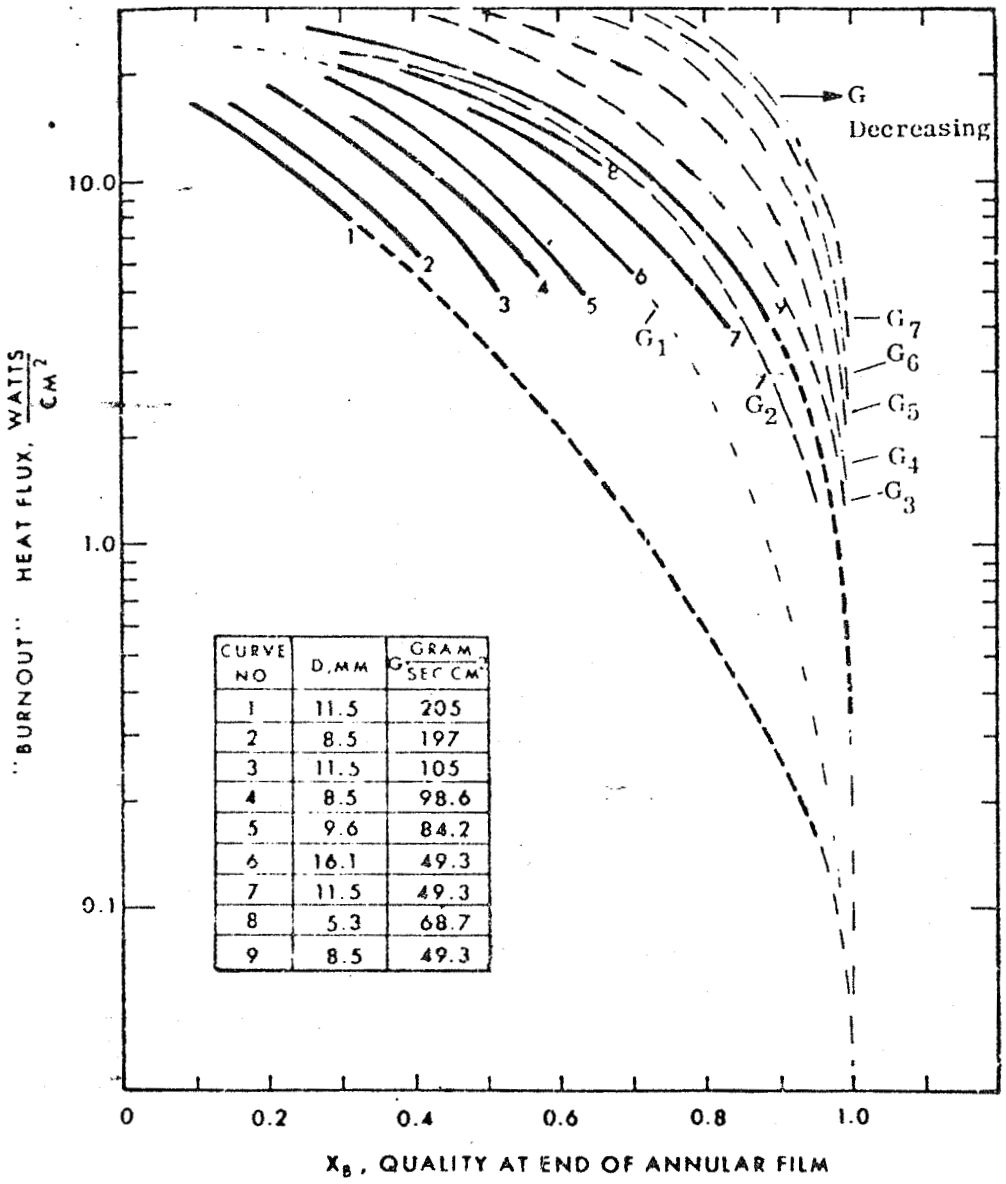


Figure 3-5. Freon 12 Dryout Data Indicates Dependence on Mass Velocity (Kirby, Ref. 29)

maximum design heat flux is 1.55 watts/cm$^2$ for $G_1$ with lower fluxes decreasing by factors of 2 to maintain Q/G constant (Figure 3-3 refers) except in the 5 psia range where Q is held constant for the highest five mass fluxes. With the selected heater size of 679 watts, Q/A = 1.55 watts/cm$^2$, required dryout qualities will typically exceed 0.85 for the flow rates under consideration. Table 3-2 indicates the burnout heat flux for our experimental configuration based on design flow rates and the extrapolation in Figure 3-5. It can be seen that the qualities required for dryout to occur are in excess of those expected for the experiment design proposed, therefore, to achieve burnout, the heater power would have to be increased over the design value for mass velocities

Table 3-2. Burnout Qualities and Heater Power

| G kg/sec-$m^2$ | 640 | 320 | 160 | 80 | 40 | 20 | 10 |
|---|---|---|---|---|---|---|---|
| Planned Q/A watts/ watts/$cm^2$ | 1.55 | 1.55 | 1.55 | 1.55 | 1.55 | 0.775 | 0.388 |
| Outlet Quality at Burnout $x_B$ | ~0.85 | ~0.91 | ~0.94 | ~0.96 | ~0.97 | ~0.98 | ~0.99 |

$G_1$ through $G_5$. The proposed experiment does not include test points for these conditions due to the excessive heater power required, however this matter should be examined further in the detailed design phase. It should also be noted that in low gravity flow regime changes may initiate dry out conditions at lower flow rates and qualities than in normal gravity.

3.2.4 TEST SECTION HEATING. Criteria for the test section heating concept include the following:

1. A uniform Q/A is required so that measurement of total Q and total A will yield an accurate Q/A for any position on the test section.

2. Since visibility and photographic recording of fluid behavior are important, the heating technique must not significantly degrade this capability.

3. The technique must be compatible with the maximum rate desired and with Spacelab utilities capabilities.

The concept of a forced-convection hot water jacket surrounding the test section was analyzed but rejected because it did not provide a uniform source temperature or uniform Q/A. The concept of an electrically conductive, transparent coating on or inside a 1.5 cm (0.6 in) ID by 90 cm (36 in) long tube was pursued with a manufacturer of electrically heated aircraft windshield materials. The performance parameters representative of current technology were a power input of up to 0.78 watts/$cm^2$ (5 watts/$in^2$), visible light transmittance of 70 to 80%, and recommended film resistivity in the range of 6 to 25 ohms/square. While this performance would have been minimally acceptable (less than 10 watts/$in^2$), the manufacturer rejected the concept of film deposition in or on the tube as technically too difficult. An earlier investigator used a thin transparent metal film deposited on the inside of a glass tube with Freon 22 as the test fluid at heat fluxes up to 6 watts/$cm^2$, (Ref. 30). This approach should be pursued further during the detailed design phase to evaluate light transmittance in their work. Also, his data indicates an alarming difference in surface finishes for glass versus stainless which must be considered further.

The third concept analyzed was a spiral wrapping of electrical resistance wire around a transparent tube. With fine wire and some spacing of turns, the view of the interior would not be significantly obscured. The material of the tube should have high thermal

conductivity to promote heat transfer in the intended direction. Representative conductivities are K = 0.20 watts/m-K (1.4 Btu-in/hr-ft$^2$-F) for clear acrylic (Lucite), K = 1.25 watts/m-K (8.7 Btu-in/hr-ft$^2$F) for glass, and K = 1.9 watts/m-K (13.2 Btu-in/hr-ft$^2$-F) for fused silica (quartz).

Resistance wire calculations were based on compatibility with the flow boiling experiment operating region described in Section 3.2.3.2 and shown in Figure 3-3. The maximum power stated is 679 watts, and minimum power, corresponding to $G_{min}$ = 1/64 $G_{max}$, is 10.6 watts. This implies a controllable voltage supply from an ac source. At 115 VAC maximum, the minimum would be 1.8 volts. The resistance corresponding to 115 volts and 679 watts is 19.5 ohms. Table 3-3 shows some candidate wire materials and sizes, and the lengths having 19.5 ohms resistance. Figure 3-6 shows the relationship of wire length, axial pitch, and number of helical turns at 1.78 cm (0.7 inch) pitch diameter round a tube of 90 cm (36 in) length. The alloy 55% Cu 45% Ni (commercial names Copel, Constantan) shown in Table 3-3 has the favorable characteristic of an unusually low temperature coefficient of resistance, this being $\pm 0.2 \times 10^{-4}$ ohms/ohm/C (Ref. 31). From Table 3-3, the Copel AWG 24 size has a length of 8.2 m (26.9 ft) for 19.5 ohms, and from Figure 3-6, 8.2 m (26.9 ft) length would make 145 turns at an axial pitch of 6.4 mm (0.25 in). The wire diameter being 0.51 mm (0.020 in), there would be a view obstruction of 0.51 mm (0.020 in) per 6.4 mm (0.25 in) tube length, or 8%. One could choose another size, such as AWG 30, having a diameter of 0.254 mm (0.010 in). The corresponding parameters are a length of 2.04 m (6.69 ft), 32.5 turns, an axial pitch of 27.9 mm (1.1 in), and a view obstruction of 1%. The AWG 24 size at 0.64 mm

Table 3-3. Resistance Wire Characteristics

| Size, AWG | Area, Circular mils | Diam, mils* | Length of Wire Having Resistance R = 19.5 ohms: Chromel-R $R_0$ = 800 ohms - cmf** Length, ft | Chromel-P $R_0$ = 425 ohms - cmf Length, ft | Copel $R_0$ = 293 ohms - cmf Length, ft | Alloy 667 $R_0$ = 130 ohms - cmf Length, ft | Copper $R_0$ = 10.37 ohms - cmf Length, ft |
|---|---|---|---|---|---|---|---|
| 24 | 401.0 | 20.10 | 9.85 | 18.5 | 26.9 | 60.6 | |
| 26 | 251.1 | 15.91 | 6.19 | 11.7 | 16.9 | 38.1 | |
| 28 | 159.8 | 12.61 | 3.90 | 7.33 | 10.6 | 24.0 | |
| 30 | 100.5 | 10.03 | | 4.61 | 6.69 | 15.1 | 189 |
| 32 | 63.21 | 7.950 | | | 4.21 | 9.48 | 119 |
| 34 | 39.75 | 6.305 | | | | 5.96 | 74.8 |
| 36 | 25.00 | 5.000 | | | | 3.75 | 47.0 |
| 38 | 15.72 | 3.965 | | | | | 29.6 |
| 40 | 9.89 | 3.115 | | | | | 18.6 |

*1 mil = 0.001 inch = 0.0254 mm
**cmf = circular mil/foot
1 ft = 0.3048 m

$$\text{Length} = \frac{19.5\ A}{R_0} \quad \frac{\text{ohms - circular mils}}{\text{ohms - circular mils/ft}}$$

Experimental conditions are:

E = 115 volts W = 679 watts R = 19.5 ohms

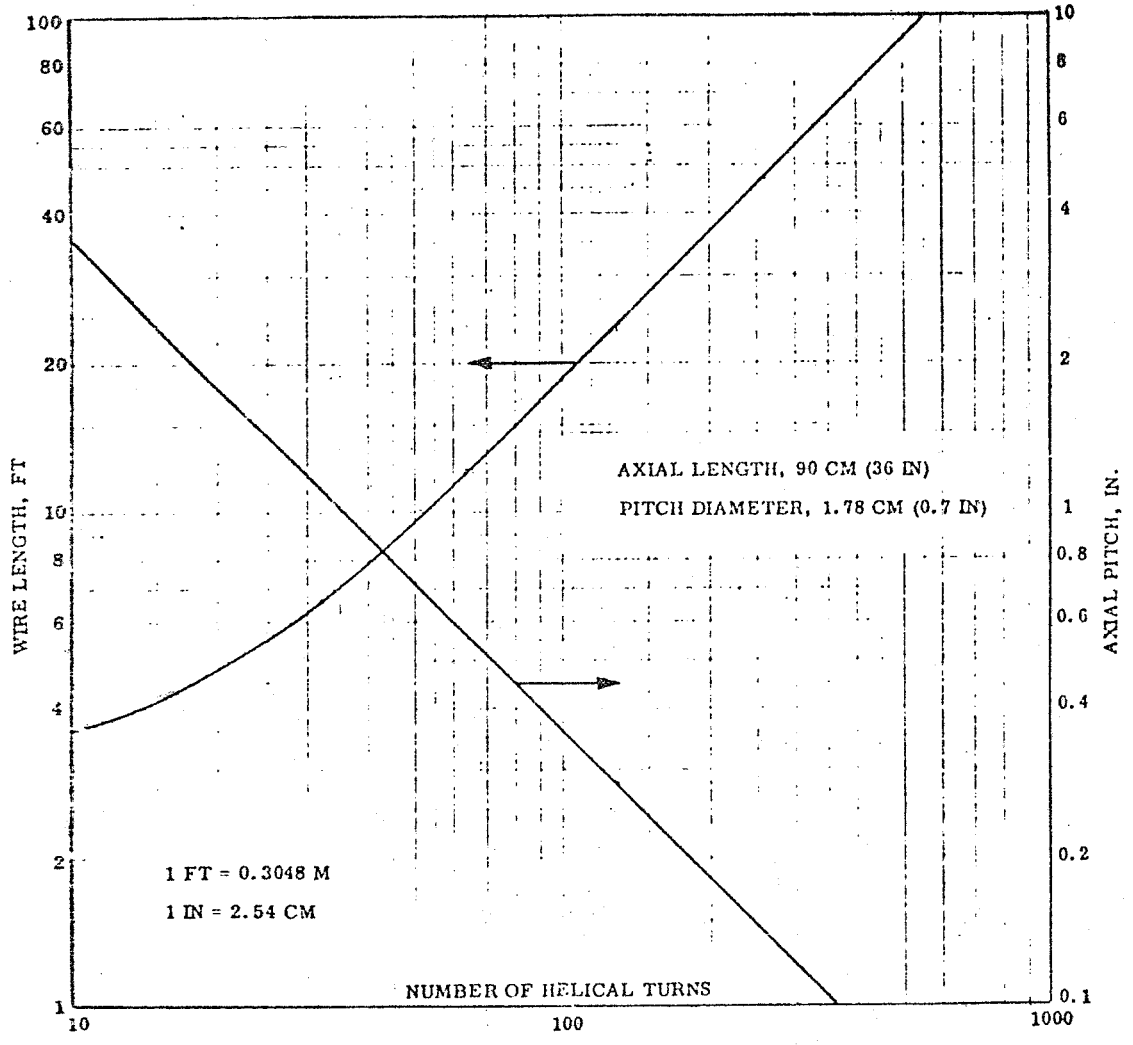


Figure 3-6. Helical Configuration Resistance Wire Winding

(0.25 in) axial pitch is preferable for uniformity of heating and the resulting 8% view obstruction is considered acceptable.

Another part of the tube heating concept is that a transparent, insulating jacket may be used to reduce heat loss from the resistance wire to ambient. Figure 3-7 is a transverse section view showing a jacket of clear acrylic (Lucite). The square section provides flat surfaces which are preferable optically to a curved surface. The space between the quartz tube OD and the jacket ID will contain the helical tube wrapping of resistance wire, and may additionally be filled with a clear, inert dielectric liquid of low vapor pressure. The purpose of the liquid is to improve uniformity of heat conduction from the resistance wire to the tube wall. A candidate fluid for this application is FC-43, which is reported by the manufacturer to be nonflammable, highly inert to chemical reactions, and "essentially non-toxic under normal industrial

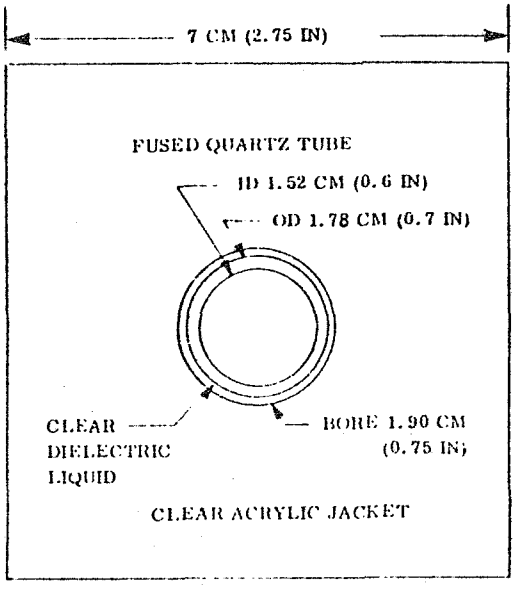


Figure 3-7. Transverse Section, Tube and Jacket

conditions." Some of the properties of FC-43 at room temperature are a vapor pressure of 0.3 mm Hg, a dielectric strength of 56 kV per 0.254 cm (0.1 in), a thermal conductivity of 0.085 watts/m-K (0.049 Btu-ft/hr-ft$^2$-F), and visible light transmittance of about 99% through 1 cm thickness.

Calculations indicate that with a jacket of the configuration described, heat loss to ambient will not exceed 2% when power is applied at the maximum rate of 679 watts.

The jacket described may also be designed so that it constitutes a secondary containment barrier providing added assurance that test fluid will not escape into the Spacelab module atmosphere. The jacket of clear acrylic is also a protective covering for the quartz tube against damage in handling.

3.2.5 FLUID MANAGEMENT CANDIDATE CONCEPTS. The term "fluid management" is used to mean the basic flow configuration involving the fluid source(s), the test section, and the hardware for disposition of the mixed phase fluid after exit from the test section. The approach taken was to assess fundamental practicality of several candidate configurations in order that the least practical could be dropped from further consideration. The remaining candidates were subjected to a more detailed study. Initially, the two experiments were considered separately for evaluation of the candidates. Later the amenability of candidates for integration was one of the evaluation criteria. Also, evaluation was within the context that the experiment hardware shall be contained within a double rack of the Spacelab module. Each candidate concept was given a title reflecting fluid management characteristics and has been illustrated by a flow schematic of only sufficient detail to enable this initial screening.

3.2.5.1 Single Pass, Overboard Dump (Figure 3-8).

a. Flow Regime/Pressure Drop Experiment (1a). The volume of stored gaseous $N_2$ corresponding to the 46 data points of Figure 3-1 at one minute per data point is about 0.113 m$^3$ (4 ft$^3$) at 6895 kN/m$^2$ (1000 psia). While this volume is not excessive relative to the volume in a Spacelab double rack, the concept does not comply with the safety constraint in Reference 32 that "pressure vessels shall normally be installed exterior to the Spacelab cabin;" and it does not conform with the principle of "design for minimum hazard" (Ref. 32 ). Therefore, this concept was dropped from further consideration.

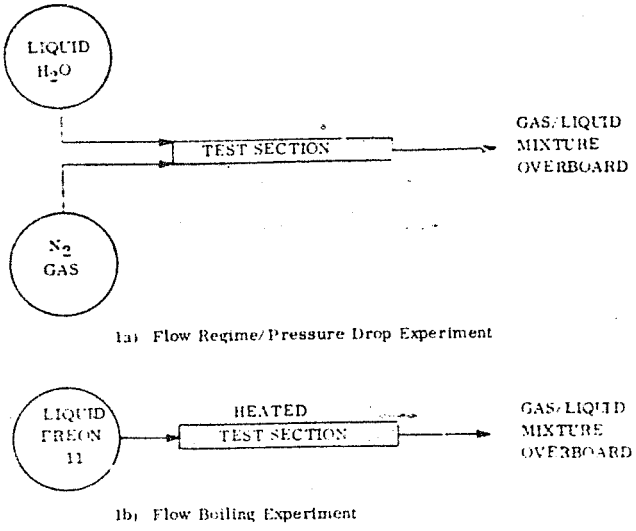


Figure 3-8. Single Pass, Overboard Dump Concept

b. Flow Boiling Experiment (1b). The quantity of stored Freon-11 corresponding to the 28 set points of Figure 3-3 at 2 minutes per set points is 111 Kg (245 lb) with a volume of 0.075 $m^3$ (2.64 $ft^3$). It appears that the safety requirements relating to pressure vessels can be met by operating at pressures of ambient and lower. The safety requirements relating to toxic materials (Ref. 32 ) can be met by double containment. Some question remains as to whether overboard discharge of Freon-11, or any fluid, will be permissible at the rates for this experiment. It is assumed that timing of the experiment and direction of the discharge from the vehicle can be such that this approach will be approved.

3.2.5.2 Single Pass, Collection Concept (Figure 3-9).

a. Flow Regime/Pressure Drop Experiment (2a). This configuration does not resolve the pressure vessel safety problem described for the preceding concept. Also, the low pressure receiver would have a volume of 7.5 $m^3$ (265 $ft^3$). This configuration was dropped from further consideration.

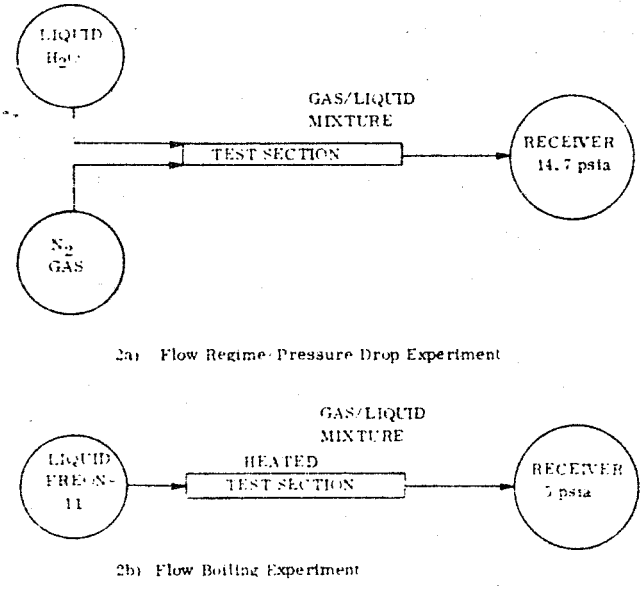


Figure 3-9. Single Pass, Collection Concept

b. Flow Boiling Experiment (2b). The low pressure receiver volume would have to be over 5.4 $m^3$ (190 $ft^3$) for the series of set points of Figure 3-3. This configuration was dropped from further consideration because the volume is excessive for a location within the Spacelab module.

3.2.5.3 Fluid Collection, Batch Recycle (Figure 3-10).

a. Flow Regime/Pressure Drop Experiment (3a). The operating

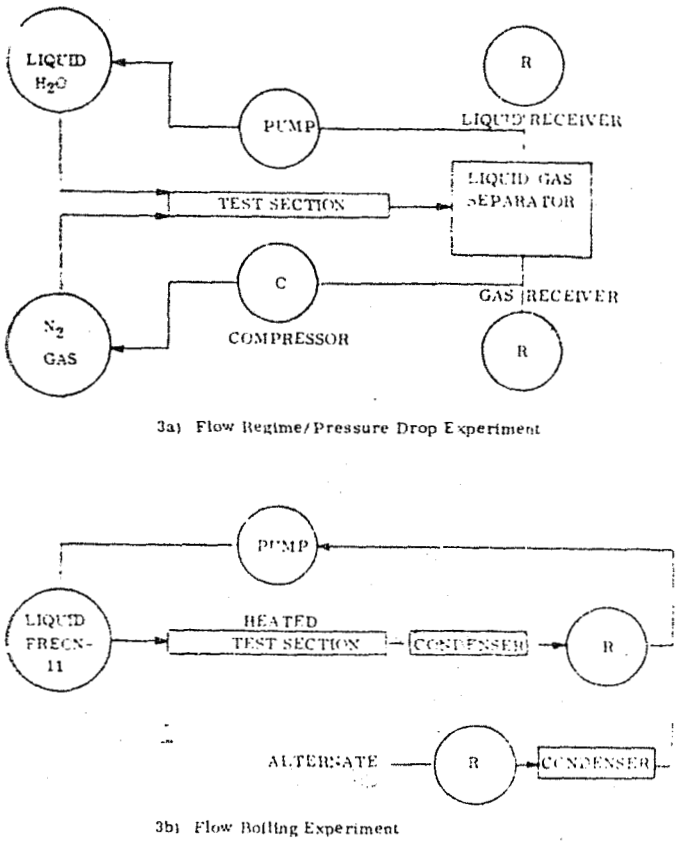


Figure 3-10. Fluid Collection, Batch Recycle

scheme is that test section discharge for a few minutes of operation undergoes phase separation and collection, the test section flow is interrupted, and the collected fluids are pumped back into the supply vessels. The recycle rates are much lower than and essentially independent of test section flow rates. Supply and collection vessels are small relative to those in previous configurations, and Reference 32 allows that "small pressure vessels may be permitted inside the cabin provided they do not have a credible explosive failure mode and their failure will not expose the crew of vehicle to hazard."

Minimum gas vessel volumes are determined by the data point of maximum mass velocity and maximum quality shown in Figure 3-1, and by a criterion of one minute of flow per data point. These volumes are 0.5 $ft^3$ at 1060 psia for the gas supply vessel and 34.1 $ft^3$ at 14.7 psia for the gas receiver. Since the latter volume is excessive, and the fluid management configuration is undesirably complex, this concept was dropped from further consideration.

b. Flow Boiling Experiment (3b). In this concept there are no large volumes because the test fluid vapor is condensed. The alternate configuration shown in Figure 3-10b has an advantage of some levelling of the condenser flow rate. However, design and development of any zero-g condenser would be a much more extensive and uncertain undertaking than for the other components being evaluated. This was judged to be sufficient reason to drop the concept from further consideration.

3.2.5.4 Continuous Liquid and Gas Recycle (Figure 3-11)

a. Flow Regime/Pressure Drop Experiment (4a). In this concept the gas is cabin air and the entire cabin serves as a collection and source vessel. Control of flow rates is by variable speed controls on the blower and pump. This approach was successful in recent aircraft flight experiments on two phase fluids behavior (Ref. 20). The combined electrical power demand of the pumping components is fairly high.

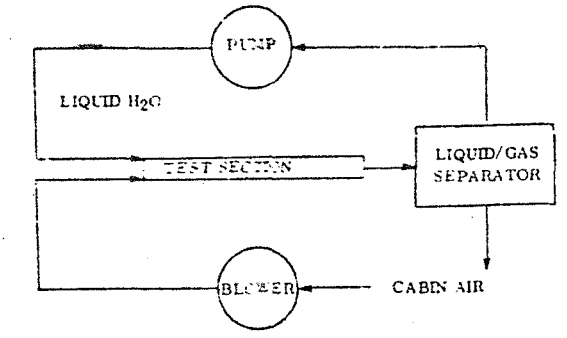


4a) Flow Regime/Pressure Drop Experiment

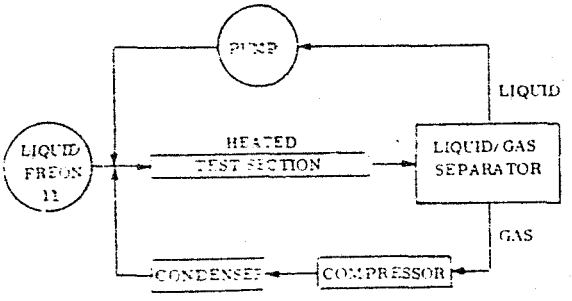


4b) Flow Boiling Experiment

Figure 3-11. Continuous Liquid and Gas Recycle

b. Flow Boiling Experiment (4b). Continuous recycle involves condensing. For reasons stated earlier, a condenser requirement is sufficient reason to drop this concept from further consideration.

3.2.5.5 Continuous Liquid Recycle, Gas Overboard (Figure 3-12)

a. Flow Regime/Pressure Drop Experiment (5a). This concept includes a high pressure gas storage vessel and is dropped for reasons stated earlier.

b. Flow Boiling Experiment (5b). Compared with total overboard discharge this concept can reduce the quantity of stored Freon-11 from 111.1 kg (245 lbs) to 13.6 kg (30 lbs). The quantity expended overboard is likewise about 13.6 kg.

3.2.5.6 Concepts Screening Summary. All of the concepts having high pressure gas storage were dropped because of the safety constraint. The objection to high pressure gas storage would be diminished if the pressure vessel were located on a pallet, but even then, the concept would violate the principle of design for minimum hazard. If use of a pallet were acceptable, then cryogenic storage could be considered.

Also, all of the concepts having collection vessels for test section effluent were dropped because of excessive volumes for the collected gaseous phase. The volume requirements are directly related to parameters of test section flow area, maximum mass velocities, and flow durations per set point which were established earlier. If the collection volume could be reduced by about an order of magnitude through an equal reduction in the product of the parameters named, then the concepts with batch recycle could remain in consideration. However, the batch recycle would be undesirably complex and time consuming.

Table 3-4 summarizes the concepts screening results. Preferred concepts are 1b, 4a, and 5b. In the event overboard discharge is not acceptable, the alternate flow boiling concept preference is 4b.

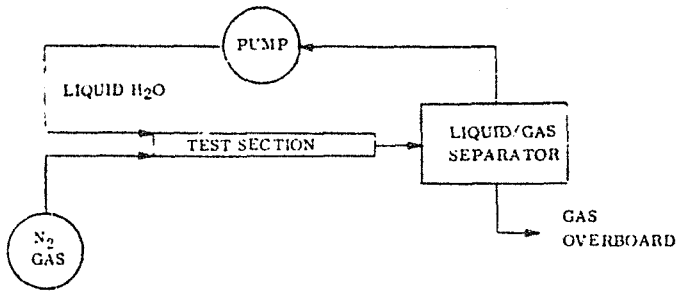


5a) Flow Regime/Pressure Drop Experiment

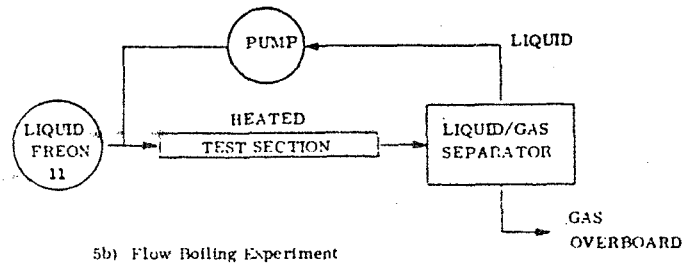


5b) Flow Boiling Experiment

Figure 3-12. Continuous Liquid Recycle, Gas Overboard

3.2.6 EXPANDED CONCEPTS DEFINITION. The concepts which passed the screening are here defined in greater detail for the purpose of further evaluation. The two experiments are first dealt with separately, and subsequently the integration of experiments is addressed.

3.2.6.1 Flow Regime/Pressure Drop Experiment. Figure 3-13 is a detailed flow schematic based on the concept 4a shown in Figure 3-11. The test section has been previously described in Sections 3.2.1 and 3.2.4. The controls include valves V-1, V-2, and V-3 for isolating the test section from fluid management components.

From Figure 3-1, a requirement is calculated for a 176 to 1 range in water flow and for a 1024 to 1 range in air flow. Experiment operation may reveal that even greater ranges are desirable. Figure 3-13 shows variable speed controls (also known as

Table 3-4. Concepts Screening Summary

| Concept | Experiment | Onboard Fluids | | Fluids Overboard | Concept Rejected ? | Rejection Criteria |
|---|---|---|---|---|---|---|
| | | Weight, kg (lbs) | Volume $m^3$ ($ft^3$) | kg (lb) | | |
| 1a Single Pass, Overboard Dump | Flow Regimes/ Pressure Drop | 289 (637) | 0.68 (24) | 289 (637) | Yes | Safety |
| 1b Single Pass, Overboard Dump | Flow Boiling | 111 (245) | 0.076 (2.7) | 111 (245) | No | — |
| 2a Single Pass, Collection | Flow Regimes/ Pressure Drop | 289 (637) | 99.1 (3500) | None | Yes | Excessive Volume |
| 2b Single Pass, Collection | Flow Boiling | 111 (245) | 5.38 (190) | None | Yes | Excessive Volume |
| 3a Collection, Batch Recycle | Flow Regimes/ Pressure Drop | 9 (20) | 4.0 (140) | None | Yes | Excessive Volume |
| 3b Collection, Batch Recycle | Flow Boiling | 16 (35) | 0.51 (18) | None | Yes | Zero-g Condenser Development |
| 4a Continuous Recycle, Air/$H_2O$ | Flow Regimes/ Pressure Drop | 5 (10) | 0.006 (0.2) | None | No | — |
| 4b Continuous Recycle | Flow Boiling | 5 (10) | 0.006 (0.2) | None | Yes | Zero-g Condenser Development |
| 5a Continuous Recycle, Liquid Only | Flow Regimes/ Pressure Drop | 116 (255) | 0.051 (1.8) | 111 (245) | Yes | Safety |
| 5b Continuous Recycle, Liquid Only | Flow Boiling | 14 (30) | 0.008 (0.3) | 14 (30) | No | — |

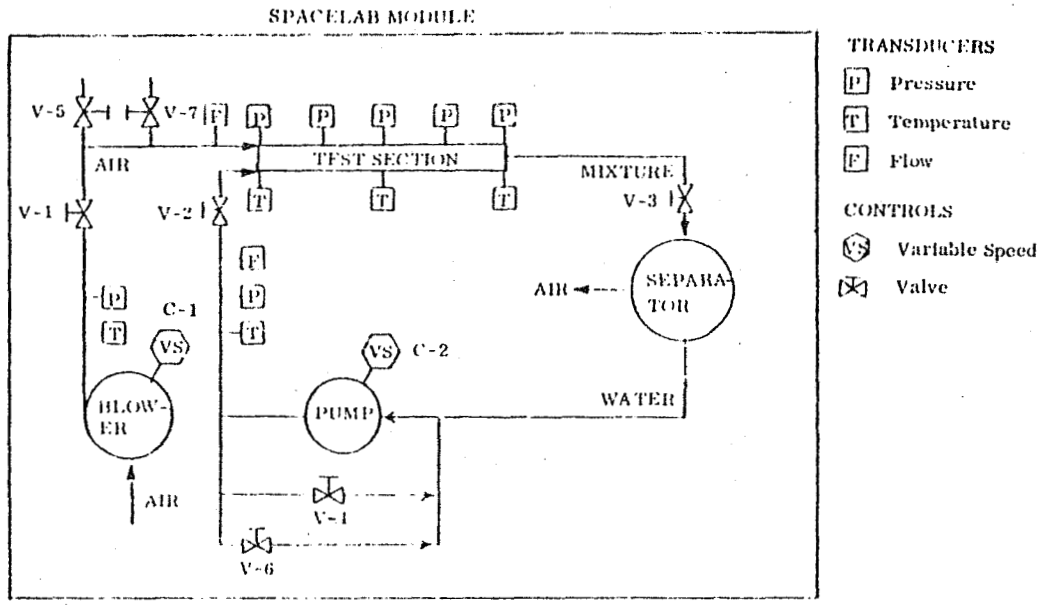


Figure 3-13. Flow Regime/Pressure Drop Experiment Flow Schematic

adjustable speed controls) for the pump and blower motors. The performance available from such controls is precision, stepless speed adjustment over ranges up to about 1000 to 1. It may be necessary to limit the speed range due to performance characteristics of the pump and blower. The valves V-4 and V-5 shown in Figure 3-13 provide a variable bypass capability for control of low flows to the test section. Valves V-6 and V-7 are like V-4 and V-5 except that they are much smaller and are for vernier control of bypass. The combination of variable speed and variable bypass has at least three objectives: (a) to achieve the extreme flow ranges desired, (b) to enable precise flow settings, and (c) to avoid extreme power inefficiencies.

The liquid/gas separator operating range is the same as the test section range (Figure 3-1) and is extreme in both flow and quality. Figure 3-14 is the specification control drawing for the motor-driven, centrifugal liquid/gas separator which is mentioned in Reference 20. This unit operated satisfactorily over wide flow and quality ranges, and during aircraft flights, with a g-level exposure range from near zero to slightly more than +2. It also operated in sustained 1-g during ground tests. A unit of this type is proposed for the concept of Figure 3-13. A two-speed motor control is adequate to enable the higher speed for sustained 1-g ground operation and the lower speed for sustained near 0-g operation in Spacelab. The liquid capacity of the separator is sufficient to serve as an accumulator, thereby accepting variations in test section liquid hold-up.

Tentative locations of flow, pressure, and temperature transducers are shown in Figure 3-13, but further definition of the measurements and data concept is in a subsequent section.

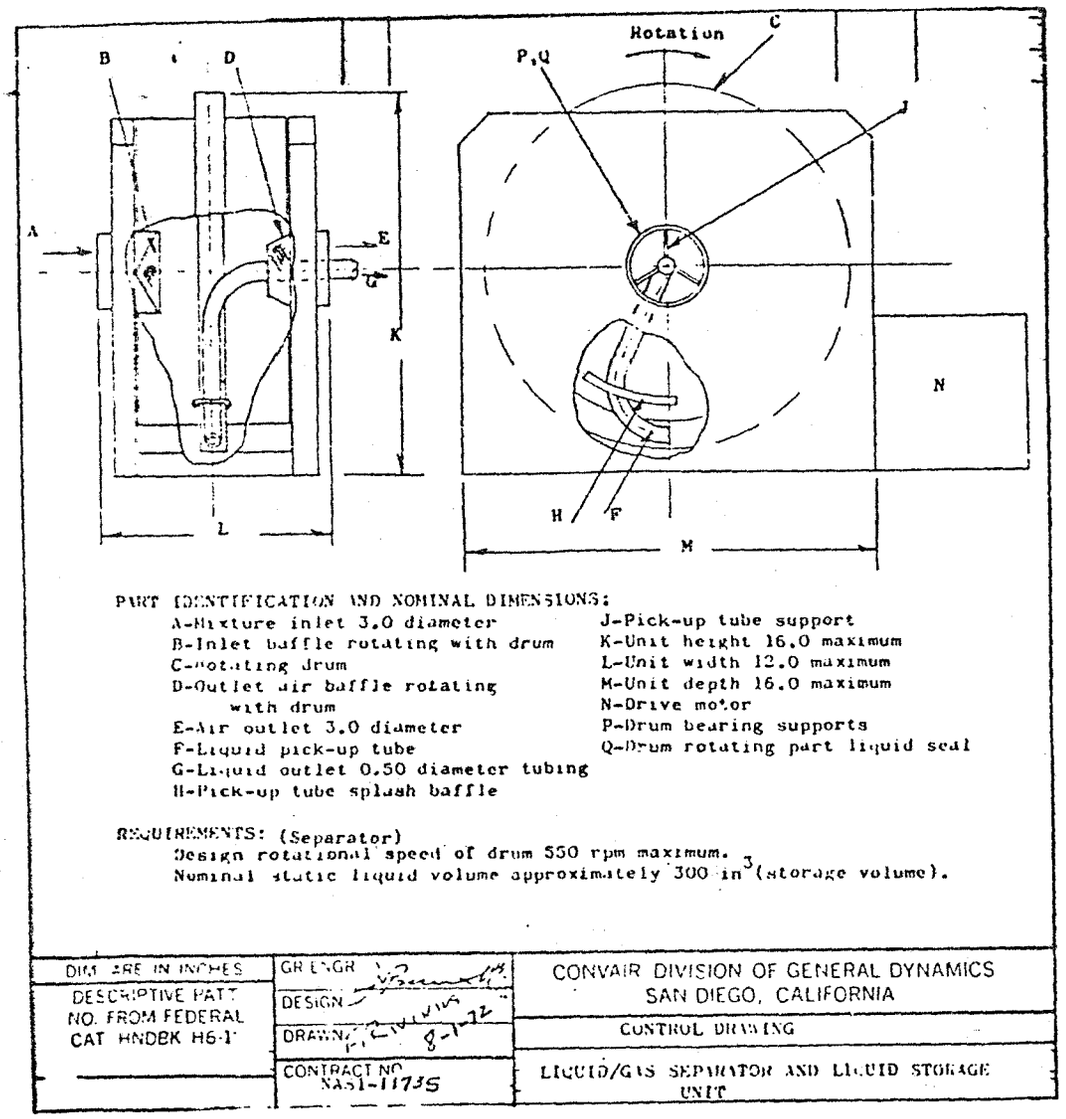


Figure 3-14. Liquid/Gas Separator Concept

The principal performance parameters are shown in Table 3-5 and are based on the operating region shown in Figures 3-1 and 3-2. The maximum test section pressure drop estimate is an extrapolation from measurements in a similar system (Ref. 20) and is reasonably consistent with calculation by a method applicable to two-phase, homogeneous, turbulent flow (Ref. 22). Maximum input power to the pump and blower was calculated from the maximum pressure drop and the estimated efficiencies of components as shown in Table 3-6. The estimated power requirement for a liquid/gas separator of the type described in Reference 20 is 75 watts. The estimated total maximum power to flow components only (i.e., excluding lights, camera, and other data acquisition components) is 857 watts.

Table 3-5. Hardware Performance Estimate, Flow Regime/Pressure Drop Experiment

| | |
|---|---|
| Total Mass Velocity, Controllable | 0 to 640 kg/sec-m$^2$ (0 to 54.6 lb/min-in$^2$) |
| Pump Liquid Flow, Controllable | 0 to 0.116 kg/sec (0 to 15.3 lb/min) |
| Blower Gas Flow, Controllable | 0 to 0.019 kg/sec (0 to 2.45 lb/min) |
| Quality, Controllable | 0 to 0.64 |
| Separator $\Delta p$ | TBD* |
| Test Section $\Delta p$, Maximum | 20.7 kN/m$^2$ (3 lb/in$^2$) |
| Blower $\Delta p$, Max. | TBD** |
| Pump $\Delta p$, Max. | TBD** |

*Assuming a motor-driven, rotary separator, the separator will deliver liquid at a $\Delta p$ that is positive but low compared with pump maximum $\Delta p$.

**By sizing the plumbing other than the test section for low pressure drop, the pump and blower $\Delta p$'s will be nearly equal and only slightly higher than test section $\Delta p$.

Table 3-6. Flow Components Power Estimate, Flow Regimes/Pressure Drop Experiment

| | Water Pump | Air Blower |
|---|---|---|
| Maximum Flow Power, watts | 2.4 | 320 |
| Pump/Blower Efficiency | 0.5 | 0.7 |
| Motor Efficiency | 0.5 | 0.7 |
| Speed Control Efficiency | 0.7 | 0.95 |
| Maximum Input, watts | 13.6 | 768 |

Table 3-7. Hardware Performance Estimate, Flow Boiling Experiment

| | |
|---|---|
| Total Mass Velocity, Controllable | 0 to 640 Kg/sec-m$^2$ (0 to 54.6 lb/min-in$^2$) |
| Total Flow, Controllable | 0 to 0.117 Kg/sec (0 to 15.42 lb/min) |
| Heating Rate, Controllable | 0 to 680 watts |
| Quality | 0 to 0.6 |
| Liquid Flow, Maximum | 0.116 Kg/sec (15.34 lb/min) |
| Vapor Flow, Maximum | 0.016 Kg/sec (2.34 lb/min) |
| Test Section $\Delta p$, Maximum | 20 kN/m$^2$ (2.9 lb/in$^2$) |
| Test Fluid Storage Capacity | 111 Kg (245 lb) |



3.2.6.2 Flow Boiling Experiment, Overboard Dump Concept. Figure 3-15 is a detailed flow schematic based on concept 1b shown in Figure 3-9. The test section and heater have been described in Sections 3.2.1 and 3.2.4, respectively. The supply tank for liquid Freon 11 will contain a zero-g acquisition device as described in Section 3.2.9.4. Isolation valves V-1, V-2 and V-3 are open only during experiment operation. R-1 and R-2 are adjustable static pressure regulators. Forward pressure regulator R-1 is set and reset to deliver each of the several lower test section pressures shown in Figure 3-3. Back pressure regulator R-2 is adjusted to obtain the desired flow rate at each selected test section pressure. The R-1 to R-2 pressure difference will be the pressure drop of the test section. An alternate procedure is to set R-2 first and adjust R-1 to obtain the desired flow rate. Tentative locations of transducers are shown in Figure 3-15, but further definition of the measurements and data concept is in a subsequent section.

Table 3-7 summarizes major performance characteristics of the experiment flow components. Maximum electrical power

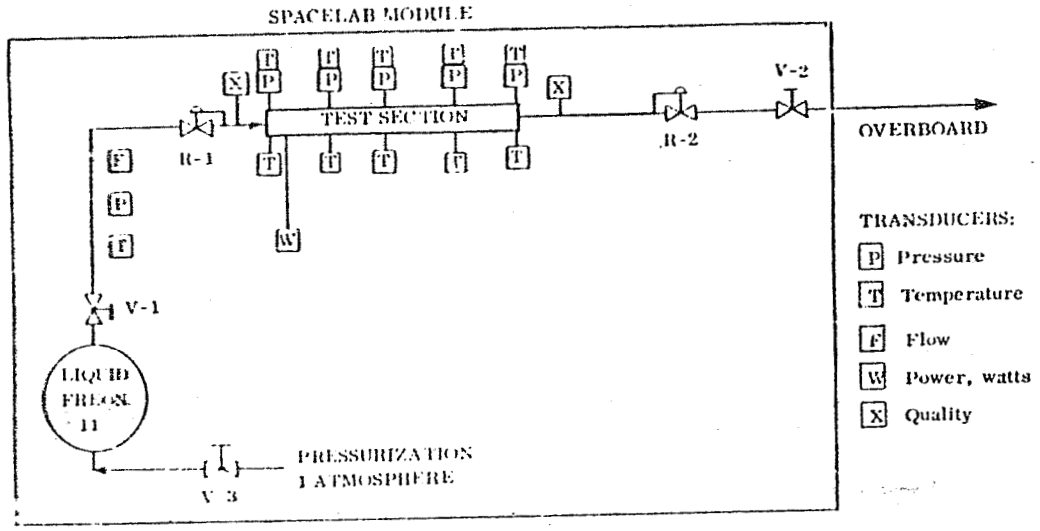


Figure 3-15. Schematic , Flow Boiling Experiment, Overboard Dump Concept

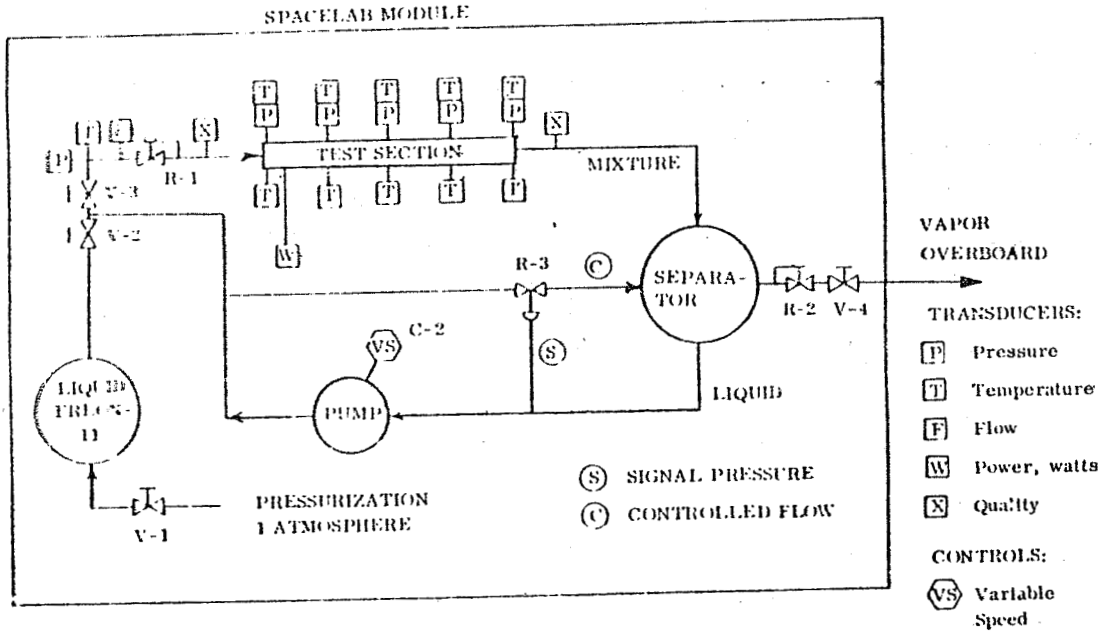


Figure 3-16. Schematic, Flow Boiling Experiment, Liquid Recycle Concept

consumption for these components only (excluding lights, camera, and other data acquisition elements) is estimated to be 700 watts and is due to the electrical heating element on the test section.

3.2.6.3 Flow Boiling Experiment, Liquid Recycle Concept. Figure 3-16 is a detailed flow schematic based on concept 5b shown in Figure 3-12. The test section and heater have been described in Sections 3.2.1 and 3.2.4, respectively. The supply tank for liquid Freon-11 will contain a zero-g acquisition device as described in Section 3.2.9.4.

Isolation valves V-1, V-2, V-3 and V-4 are normally open only during experiment operation. The liquid loop can be scavenged in a manner to return liquid to the supply tank by operating the pump while V-1 and V-2 are open and V-3 and V-4 are closed. The loop can also be scavenged to vacuum by opening V-4 with V-2 closed.

Adjustable static pressure regulator R-1 is set to deliver each of the several lower test section pressures shown in Figure 3-3. Back pressure regulator R-2 is then adjusted to obtain the desired flow rate. The R-1 to R-2 pressure difference will be the pressure drop of the test section.

There is a 1780 to 1 range in vapor flow and 159 to 1 range in liquid flow from the test section, as calculated from the operating range shown in Figure 3-3. Flow control is based on a liquid/gas separator of the type shown in Figure 3-14. The bypass line with regulator R-3 (Figure 3-16) is for maintaining a nearly constant liquid level in the liquid/gas separator so that (a) the separator will not overflow and allow liquid discharge overboard, and (b) the separator will not be pumped dry and allow vapor ingestion into the pump.

With the separator rotating at constant speed, the liquid discharge pressure responds to liquid volume (radial height) in the separator. This discharge pressure is sensed as the signal pressure to regulator R-3 (Figure 3-16) which responds by varying the bypass flow. The manually set variable speed control on the pump motor (Figure 3-16) is for reducing the extreme range in bypass flow. A 20 to 1 range in pump delivery together with a 10 to 1 regulator range will provide up to a 200 to 1 bypass flow range.

Tentative locations are shown in Figure 3-16, but further definition of the measurements and data concept is in a subsequent section.

Estimates of performance parameters are the same as shown in Table 3-7 except that the test fluid storage capacity requirement is about 14 Kg (31 lb) expended plus 4 Kg (9 lb) inventory in the recycle loop for a total of 18 Kg (40 lb). The estimated electrical power (excluding lights, camera, and other data acquisition elements) is 700 watts to the electrical heating element plus 37 watts to the pump motor for a total of 812 watts including 75 watts for separator.

3.2.7 PRELIMINARY CONCEPTS COMPARATIVE EVALUATION. The screening of Sections 3.2.5.6 reduced the candidates to one for the Flow Regime/Pressure Drop Experiment and two for the Flow Boiling Experiment. Comparing Figure 3-15 with 3-16, together with the text of Sections 3.2.6.2 and 3.2.6.3, it is evident that the overboard dump concept is much less complex than the liquid recycle concept. Weight, volume, input electrical power, and heat rejection are estimated to be close enough in the two concepts that a selection would not be significantly influenced by these properties. An important consideration is whether fluids may be dumped overboard from Spacelab in the quantities shown in Table 3-4. In terms of quantity overboard, the liquid recycle concept is about eight times better than total overboard dump. Both concepts are retained for further consideration.

3.2.8 EXPERIMENT INTEGRATION CONCEPTS. Some degree of integration of the Flow Boiling Experiment with the Flow Regime/Pressure Drop Experiment is attainable by sharing components. Figure 3-17 shows the Flow Boiling with overboard dump concept of Figure 3-15 added to the Flow Regime/Pressure Drop experiment that was shown in Figure 3-13. Additional valves make it possible to isolate each experiment from the other. The shared components are the test section and the attached transducers.

Figure 3-18 shows the Flow Regime/Pressure Drop concept of Figure 3-12 added to the Flow Boiling with liquid recycle concept of Figure 3-16. Here the shared components are the test section with transducers, the liquid/gas separator and the liquid pump.

In Figures 3-13, 3-17 and 3-18 there is no water storage vessel shown, the concept being that the liquid loop contains enough water for continuous recycle in the Flow Regime/Pressure Drop experiment. This requires that the Flow Regime/Pressure Drop experiment be performed first. Upon completion, the water may be evacuated overboard from the liquid loop by appropriate opening and closing of valves. In Figure 3-17, the evacuation of water would be achieved by closing valves V-1, V-5, V-7, V-9, and V-11, followed by opening all other valves of the liquid loop. For the configuration of Figure 3-18, the valves to be closed for the same purpose are V-2, V-5, V-7, and V-9. Following evacuation of the water, the valves may be re-set to perform the Flow Boiling experiment.

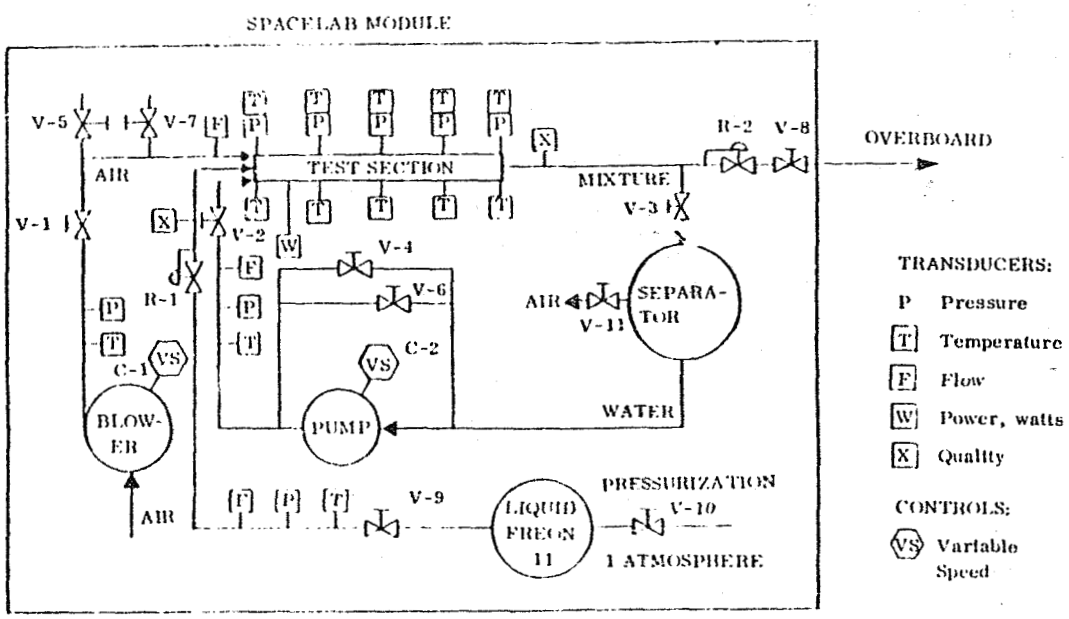


Figure 3-17. Integrated Experiments, Liquid Overboard

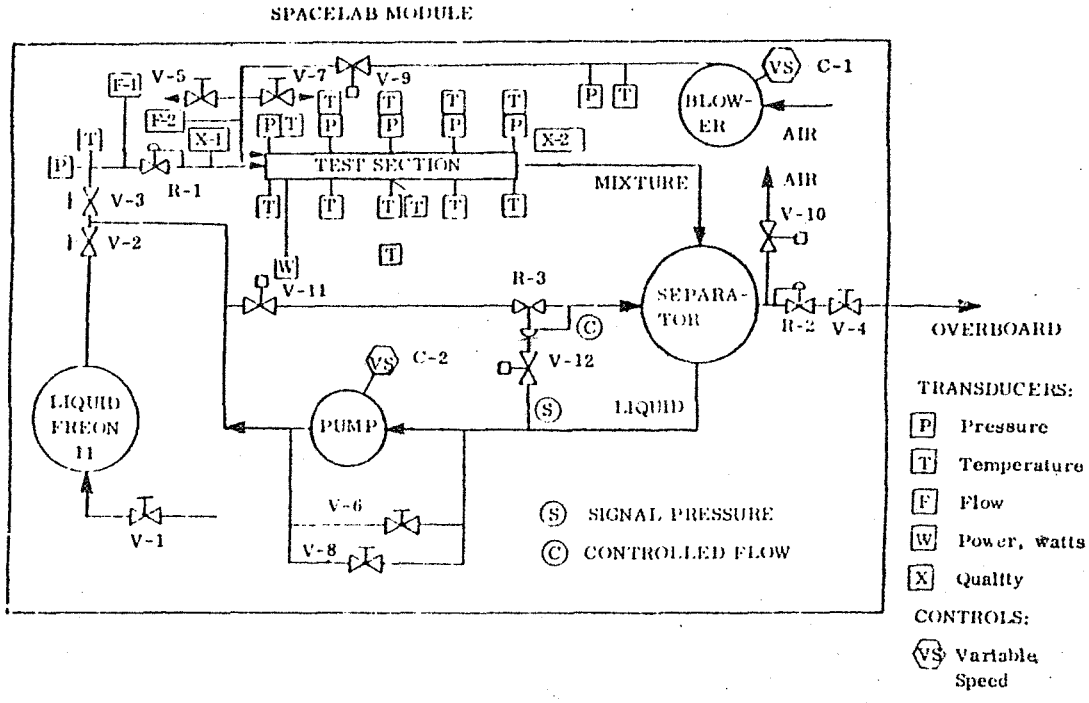


Figure 3-18. Integrated Experiments, Liquid Recycle

3.2.9 EXPERIMENT HARDWARE COMPONENTS

3.2.9.1 Controls. Table 3-8 is a list of the controls corresponding to the concepts of Figure 3-18. The two-speed control for the liquid/gas separator can be pre-set at high speed for the 1-g environment of ground operation and again at low speed for the near 0-g of Spacelab operation, so that during experiment operation the switch position will not be changed. All other controls will be used during experiments and must be readily accessible and operable.

3.2.9.2 Instrumentation. Table 3-9 is a list of transducers corresponding to Figure 3-18. The ranges given reflect requirements of the experiment operating regions shown in Figures 3-1, 3-2, 3-3 and 3-4. The voltage measurement shown is for determining heater power input and suffices because heater impedance is constant. The two temperature measurements at each of five stations along the test section are fluid bulk temperature and tube inner surface temperature, respectively.

Table 3-10 lists four digital displays and 18 indicator lights. The digital displays are of parameters the experiment operator must observe as he positions controls to establish each of the flows and qualities previously discussed. The lights are indicators that electrical power is applied to each component listed.

Table 3-8. Controls List (Reference Figure 3-18)

| Item | | Function | Description |
|---|---|---|---|
| 1. | C-1 | Adjust blower speed and output, manual set. | Variable frequency input to 400 Hz motor. |
| 2. | C-2 | Adjust pump speed and output, manual set. | Variable frequency input to 400 Hz motor. |
| 3. | R-1 | Adjust test section inlet pressure, manual set. | Forward press. regulator -5/-10 psi. |
| 4. | R-2 | Adjust flow of Freon 11, manual set. | Back pressure regulator. |
| 5. | R-3 | Maintain liquid level in separator, automatic. | Pneumatic relay. |
| 6. | C-3 | Heater power control, manual set. | Variable transformer, 400 Hz. |
| 7. | V-1, V-2, V-3, V-4, V-9, V-10 V-11, V-12 | Flow on-off select. | Solenoid valve, normally closed, switch operated. |
| 8. | V-5, V-6, V-7, V-8 | Flow modulating. | Manual set flow control valve. |
| 9. | Switch | Select separator speed. | Two-speed selector switch. |
| 10. | Switches | Electrical power on-off select. | Main power to experiment; blower; pump; separator; heater; cine camera, each photo light; each solenoid valve. |

Table 3-9. Transducers List (Reference Figure 3-18)

| | Type | Fluid | Range |
|---|---|---|---|
| F-1 | Flow | Air | 0-.02 kg sec |
| F-2 | Flow | Water or Freon-11 | 0-0.12 kg sec |
| X-1 | Quality | Freon-11 | 0-0.2 kg sec |
| X-2 | Quality | Freon-11 | 0-0.9 kg sec |
| V | Volts | - | 0-125 V ac |
| P-1 | Pressure | Water or Freon-11 | 96.5-110.3 kN/m$^2$ abs. (14-16 psia) |
| P-2 | " | Air | 0-35 kN m$^2$ (0-5 psig) |
| P-3 | " | Freon-11 or Mixed Air/Water | -105 to -35 kN/m$^2$ (-15 to -5 psig) |
| P-4 | " | " | " |
| P-5 | " | " | " |
| P-6 | " | " | " |
| P-7 | " | " | " |
| T-1 | Temperature | Water or Freon-11 | 283-305K (50-90F) |
| T-2 | " | Air | 283-305K (50-90F) |
| T-3 | " | Freon-11 or Mixed Air Water | 267-305K (20-90F) |
| T-4 | " | " | " |
| T-5 | " | " | " |
| T-6 | " | " | " |
| T-7 | " | " | " |
| T-8 | " | Test Section Wall | " |
| T-9 | " | " | " |
| T-10 | " | " | " |
| T-11 | " | " | " |
| T-12 | " | " | " |
| T-13 | " | Jacket Outer Wall | " |
| T-14 | " | " | " |
| T-15 | " | Air, Ambient | " |

3.2.9.3 Test Section. Some characteristics of the test section were discussed in Sections 3.2.1 and 3.2.4. Line sizes for air flow to and from the test section are 5 cm (2 in). There are conical adapters at each end which taper to the 1.5 cm (0.6 in) bore of the test section.

3.2.9.4 Tank and Capillary Acquisition Device. The Freon-11 storage tank is shown schematically in Figure 3-17 and 3-18 for the liquid overboard and liquid recycle systems. For the liquid overboard system, the 111 kg of Freon-11 requires a storage volume of 0.0784 m$^3$ (2.77 ft$^3$). This is achieved with two tanks (for convenience in installation) each 12.2 cm (16.6 in) in diameter. For liquid recycle the 14 kg of Freon-11 requires a tank volume of only 0.0125 m$^3$ (0.94 ft$^3$), therefore a single tank of diameter 28.5 cm (11.24 in) is adequate.

A choice of two fluid expulsion systems were selected dependent on a requirement to conduct experiments in this tank. This requirement would necessitate a rigid,

Table 3-10. Displays List

| Measurement | Fluid | Range | Display |
|---|---|---|---|
| Flow | Air | 0-0.02 kg/sec | Digital |
| Flow | Liquid | 0-0.12 kg/sec | Digital |
| Temperature, Inlet | Freon | 265-300K | Digital |
| Heater Power | - | 0-125 Volts | Digital |
| Main Power - On | - | Discrete | Light |
| Pump - On | - | " | " |
| Blower - On | - | " | " |
| Separator On - Low | - | " | " |
| Separator On - High | - | " | " |
| Heater On | - | " | " |
| Camera On | - | " | " |
| Photo Lights (3) On | - | " | " |
| V-1 Open | - | " | " |
| V-2 Open | | " | " |
| V-3 Open | | " | " |
| V-4 Open | | " | " |
| V-5 Open | | " | " |
| V-10 Open | | " | " |
| V-11 Open | | " | " |
| V-12 Open | | " | " |

transparent tank with no moving parts. For this option, a surface tension capillary screen acquisition system has been chosen similar to that reported in detail in Reference 33.

The surface tension device is shown in Figure 3-19 in a spherical storage tank in conceptual detail. It could be modified to a cylindrical configuration if packaging in our Spacelab rack so requires. The channels would be 2.5 cm by 0.7 cm in width comprising two great circles intersecting at the outlet. A 200 × 600 mesh screen is recommended for retention of the Freon-11.

An alternative bladder concept for the Freon-11 storage tank may be less expensive since such systems are now in use in the space program. This bladder concept may be chosen if the transparent surface tension concept is not suitable or desirable for heat transfer experiments and the non-transparent tank option can be selected. This concept utilizes a metal tank with a Teflon bladder which is collapsed by ambient pressure since system operating pressure is less than one atmosphere.

This configuration is also shown in Figure 3-19. The center tube can be either aluminum or Teflon. A similar 53.3 cm (21 in) diameter tank is now in use with the Centaur hydrogen peroxide system and has been flight qualified; that assembly uses 100 psi helium gas for expulsion and a Dow Corning 9711 silicon rubber bladder.

3.2.9.5 Quality Meter. General Dynamics Convair has had experience in the use of the Quantum Dynamics quality meter to measure the quality of hydrogen in a one-g laboratory experiment. An inquiry to the manufacturer revealed that their meter would perform very satisfactorily and had been used with Freon in the LEM program with success. He reports an accuracy of ± 0.5% for the density measurement which translates to a higher accuracy for quality above qualities of one per cent. The accuracy of the instrument is sufficient over the range of interest. Instrument drift for cryogenic hydrogen service is reported to be a problem, but this is possibly a temperature problem which should be absent with Freon. Williamson (Ref. 34) discusses devices to measure quality of two-phase flow and reports a high degree of accuracy for void fraction and quality appears feasible with the capacitance meter technique.

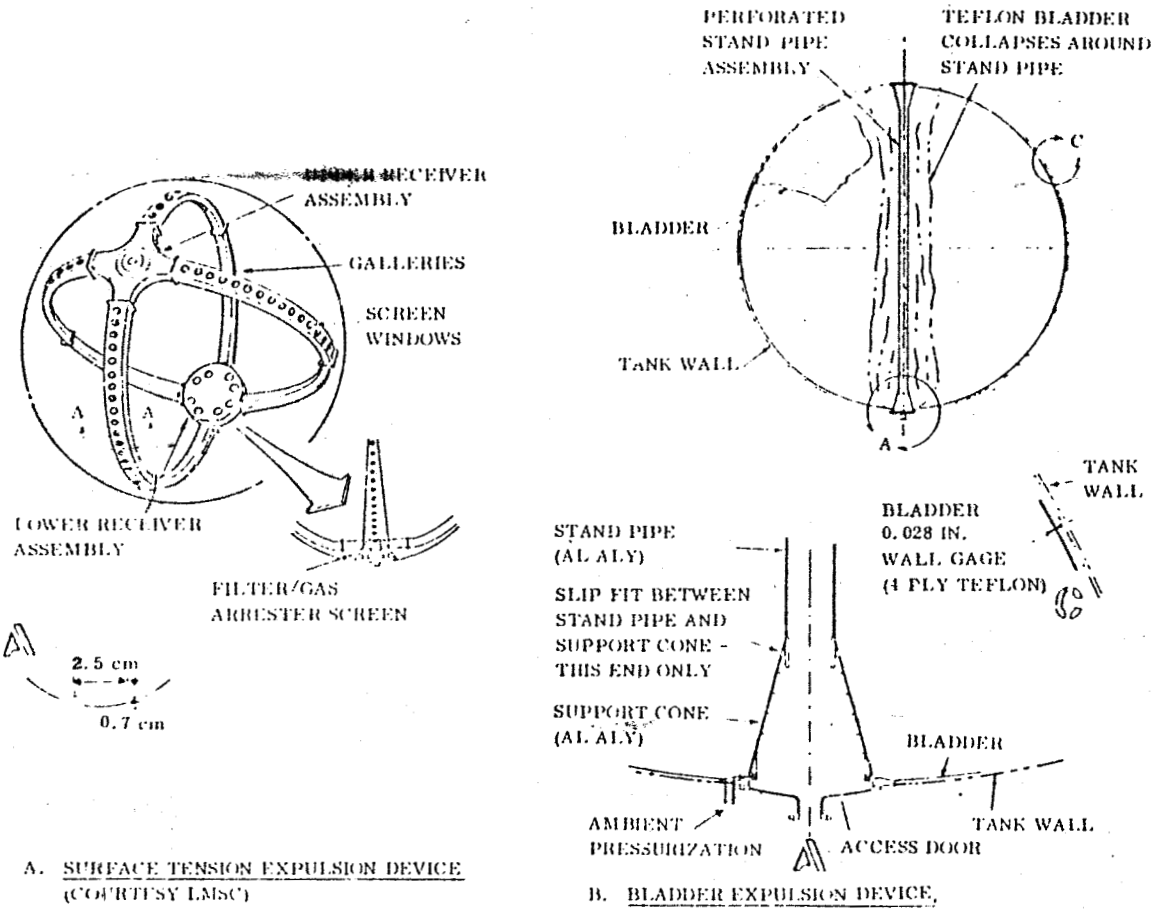


A. SURFACE TENSION EXPULSION DEVICE (COURTESY LMSC)

B. BLADDER EXPULSION DEVICE

Figure 3-19. Two Fluid Acquisition Systems Meet Experiment Options

3.2.10 INSTALLATION IN SPACELAB DOUBLE RACK. The installation shown in Figure 3-20 corresponds to the flow schematic of Figure 3-18 and is for the Flow Regime/Pressure Drop experiment integrated with the liquid recycle option of the Flow Boiling experiment. In the discussion of test fluids (Section 3.2.2) it was proposed that safety requirements relating to toxicity of Freon-11 could be met by double containment. The transparent Lexan panels shown provide for a secondary enclosure. The need for this enclosure applies only to components containing Freon-11. Thus the cameras, lights, and some other components are positioned outside the enclosure so as to be readily accessible for operation and maintenance.

The test section was placed outside the enclosure with the objective of minimizing degradation of photographic images. The test section jacket inherently provides double containment of test fluids.

FOLDOUT FRAME

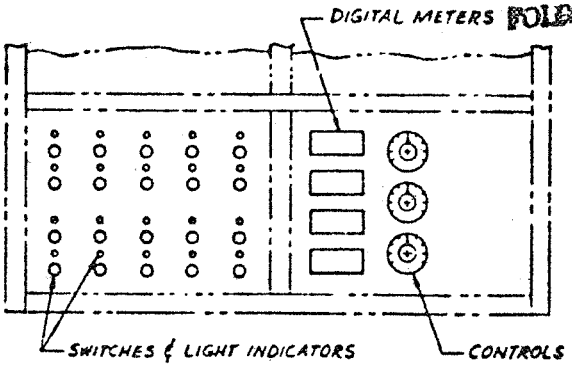


VIEW D-D

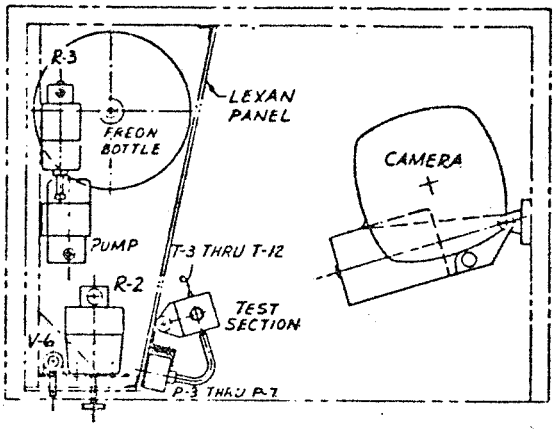


VIEW C-C

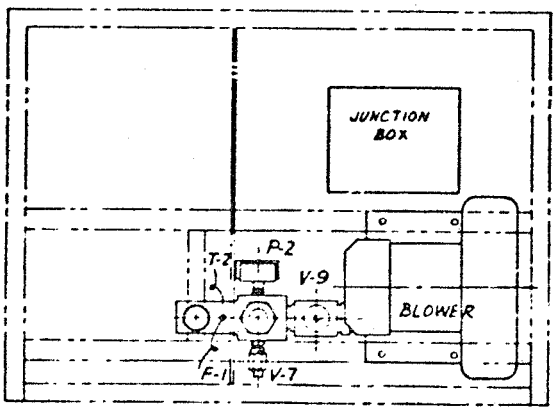


VIEW B-B

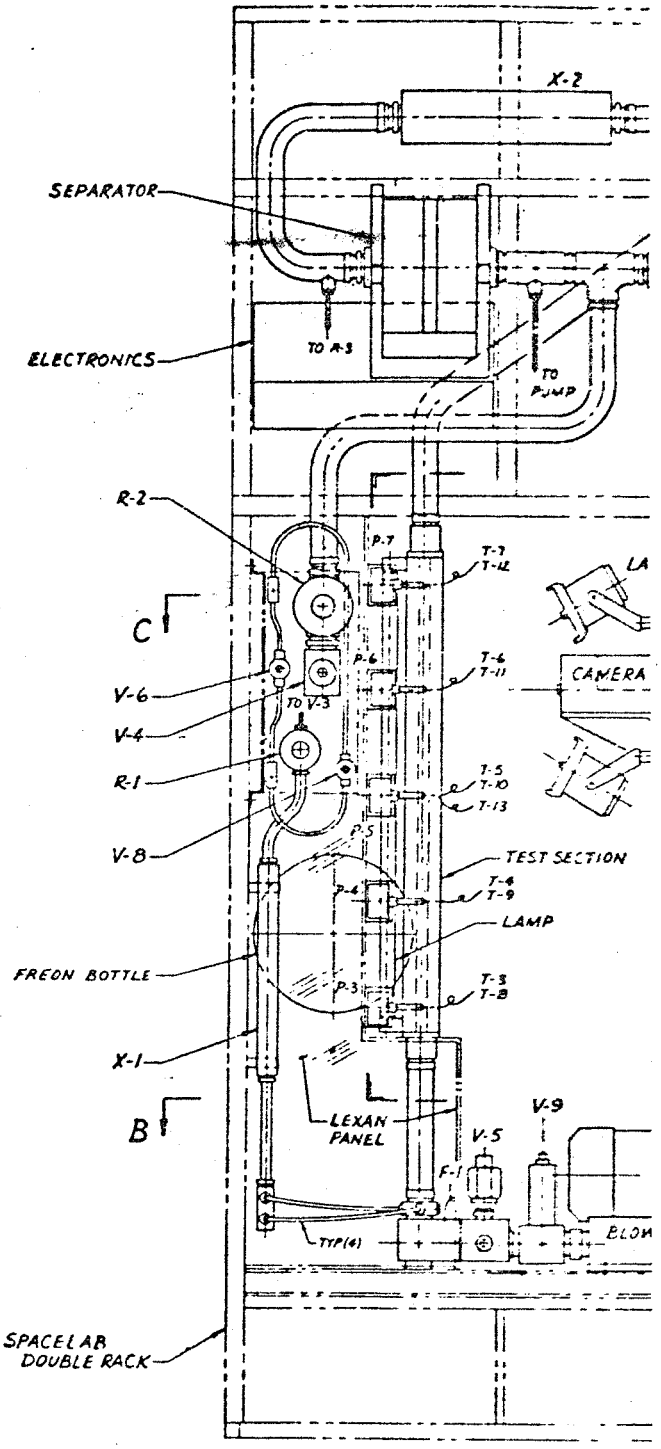


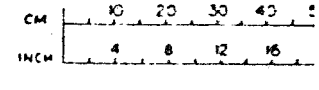


SCALE

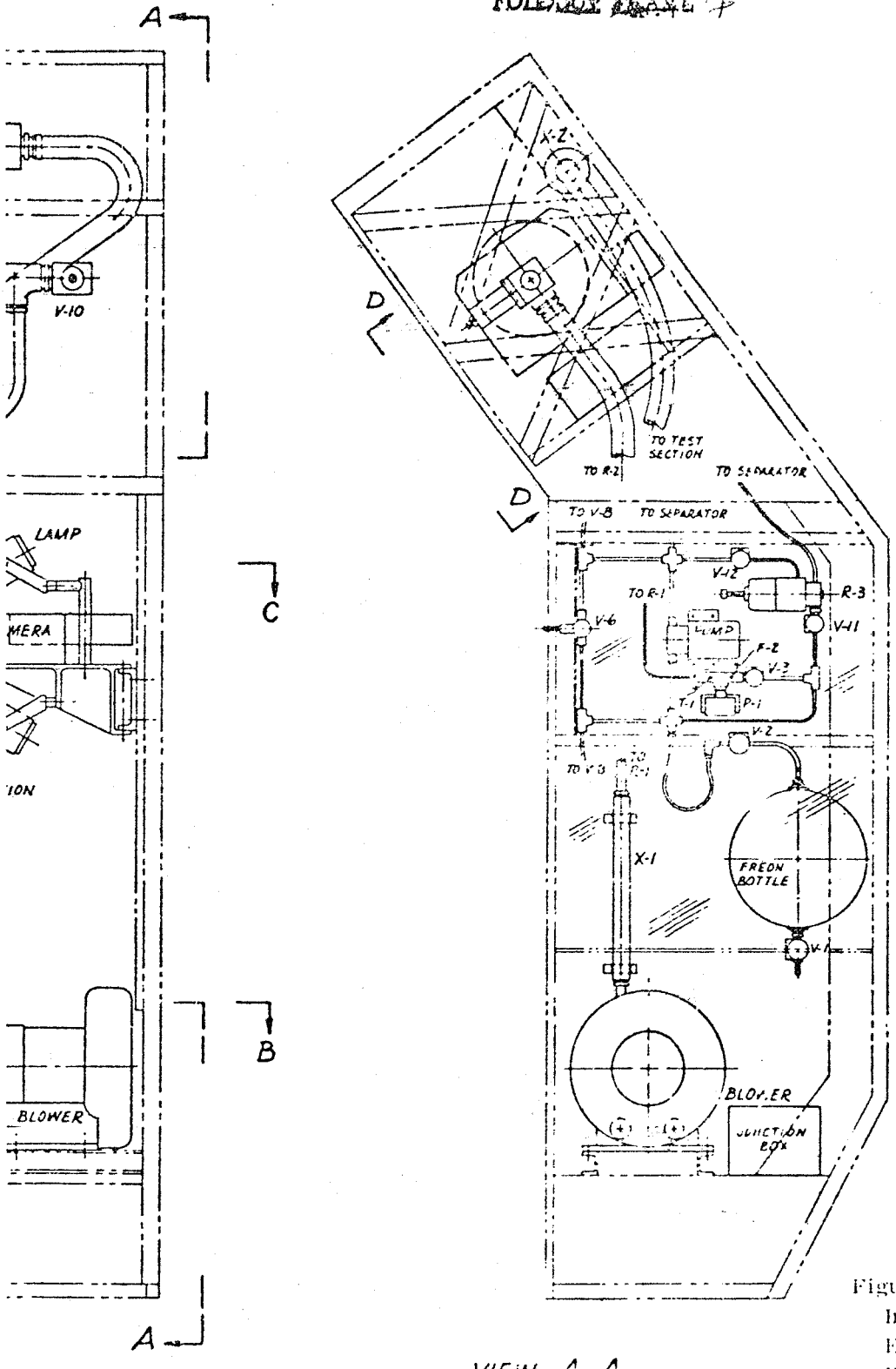


Figure 3-20. Experiment Installation for Integrated Experiments With Liquid Recycle of Freon



D. CHU 6-27-77
REV 8 22-77

The installation scheme shown provides for flexibility in angle and location of cameras and lights. The cameras can be traversed in a direction parallel to the test section, and they can be pivoted about an axis normal to the floor.

The enclosure for the Freon-containing components is not required to be transparent on all sides. Light metal sheets can be used to complete side sections and the back of the enclosure; it should not have gross leaks to cabin ambient. Safety will be enhanced if the enclosure is operated at a pressure slightly below cabin ambient. This can be done by providing a line from the enclosure to the small experiment venting assembly (Reference 32), with the line containing a shutoff valve and calibrated orifice that allows overboard bleed of a few $cm^3$/sec. This bleed would be in operation only during the Flow Boiling experiment and inboard leakage of cabin air would maintain the pressure balance in the enclosure.

Figure 3-21 corresponds to the flow schematic of Figure 3-17 and is for the Flow Regime/Pressure Drop experiment integrated with the overboard dump option of the Flow Boiling experiment. The two spherical tanks for Freon-11 were selected because they have the stated capacity (Table 3-7) and they represent existing hardware from another program. Other number of tanks, sizes, and shapes could have been selected.

## 3.3 SUPPORTING REQUIREMENTS

3.3.1 VOLUME. The arrangement of Figures 3-20 and 3-21 show that the volume of a Spacelab double rack is adequate for the concept of integrated experiments. Storage tank volumes were presented in Section 3.2.9.4.

3.3.2 WEIGHT. Table 3-11 is an estimate of weights for fixed hardware and consumables for the liquid recycle concept of Figure 3-18. It is assumed that all test fluids are jettisoned during preparations for Orbiter re-entry, so that photographic film is the only consumable returned to the earth. The quantity of cine film is based on 120 data points, 7 seconds of film per data point, 100 frames/second, and packaging in 1200 ft magazines with one spare loaded magazine. The estimated delta weights for a total overboard dump in the flow boiling experiment (Reference Figure 3-7) are 25 kg (55 lb) of hardware for a larger Freon storage tank and 111 kg (245 lb) of additional consumables not returned to earth. The total weight in either case is within allowables for a Spacelab double rack (Reference 32).

3.3.3 ELECTRICAL POWER. An estimate of electrical power and energy requirement is shown in Table 3-12. The watt-hours column for the flow regime/pressure drop experiment is for 80 data points at one minute per data point, except that the cine camera and lights are on 7 seconds per data point. The watt-hours column for the flow boiling experiment is for 10 data points at two minutes per data point, except that the cine camera and lights are on 7 seconds per data point. The concepts described earlier indicate ac inputs in the blower and pump motors in order that variable frequency

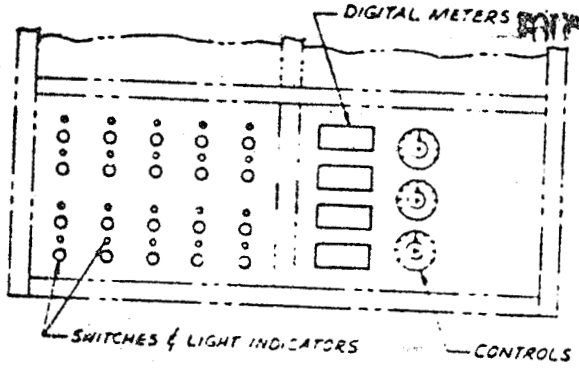


VIEW D-D

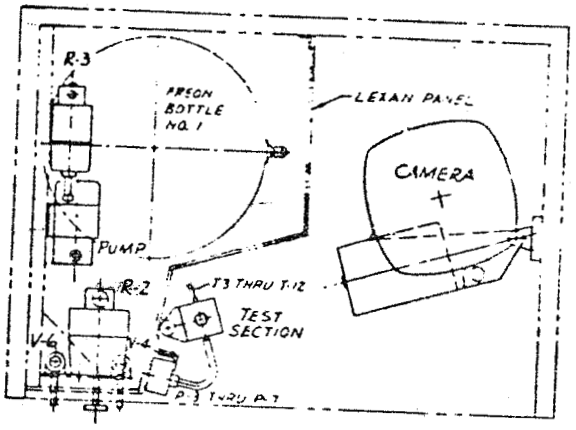


VIEW C-C

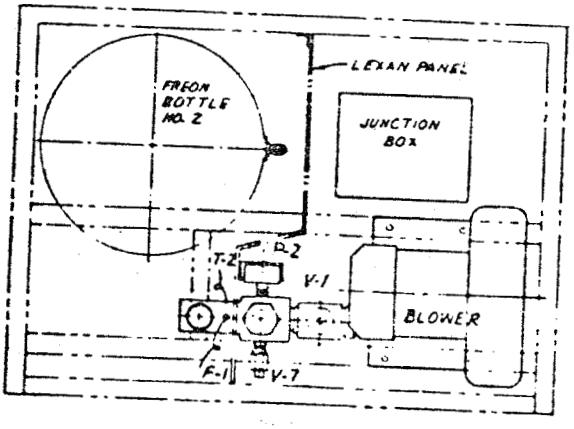


VIEW B-B

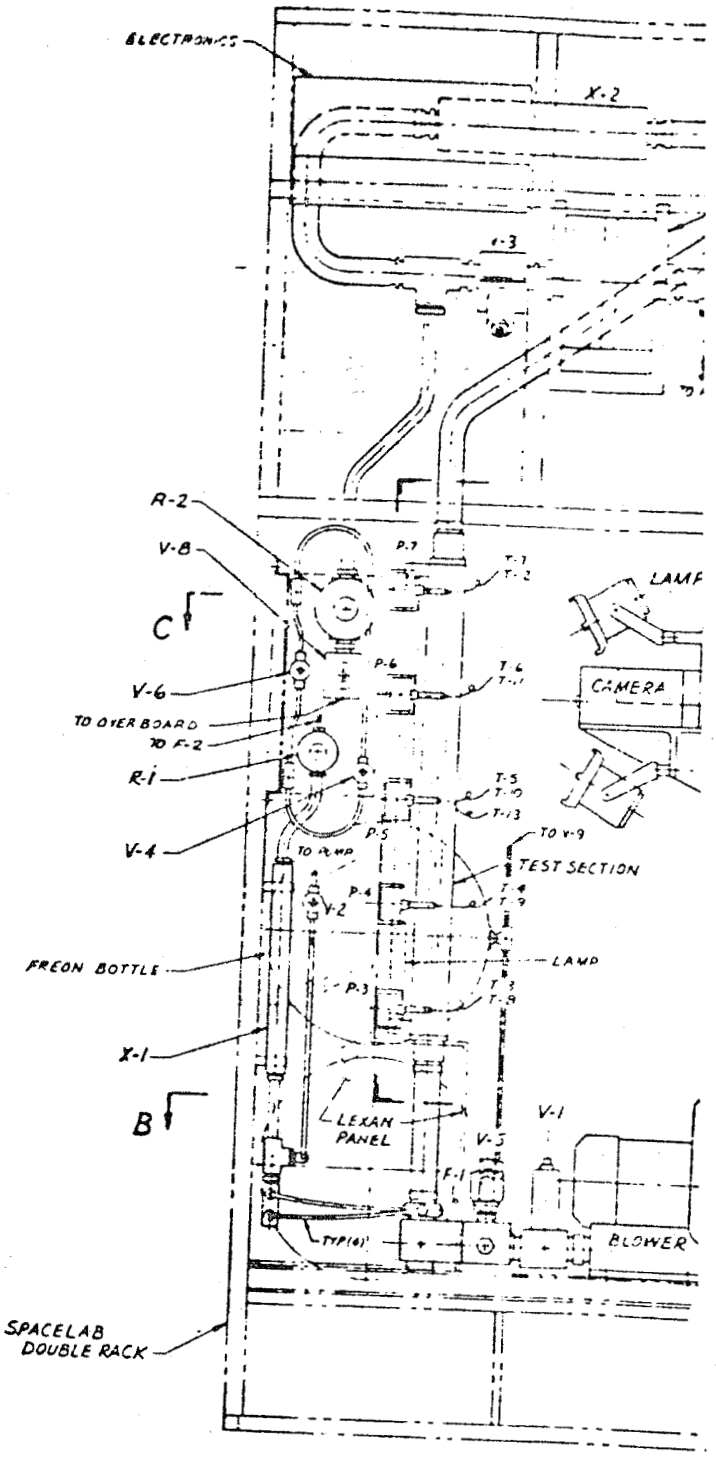


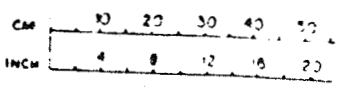


SCALE

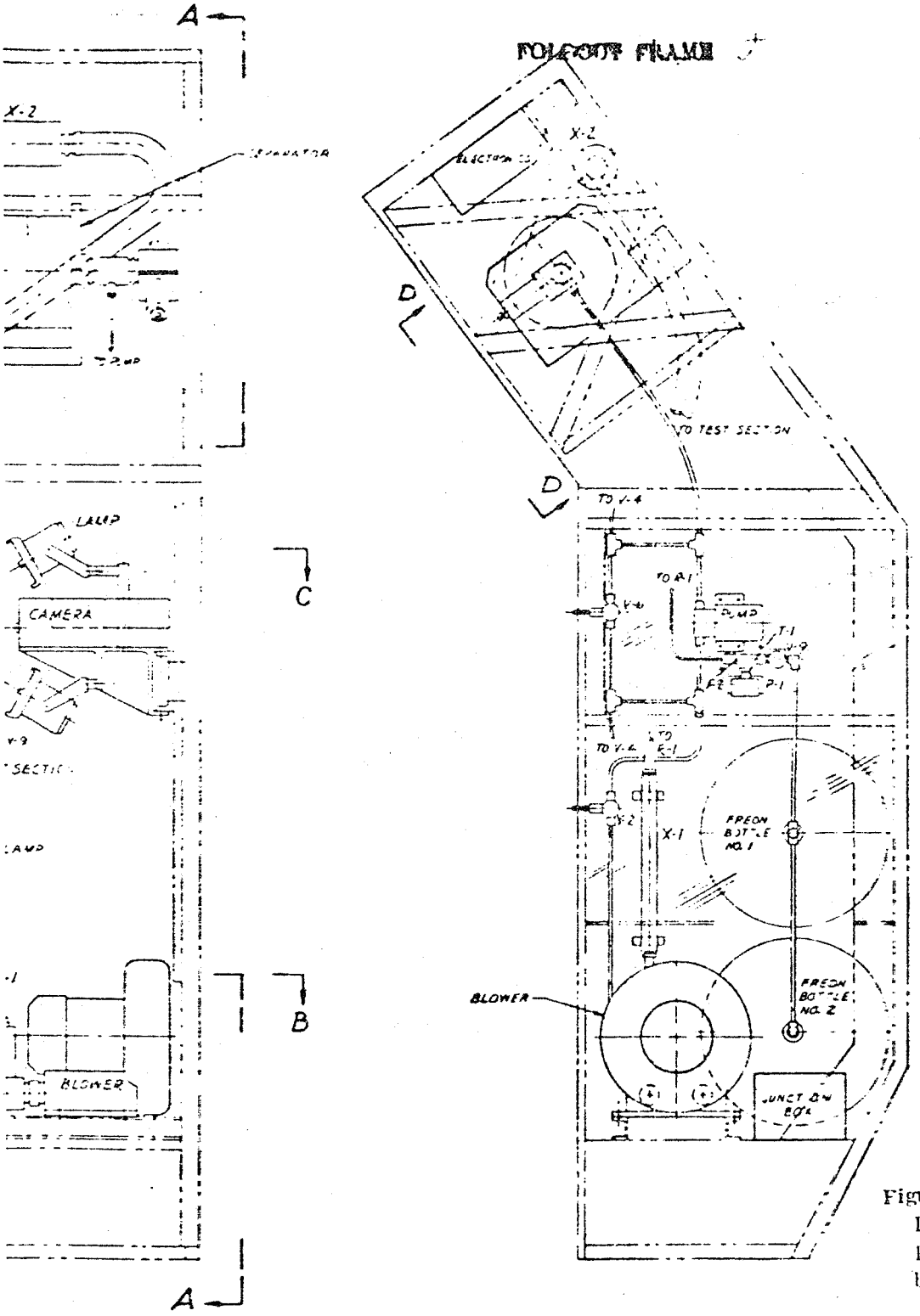


VIEW A-A

ORIGINAL PAGE IS
OF POOR QUALITY

Figure 3-21. Experiment Installation for Integrated Experiments With Overboard Dump of Freon

D.CHU 6-27-77
REV 8-26-77

Table 3-11. Weights Estimate for Liquid Recycle Concept (Ref. Figure 3-13)

| Hardware, Fixed, Dry | kg | lb |
|---|---|---|
| Test Section | 5.9 | 13.0 |
| Blower and Motor | 30.0 | 66.2 |
| Pump and Motor | 4.8 | 10.6 |
| Separator and Motor | 10.4 | 23.0 |
| Freon Supply Tank | 10.2 | 22.5 |
| Camera, Motion Picture | 2.7 | 6.0 |
| Camera, Still | 1.8 | 4.0 |
| Lights, Photographic, Frontal (2) | 1.7 | 3.8 |
| Light, Photographic, Back | 1.4 | 3.1 |
| Valves, Solenoid (V-1, V-2, V-3) | 1.3 | 2.8 |
| V-4) | 0.9 | 2.0 |
| V-9, V-10) | 2.5 | 5.5 |
| V-11, V-12) | 0.9 | 2.0 |
| Valves, Flow Control (V-5, V-6, V-7, V-8) | 0.9 | 2.0 |
| Digital Panel Meters (4) | 1.8 | 4.0 |
| Panel Switches, Panel Lights | 0.5 | 1.1 |
| Motor Speed Controls (2) | 1.4 | 3.0 |
| Pressure Regulators (3) | 1.4 | 3.0 |
| Heater Control, 3-Phase | 4.8 | 10.5 |
| Flowmeter, Air | 1.0 | 2.2 |
| Flowmeter, Liquid, Turbine Type | 0.5 | 1.0 |
| Quality Meters (2) | 12.7 | 28.0 |
| Pressure Transducers (7) | 2.0 | 4.4 |
| Temperature Transducers (14) | 0.1 | 0.2 |
| Sensor Electronics, Signal Conditioning | 5.0 | 11.0 |
| Electrical Wiring | 2.0 | 4.4 |
| Piping | 4.0 | 8.8 |
| Structure, Panels, Fasteners | 31.8 | 70.0 |
| Subtotals | 155.1 | 341.8 |
| Consumables | | |
| Returned to Earth: | | |
| Film, 16 mm, 1200 ft Magazines (8) | 34.4 | 120.0 |
| Film, 35 mm | 0.5 | 1.0 |
| Not Returned to Earth: | | |
| Water | 5.4 | 12.0 |
| Freon-11 | 19.1 | 42.0 |
| Subtotals | (79.4) | (175.0) |
| Total, Hardware and Consumables | 233.5 | 514.8 |

Table 3-12. Electrical Power Estimate

| | Flow Regime Pressure Drop Experiment | | Flow Boiling Experiment | |
|---|---|---|---|---|
| | Watts, max. | Watt-hours | Watts, max. | Watt-hours |
| Blower | 769 | 1021 | - | - |
| Pump | 11 | 10 | 11 | 10 |
| Liquid/Gas Separator | 75 | 100 | 75 | 100 |
| Camera | 100 | 17 | 1200 | 24 |
| Photographic | 320 | 42 | 320 | 41 |
| Valves, Solenoid | 95 | 127 | 80 | 107 |
| Valves, Flow Control and Meters | 25 | 38 | 25 | 38 | |
| Heaters | - | - | 2700 | 1800 |
| Sensors, Signal Conditioning | 90 | 120 | 90 | 120 |
| Data Recording | | | | |
| Totals | 1485 | 1552 | 1811 | 1677 |
| Total Watt-Hours | 2029 | | | |

speed controls can be used and to the test section heater in order that a variable transformer can be used to control heater power input. The blower and heater components are not used at the same time. The maximum dc load is about 1100 watts and the maximum ac load is about 800 watts. The latter is within the capacity of a single Spacelab inverter (Reference 32).

3.3.4 HEAT REJECTION. The maximum heat load corresponds to the 1552 watt-hours of electrical energy (Table 3-12) expended over 80 minutes duration of the flow regime/pressure drop experiment. This is an average rate of 1164 watts, all of which is released within the double rack. The major part of this heat load is rejected to the cabin environment outside the Lexan enclosure. The flow boiling experiment heat load is lower than the case above. Concepts for accommodating this load are beyond the scope of the present effort. This heat load for the cabin is consistent with Spacelab power to cooling capability relation.

3.3.5 CREW. The concepts presented are compatible with experiment operation by a crew of one. The maximum crew size for effective access to controls is limited by rack width to no more than two persons. An analysis to determine optimum crew size is beyond the scope of the present effort. The experiment operating time totals 160 minutes, to which must be added the time increments for set-up, check-out, change from the first experiment to the second, shut-down, and experiment securing for

landing. The total time, including experiment operation, is estimated to be four hours for a crew of two and six hours for a crew of one.

3.3.6 DATA ACQUISITION. It is assumed that the Command and Data Management Subsystem (CDMS) of Spacelab will be utilized to the extent that its capabilities meet experiment needs for data quality, and that it may be supplemented by experiment-specific signal-conditioning equipment where justified by need for higher response or accuracy. Experiment to CDMS data signals will be via a standard CDMS Remote Acquisition Unit (RAU).

No high frequency response requirements have been identified. In previous flow regime/pressure drop experiments (Ref. 20 ) the maximum recorded frequency of pressure fluctuations was only 30 Hz.

Table 3-13 lists in two groups the 27 analog signals corresponding to the 27 transducers shown in Table 3-9. The first group contains the nine measurements in which high accuracy is most critical to experimental results. The accuracies listed are representative of good transfer capabilities and impose a requirement for experiment-specific signal processing to preserve high accuracy. The operational amplifiers, A/C converters, shift registers, and/or other electronic components are estimated to have a volume of 0.028 $m^3$ (1 $ft^3$) and a weight of 5 kg (11 lb).

Table 3-13. Measurement Accuracies

| | Measurement | Accuracy |
|---|---|---|
| | First Priority Analog Signals | |
| P-3 | Test Section Entrance Pressure | ± 0.1% |
| P-7 | Test Section Exit Pressure | ± 0.1% |
| T-3 | Fluid Temperature, Test Section Entrance | ± 0.05K |
| T-7 | Fluid Temperature, Test Section Exit | ± 0.05K |
| F-1 | Liquid Flow | ± 0.25% |
| F-2 | Gas Flow | ± 0.25% |
| X-1 | Test Section Entrance Quality | |
| X-2 | Test Section Exit Quality | |
| W | Heater Voltage Input | ± 0.1% |
| | Second Priority Analog Signals | |
| P-1 | Liquid Supply Pressure | ± 0.5% |
| P-2 | Gas Supply Pressure | ± 0.5% |
| P-4 | Test Section 1/4-Point Pressure | ± 0.5% |
| P-5 | Test Section Mid-Point Pressure | ± 0.5% |
| P-6 | Test Section 3/4-Point Pressure | ± 0.5% |
| T-1 | Liquid Supply Temperature | ± 0.1K |
| T-2 | Gas Supply Temperature | ± 0.1K |
| T-4 | | |
| T-5 | Fluid Temperatures, Test Section | ± 0.1K |
| T-6 | | |
| T-8 | | |
| T-9 | | |
| T-10 | Test Section Wall Temperatures | ± 0.1K |
| T-11 | | |
| T-12 | | |
| T-13 | Jacket External Surface Temp. | ± 0.1K |
| T-14 | | |
| T-15 | Ambient Air Temperature | ± 0.1K |
| | [illegible] | |
| 19 | [illegible] | Discrete |

The second group in Table 3-13 has 19 measurements that are of interest but may be of lower accuracy. These analog signals may be input directly to the RAU. It is also desirable to record on-off cycles of all electrical components, including cameras, lights, blower, pump, separator, and all valves. This gives rise to the 19 discrete signals stated in Table 3-13.

Visual records will constitute an important part of the data. High speed color motion pictures have already been discussed The estimate of experiment weight further includes allowance for a standard 35 mm camera and film for one exposure per data point. Prior evaluation of flowing boiling phenomena has been productive. The

changes in the fluid behavior in the reduced-gravity environment should be enlightening. Early photographic evaluation of Freon boiling by General Electric (Reference 30) indicates the clarity of the observation for changes in vapor quality with distance along the tube. The change of quality with heated surface area is shown in Figure 3-22.

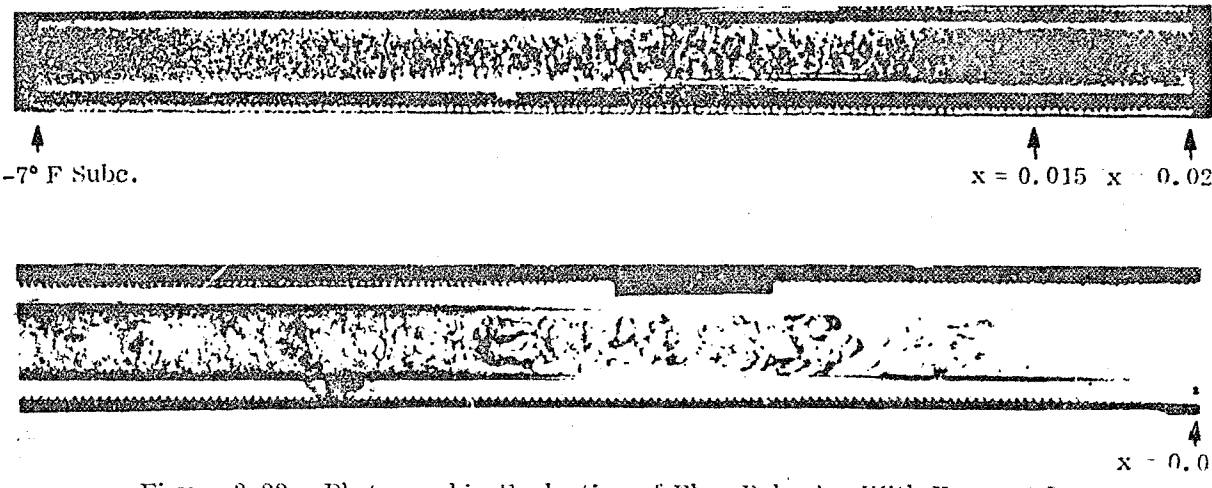


Figure 3-22. Photographic Evaluation of Flow Behavior With Freon at Low Vapor Quality, Nucleate Boiling Above and Slug Flow Below (General Electric Co., Schenectady, New York, Ref. 35)

## 3.4 OPERATING PROCEDURES

The procedures outlined below are consistent with the assumption of integrated experiments as represented by Figure 3-18. In scope, the procedures defined are limited to pre-experiment preparation and once-through performance of each experiment at a scheduled time during a Spacelab mission. It is assumed that the experiments will be performed several times in a ground facility prior to flight. While there may be minor differences between ground and in-flight procedures, the objective should be to keep them as nearly identical as possible. It is also assumed that the two-phase flow regime/pressure drop and the flow boiling experiments will be performed consecutively without interruptions.

### 3.4.1 PRE-EXPERIMENT PREPARATION

a. Remove and stow any equipment covers and/or restraints that may be required as launch environment protection.

b. Confirm all switches are in the OFF position.

c. Assure all regulators are set at a zero flow position.

d. Assure that all manual valves are closed.

e. Confirm that all motor variable speed controls are set at minimum speed.

f. Check that camera position, aim, and focus are correct, and that a loaded film magazine is in place.

g. Switch experiment main power ON.

h. Switch photographic lights and camera ON, observe for correct function, then switch OFF. Time on should be just long enough to verify function.

i. Switch power ON to transducers, signal conditioning electronics, and displays.

j. Operate Command and Data Management Subsystem (CDMS) as required for input of data signals.

If the foregoing reveals any defects or deficiencies that would prevent correct and safe experiment operation, including data acquisition, correction should be accomplished for each defect at the time observed and before proceeding to the next step.

3.4.2 FLOW REGIME/PRESSURE DROP EXPERIMENT PROCEDURE. (Refer to Figures 3-18 and 3-23.

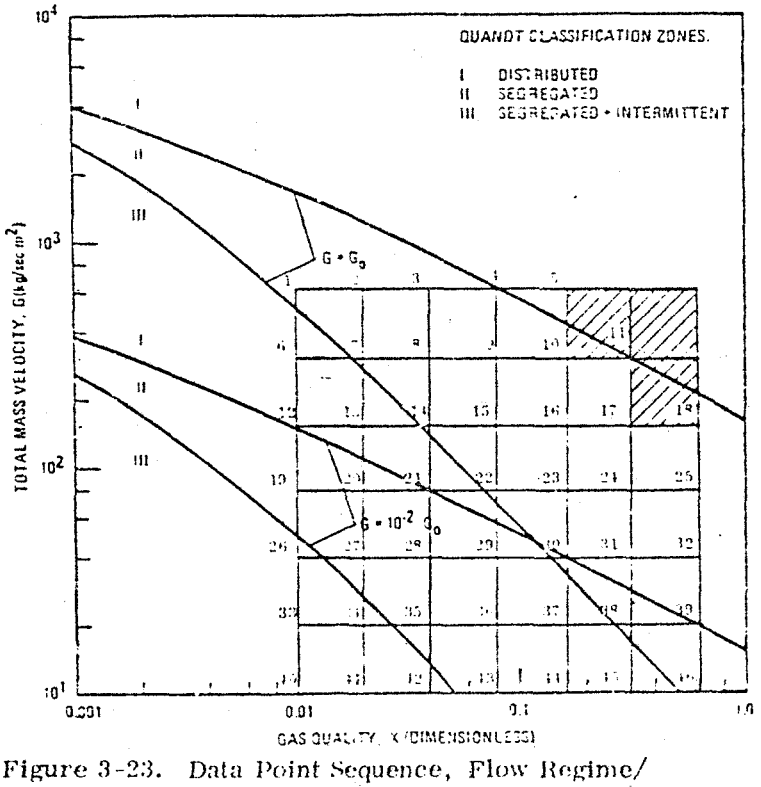


Figure 3-23. Data Point Sequence, Flow Regime/ Pressure Drop Experiment

a. Switch separator ON.

b. Switch V-9 OPEN.

c. Switch V-10 OPEN.

d. Switch blower ON.

e. Advance blower speed control C-1 to approximately half speed.

f. Switch V-3 OPEN.

g. Turn regulator R-1 fully OPEN.

h. Switch pump ON.

i. Adjust pump speed control C-2 and/or bypass valves V-6 and V-8 to obtain the liquid flow data point 1.

j. Adjust blower speed control C-1 and/or bypass valves V-5 and V-7 to obtain the gas flow for data point 1.

k. Trigger lights/camera operation (automatically timed).

l. Repeat i., j., and k. sequentially for data points 2 through 46. Interrupt as necessary to change film magazines.

m. Repeat i., j., and k. for any unscheduled data points suggested by observations of flow patterns and data.

3.4.3 EXPERIMENT CHANGEOVER PROCEDURE (Refer to Figure 3-18).

a. Switch pump OFF.

b. Switch blower OFF.

c. Switch V-9 CLOSED.

d. Switch V-10 CLOSED.

e. Turn V-5 CLOSED.

f. Turn V-7 CLOSED.

g. Turn V-6 OPEN.

h. Turn V-8 OPEN.

i. Turn R-2 OPEN.

j. Slowly turn V-4 OPEN to discharge water overboard. Wait long enough to dry all interior surfaces of the apparatus.

k. Turn R-2 CLOSED.

l. Slowly turn V-2 OPEN to partially re-pressurize recycle loop.

m. Slowly turn V-1 OPEN to fully re-pressurize recycle loop.

n. Adjust pump speed control C-2 to approximately half speed.

o. Switch V-12 OPEN.

p. Switch V-11 OPEN.

q. Switch pump ON.

r. Turn V-6 CLOSED.

s. Turn V-8 CLOSED.

t. Adjust heater power control to ZERO.

u. Switch heater power ON.

3.4.4 FLOW BOILING EXPERIMENT PROCEDURE (Refer to Figures 3-18 and 3-24). The following is consistent with the data point sequence shown in Figure 3-24.

a. Adjust R-1 to the approximate test section inlet properties (pressure, temperature, quality) for data point 1.

b. Adjust R-2 and pump speed control C-2 to the approximate flow for data point 1.

c. Adjust heater power control to the heat input for data point 1.

d. Re-adjust R-1 and R-2 to the set point conditions for data point 1.

e. Trigger lights/camera operation.

f. Repeat a., b., c., d., and e. sequentially for data points 2 through 28.

g. Repeat a., b., c., d., and e. for any unscheduled data points suggested by observations of flow patterns and data.

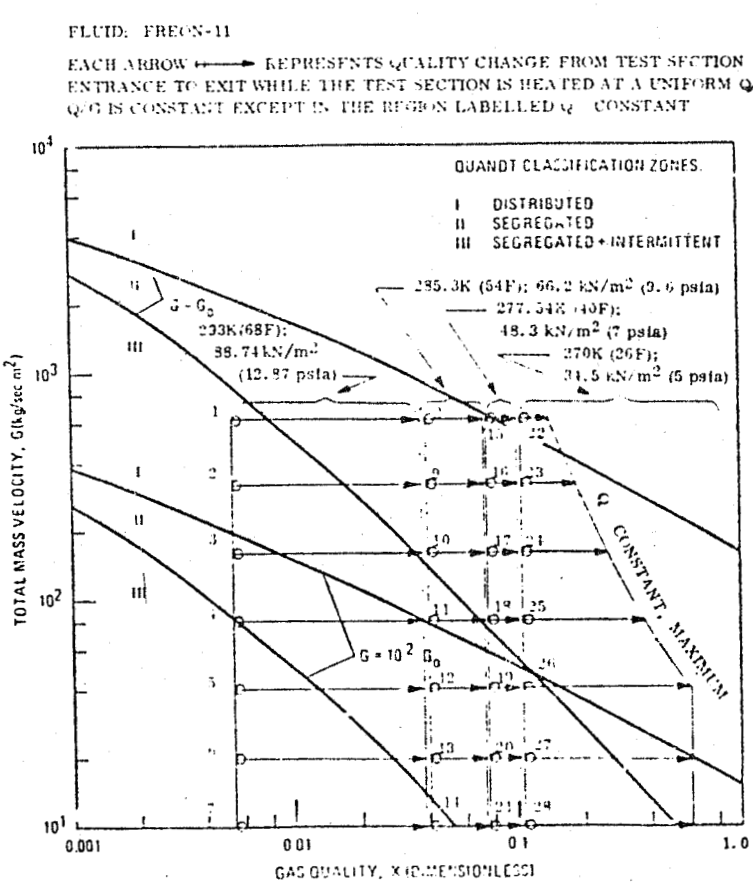


Figure 3-24. Data Point Sequence, Flow Boiling Experiment

3.4.5 SHUTDOWN PROCEDURES

a. Switch heater power OFF.

b. Turn V-1 CLOSED.

c. Turn R-2 OPEN.

d. Turn R-1 OPEN.

e. Switch pump OFF.

f. Switch separator OFF.

g. After discharge of Freon overboard. turn V-4 CLOSED.

h. Turn R-2 CLOSED.

i. Switch experiment main power OFF.

j. Stow film.

k. Replace any equipment covers and/or restraints that may be required for re-entry/ landing environment protection.

3.5 VARIABLES

In the discussion following, the term "primary variable" is used to mean one which is directly set or adjusted by the experiment operator as he manipulates controls of the experiment apparatus. Thus the adjective "primary" is specific to the hardware and is not intended to imply priority in any other context.

3.5.1 FLOW REGIME/PRESSURE DROP EXPERIMENT. The primary variables are liquid mass velocity, $G_\ell$, and gas mass velocity, $G_g$, from which are derived the parameters discussed in Section 3.2.3.1, namely total mass velocity, G, and gas quality, x. A secondary variable, dependent on $G_\ell$ and $G_g$, is the test section pressure drop, $\Delta P$, which will be measured by transducers at 5 stations along the test section. Considering that flow regimes may change along the test section, it should be possible to select the $\Delta P$ related to an observed regime. The flow regimes may be considered as variables induced by others, and a purpose of the experiment is to produce the flow regimes shown in Figure 3-23.

3.5.2 FLOW BOILING EXPERIMENT. The primary variables are the test section entrance pressure, $P_1$, the test section exit pressure, $P_2$, and the test section electrical heat input, $q_o$. The mass flow rate, W, is dependent on $P_1$ and $P_2$. The temperature of the stored Freon-11, $T_o$, together with $P_1$, determines the fluid entrance temperature, $T_1$, and quality, $x_1$. Net heat, q, to the test fluid will be $q_o$ minus losses to surroundings. W and q jointly determine quality at exit, $x_2$. Using dimensions of the test section, the heat flux, q/A, can be calculated. Also, using local temperature measurements of the fluid and the test section inner surface, a heat transfer coefficient, $q/A\Delta T$, can be calculated. This heat transfer coefficient can then

be related to the observed flow boiling pattern of that location.

## 3.6 DATA

The measurements capabilities of the proposed hardware configuration have been presented in Figure 3-18, Table 3-9, and Section 3.3.6. It is expected that data from magnetic tapes may be reproduced as a digital print-out or computer input. The following discussion relates specific measurements to experiment objectives.

### 3.6.1 FLOW REGIME/PRESSURE DROP EXPERIMENT

3.6.1.1 Quality. Liquid mass flow, $W_\ell$, from flowmeter F-1 (Reference Figure 3-18), and gas mass flow, $W_g$, from flowmeter F-2, will be used to calculate quality: $X = W_g/(W_\ell + W_g)$.

3.6.1.2 Mass Velocities. Liquid mass velocity is $G_\ell = W_\ell/A$, where A is the measured test section flow area; and gas mass velocity is $G_g = W_g/A$. Total mass velocity is $G = G_\ell + G_g$.

3.6.1.3 Flow Regime Boundaries. By viewing motion pictures, an observed flow regime may be identified with each data point. By plotting data points on G vs X coordinates, boundary maps similar to Figure 2-1c may be produced. The boundaries for low-g runs may then be compared with boundaries for 1-g runs. The results will be applied to fulfill the objective of a reliable definition of flow regime boundary shift with the change in g-level.

3.6.1.4 Other Flow Parameters. The local densities $\rho_\ell$ and $\rho_g$ may be determined from the pressure and temperature measurements at the transducer stations along the test section. Also, the liquid volumetric flow rate, $Q_\ell$, and the gas volumetric flow rate, $Q_g$, are available from flowmeters F-1 and F-2. From these, calculations can be made of gas volumetric flow fraction, $\beta_g$, Froude number, Fr, and dimensionless liquid velocity $u_\ell^+$. These parameters may be used as coordinates for flow regime boundary maps as shown in Section 2, and the boundary shifts may be identified. It may be found that each boundary shift is best defined by a unique coordinate combination.

3.6.1.5 Pressure Drop. The purpose of pressure measurements at several stations along the test section is to identify a pressure drop with that portion of the test section where a particular flow regime is observed. Pressure drop characteristics of like flow regimes can then be compared at 1-g and near zero-g. Also, pressure drops without regard to flow regime may be compared in the manner shown in Figure 2-5. The results should fulfill the objective of reliably defining frictional pressure drop change with change in g-level.

### 3.6.2 FLOW BOILING EXPERIMENT

3.6.2.1 Quality. The quality can be calculated from the primary variables which define the state and from the energy added in the test section. An isenthalpic expansion from $T_0$, $P_0$ to $T_1$, $P_1$ defines inlet quality. Outlet quality is $X_1 + (q \dot{m}_T/h_{fg})$. This method will be utilized but it will be backed-up by quality meters which define inlet and outlet quality for the test section. Ground testing will confirm the agreement between these measurements.

3.6.2.2 Local Heat Transfer Coefficients. With the heat flux to the tube from the value of q/A, the local heat transfer coefficient will be evaluated for the measured temperature differences based on local measured values of T, the fluid temperature and $T_W$, the wall temperature. These results will be used to evaluate the Nusselt number, $hD/k_f$, for verification of existing correlations or determining required modifications.

3.6.2.3 Pressure Drop. Several correlations relate the heat transfer coefficient to the friction coefficient. Pressure drop data must be taken during the heat transfer experiments if these correlations are to be confirmed. From mass velocities, qualities, and property data, the existing correlations can be examined.

3.6.2.4 Heat Transfer Regimes. Visual observations will be used in conjunction with the measured variables to define the flow regimes occurring in conjunction with the heat transfer tests. The heat transfer data is known to be sensitive to the regime, therefore correlations are frequently developed for a particular regime. These regions were indicated in Figure 2-6 showing the transition from subcooled boiling with bubbly flow to the liquid deficient region with droplet flow.

## 3.7 EXPERIMENT COSTS

Experimental costs were determined to proceed with the two-phase flow experiment through Level IV integration for SPACELAB. Cost estimating relationships (CER's) developed during past cost analysis activities performed by Convair on space experiment systems and during the Space Transportation Systems Payloads and Data Analysis (SPDA) study (Contract NAS8-29462) were used. The cost categories in this model are based on a hardware-oriented work breakdown structure. The CER's in this model relate cost to material, subsystem type, and weight. Program parameters calculate non-recurring costs (development) and recurring costs (procurement and operations). Where applicable, externally generated point estimates were used. Several specific high cost hardware items were based on vendor quotes and on similar existing hardware costs.

A total of seven high cost hardware items were identified and are specified in Table 3-14. Film magazines are used which are reloadable; in-flight loading can reduce the costs of 27.1K in the table by a factor of 4.

Table 3-14. High Cost Hardware Items

| | Quantity | Cost in 77 K Dollars Development | Unit | Total |
|---|---|---|---|---|
| Test Section | 1 | 22.9 | 11.1 | 34.0 |
| Blower/Motor | 1 | 15.0 | 10.0 | 25.0 |
| Freon Tank | 1 | 24.5 | 7.9 | 32.4 |
| Sensor Electronics/Signal Conditioning | 1 | 32.4 | 14.0 | 46.4 |
| Quality Meters | 2 | - | 25.0 | 25.0 |
| Film Magazines | 8 | - | 27.1 | 27.1 |
| Secondary Structure | 1 | 52.9 | 33.7 | 86.6 |
| Totals | | 147.7 | 128.8 | 276.5 |

In addition to high cost hardware which are covered under experiment hardware in Table 3-15, the remaining costs for the experiment were determined. A total cost summary is presented in Table 3-15.

In arriving at these costs, a series of groundrules were required and certain assumptions were made. These areas are outlined in the remainder of this paragraph.

Table 3-15. Cost Summary, Two Phase Flow Experiment

| | Cost in 77K Dollars Development | Production | Operational |
|---|---|---|---|
| Experiment Hardware | 389.8 | 238.3 | - |
| Systems Engineering and Integration | 69.0 | - | - |
| System Test(1) | 77.5 | 23.8 | - |
| Ground Support Equipment | 10.0 | - | - |
| Support Operations | - | - | TBD |
| Initial Spares | 29.7 | - | - |
| Ground Operation | - | - | 36.0(2) |
| Mission Operations | - | - | TBD |
| Facilities | 0 | - | - |
| Program Management/Administration | 28.8 | 13.1 | 1.8 |
| Total | 604.8 | 275.2 | 37.8 |
| Grand Total | | 917.8 | |

(1) No system test hardware - test performed on flight articles.
(2) Level IV Integration only. Level III/II, I, Post Mission, and Maintenance Refurbishment TBD.

The costs are estimated in current/constant FY '77 dollars. The costs are estimated for nonrecurring (development), recurring production (unit flight hardware), and certain portions of the recurring operation phases. Prime contractor fee is not included in these estimates. It is assumed that only one article (the flight article) is produced and all engineering development tests, qualification tests as necessary are carried out using the one unit which is refurbished prior to flight. All purchased components are assumed qualified aerospace type off-the-shelf hardware and little or no development or testing effort is required. Fabricated components require normal design, analysis and testing.

No facilities are required chargeable to the experiment. It was assumed that eight 1200 ft film magazines were required. If these magazines can be reloaded in flight only one or two are required.

A multipurpose high fidelity Spacelab rack mockup will be required as a dimensional tooling aid, integration mockup, test stand, and experiment shipping structure. It is assumed that no flight rack will be provided prior to Level IV integration.

It was assumed that only standard and available test equipment and servicing equipment (water and Freon) was required and the only experiment chargeable GSE may be some special tools and shipping related items.

No heat exchanger interface with Spacelab is required. Finally, this cost data is provided for planning purposes only.

# 4

## CONCLUSIONS AND RECOMMENDATIONS

The review of future NASA applications indicates there are several areas where designs of hardware are not fixed which can benefit from improved correlations for reduced-gravity two-phase flow. Major applications are space storage of cryogenic propellants and space power systems as well as new cryogenic vehicles. Experiments in the early 1980's will be timely for these applications.

The correlations to date for flow regime, pressure drop, and heat transfer are all empirical indicating the need for further investigation into the mechanism of the process. More important, these empirical equations do not adequately predict the shift in flow regime with changes in gravity-level. Meanwhile, controversy continues over the nucleate boiling contribution in reduced-gravity. The test environment of Spacelab with sufficiently low-g and sufficient duration is required.

The conceptual design study confirms the feasibility of the reduced-gravity two-phase flow experiment in Spacelab and it is recommended that the detailed design proceed. A combined experiment is outlined in which the test section was selected to be a 1.52 cm fused quartz tube 90 cm in length. Water-cabin air are the test fluids for a combined flow-regime pressure drop study because of the experimental ease of an open-loop air closed-loop water system. Freon-11 is the recommended test fluid for the heat transfer study. The former experiment provides steady-state operation at a specific quality affording improved regime definition in low-g. The heat transfer study involves a change in quality with distance along the tube with the result that two or more regimes may result for a given test in some regions of the flow map.

One consideration in system operation is the overboard dumping of fluids, particularly Freon. Both liquid-recycle and overboard-dump systems are presented as options. The liquid-recycle with 14 kg (30 lbs) of Freon is more complex; however, it is volume efficient. The overboard dump with 111 kg (245 lbs) of Freon dumped is the preferred system for reasons of simplicity and it also provides two 42 cm (17 in) diameter transparent tanks for other experiments. In either case the experimental design proposed has sufficient space for integration of additional fluid/heat transfer experiments in the double rack. This experiment integration can make use of common cameras, lights, electronics/signal conditioning and controls.

A wire-resistance heating element of 679 watts will provide the design heat fluxes for the experiment. This does not provide dryout at the higher flow rates, but only at the lower two flow rates. Additional heater power could be considered. The flow regimes cover the saturated boiling regime but can be extended with ease to subcooled boiling

and to a study of the transition into the dispersed (droplet) flow regime. A metal-film resistance heater remains as an alternate concept but it is even more severely limited in maximum power. The maximum power to the total experiment is 1897 watts with a total usage of 2929 watt hours in approximately six hours.

The test duration is six hours total, comprising 80 data points in the flow regime-pressure drop sequence in 80 minutes and 40 points in the heat transfer tests in 80 minutes, with additional time for changeover and set-up.

Program costs are 605K dollars for development and 312K dollars for production of a single unit for test and flight. This total program cost of 917K dollars is reasonable and justified in view of the increased design data which can be achieved as well as the general increase in our knowledge of this complex phenomena of two-phase flow which is so widely used in our earth-bound operations.

# 5

## REFERENCES


1. "Orbital Propellant Handling and Storage Systems for Large Space Programs," NASA Contract, March 1977, General Dynamics Convair work-in-progress.

2. "Initial Technical, Environmental, and Ecenomic Evaluation of Space Solar Power Concepts," Vol. I Summary, Lyndon B. Johnson Space Center Report JSC-11568, August 31, 1976.

3. "Future Space Transportation Systems Analysis Study," NASA Contract NAS9-14323, Boeing Final Briefing, December 1976.

4. "Initial Technical, Environmental, and Economic Evaluation of Space Solar Power Concepts," Vol. II, Detailed Report, Lyndon B. Johnson Space Center Report JSC-11568, August 31, 1976.

5. "Nuclear Flight Systems Definition Study," Phase III, Final Report, Vol. II, Part B Baseline System Definition, North American Rockwell, Space Division Report SD71-466-3, April 1971.

6. "Summarized NASA Payload Descriptions - Automated Payloads," George C. Marshall Space Flight Center, July 1975.

7. "Superconducting Magnetic Spectrometer Experiment for HEAO Mission B, Part I, Preliminary Design and Performance Specifications," University of California, Berkeley, DCN 1-1-21-00090 (IF) 15 February 1972.

8. "Payload Descriptions, Vol. I, Automated Payloads," Level B Data, Marshall Space Flight Center, July 1975.

9. Bekey, Mayer, and Wolfe, "Advanced Space System Concepts and Their Orbital Support Needs (1980-2000)," Aerospace Corp., Contract NASW2727, April 1976.

10. "Space Station Systems Analysis Study," Part 2, NAS8-14958, McDonnell Douglas Astronautics Company Briefing, January 28, 1977.

11. Alvarez, L. W., et al, "The Liquid Xenon Compton Telescope: A New Technique in Gamma-Ray Ascronomy," University of California, Berkeley Space Sciences Laboratory Series 14, Issue 17, March 1973.

12. "Payload Descriptions, Volume II, Sortie Payloads," Marshall Spaceflight Center, July 1975.

13. "System Definition Manual," A Series of Manuals for the Space Shuttle/Orbiter, Rockwell International Space Division Documents, SD72-SH-0106-X, June 25, 1974.

14. "Manned Orbital Systems Concept Study," NAS8-31014, McDonnell Douglas Astronautics Company - West, 30 September 1975.

15. "Definition of Experiment Program in Space Operations, Techniques, and Subsystems, Independent Manned Manipulator," Vol. II, Technical Report LTV Astronautics Division, LTV Aerospace Corp., MSFC Alabama, 15 November 1966.

16. R. Frietag Presentation to General Dynamics/Convair, October 1976.

17. AIAA/MSFC Symposium on Space Industrialization Proceedings, Marshall Space Flight Center, Alabama, May 26 and 27, 1976.

18. "Space Industrialization Studies Orientation Meeting - MSFC Background Data," Marshall Space Flight Center, September 28, 1976.

19. "Report on NASA Five-Year Planning - Fiscal Years 1978 through 1982," Draft, NASA Planning and Program Integration, 14 February 1977.

20. King, C. D., et al, "Aircraft Flight Testing of Fluids in Zero-Gravity Experiments," Report No. CASD-NAS-74-054, General Dynamics Convair Division, Contract NAS1-11735, NASA George C. Marshall Space Flight Center, October 1974.

21. Hsu, Y., and Graham, R. W., "Transport Processes in Boiling and Two-Phase Systems," McGraw-Hill Book Company, 1976.

22. Wallis, Graham B., "One-Dimensional Two-Phase Flow," McGraw-Hill Book Co., 1969.

23. Anon., "MSFC Skylab Structures and Mechanical Systems Mission Evaluation," TM X-64824, NASA, George C. Marshall Space Flight Center, October 1974.

24. Fitzsimmons, D. E., "Two Phase Pressure Drop in Piping Components," Report No. HW-80970 Rev. 1, UC-80 Reactor Technology, Hanford Atomic Products Operation, General Electric Company, Contract No. AT(45-1)-1350, U.S. Atomic Energy Commission, March 20, 1964.

25. Merte, H. Jr. and Clark, J. A., "Boiling Heat Transfer With Cryogenic Fluids at Standard, Fractional and Near-Zero Gravity," J. Heat Trans., 86, 351, 1964.

26. Lienhard, J. H. and Ohir, V. K., "Extended Hydrodynamic Theory Theory of the Peak and Minimum Pool Boiling Heat Fluxes," NASA CR-2270, NGL 18-041-035, July 1973.

27. Merte, H., Jr., "Incipient and Steady Boiling of Liquid Nitrogen and Liquid Hydrogen Under Reduced Gravity," University of Michigan, Tech. Rep. No. 7, NASA-CR-103047, NAS8-20228, November 1970.

28. Collier, J. G., Convective Boiling and Condensation, McGraw Hill Book Co. (UK) Limited, London, 1972.

29. Kirby, G. J., "Burnout in Climbing Film Two Phase Flow, A Review of Theories of the Mechanism," AEEW-R170 UK, AEC Reactor Group, Winfrith 1966 appearing in NASA SP-5102, 1975, p. 156.

30. Bijwaard, C.; Staub, F.; Zuber, N., "A Program of Two Phase Flow Investigation," Tenth Quarterly Report, General Electric GEAP-4959, San Jose, CA, October 1965.

31. Anon., "Chromel-Alumel Thermocouple Alloys," Hoskins Manufacturing Company, Detroit, Michigan, 1961.

32. Anon., "Spacelab Payload Accommodation Handbook," NASA/ESA, ESA Ref. No. SLP/2104, Review Issue PDR-B 1976, Reprint January 1977 (Including Minor Updates).

33. Heller, W. and Cadwallader, E., "Positive Expulsion, State of the Art Study," CPIA Publication 210, May 1971.

34. Williamson, K. D., Jr., "Techniques for Determining Average Density and Related Parameters in Two-Phase Cryogenic Flow Systems," Adv. in Cryo. Engr. 17, 206, 1972.

35. Poppendick, H. F. and Sabin, C. M., "Technology of Forced Flow and Once-Through Boiling," NASA SP-5102, 1975.

END

DATE

FILMED

FEB 16 1978